2009

Novel Interactions of the Hormone Leptin Revealed by PET Imaging in Rodents and Rhesus Macaques

Robert Richard Flavell

Novel Interactions of the Hormone Leptin Revealed by PET Imaging in Rodents and Rhesus Macaques

A Thesis Presented to the Faculty of

The Rockefeller University

In Partial Fulfillment of the Requirements for

The degree of Doctor of Philosophy

By

Robert Richard Flavell

June 2009

Novel Interactions of the Hormone Leptin Revealed by PET Imaging in Rodents and Rhesus Macaques

Robert Richard Flavell, PhD

The Rockefeller University, 2009

Leptin is a polypeptide hormone, secreted principally by adipose tissue, which functions as an afferent signal in a feedback loop to maintain body weight and energy homeostasis. In addition to its well documented effects on food intake and energy expenditure, leptin modulates the function of many other physiological systems in mammals, through actions in the central nervous system and periphery. Remarkably, despite extensive studies on leptin receptor expression, the physiological biodistribution of the hormone remains essentially unknown. In order to characterize the distribution leptin in mammals, we have developed methodologies to radiolabel the hormone and visualize its biodistribution using positron emission tomography (PET). Two complementary techniques were developed to label leptin using the positron emitting isotopes ^{68}Ga and ^{18}F. ^{68}Ga labeling was accomplished by lysine-directed conjugation with the chelator 1,4,7,10-tetraazacyclododecane-1,4,7,10-tetraacetic acid (DOTA) followed by chelation of the isotope. ^{18}F labeling was accomplished using a site-specific, two step labeling procedure in which an aminooxy moiety was introduced at the C-terminus of leptin using expressed protein ligation (EPL), which was subsequently derivitized with ^{18}F-4-fluorobenzaldehyde in an aniline accelerated radiochemical

oximation reaction. These probes were used for PET imaging in mice, rats, and in rhesus macaques. PET imaging in these organisms revealed that the hormone was rapidly taken up by the cortex of the kidney, bone marrow, and visceral organs. Uptake in the kidney was partially saturable with cold ligand, and was not mediated by leptin receptor (ObR). Subsequent analysis in with a kidney specific knockout of the multiligand endocytic transporter megalin revealed loss of leptin in the urine, which was confirmed using PET imaging. Thus, megalin is required for the uptake of leptin in the proximal convoluted tubule within the cortex of the kidney. Subsequent biodistribution experiments revealed that the hormone was taken up by the brain, spleen, liver, fat, and lungs in mice, and that this uptake was leptin receptor dependant. Furthermore, PET imaging in rhesus macaques revealed that leptin was absorbed by the bone marrow and liver. Thus, leptin may activate and modulate hematopoiesis by direct action on either hematopoietic precursors or the stromal support tissue. Thus, novel physiologically significant interactions of the hormone leptin were revealed using PET.

Acknowledgements

Firstly, I would like to thank Prof. Tom Muir for his continued support, his creativity, his scientific rigor, his mentorship, and most of all his irrepressible enthusiasm for science.

I would like to thank my committee, consisting of Profs. Ali Brivanlou, Tarun Kapoor, Tim Ryan, Sandy Simon, and Jeff Friedman, for their advice. Additionally I would like to thank Dr. Phil Dawson of Scripps for serving as my outside examiner.

This thesis was the project of a very close collaboration with Dr. Giovanni Ceccarini. I would like thank him, for his patience, his creativity, and persistence in working out the difficult problems that we encountered. And I would like to again thank Prof. Jeff Friedman for his mentorship through this project.

I would also like to thank my collaborators Dr. Eduardo Butelman and Prof. Mary-Jeanne Kreek for working together on the primate imaging experiments, which turned out to be crucial in tying together all of the rest of the results.

Additionally I would like to thank Prof. Paresh Kothari for teaching me the fundamentals of radiochemistry, and Michael Synan for teaching me the basics of PET imaging analysis and for spending countless hours with us on the micro-PET scanner. Additionally I would like to thank Prof. Shankar Vallabhajosula for the opportunity to do PET imaging and radiochemistry at the Citigroup Biomedical Imaging Center.

I would also like to thank the current and former members of the Muir Lab for providing a wonderful educational environment over the years. Without the suggestions, teaching, and assistance this thesis would not have been possible. In particular, Maya Bar-Dagan provided extensive patient and careful technical assistance.

I would like to thank my family, including my mother Ellen, my stepfather Jeff, stepmother Maddy, and sister Sasha. Additionally I would like to thank my brother Steven, sister-in-law Nicole, and father Richard – all of whom are scientists- for many hours of discussions of the theory, practice, and daily joys and annoyances of science, which were helpful for me in the course of my thesis research. Finally I would like to thank my girlfriend Joanne for her continued support and love through both good and bad times.

TABLE OF CONTENTS

LIST OF FIGURES AND SCHEMES

LIST OF TABLES

Chapter 1. Introduction

1.1 Leptin: a circulating factor regulating fat homeostasis

Energy and body weight homeostasis in mammals is regulated with remarkable precision. While an average man takes in approximately one million kcal per year, the expected weight gain of the same individual is under 0.5 kilograms, an energy increase of only 1560 kcal. This small weight gain represents only 0.2% of energy intake[1]. Thus, food intake and energy expenditure must be nearly equal, suggesting the existence of a feedback system which regulates this coupling. Nevertheless, there is a clear variation in the set point of this system between individuals. Obesity is defined as a body mass index (BMI, defined as the weight of an individual in kg/height in m squared) of over 30, and is associated with significant health risks, most prominently cardiovascular disease and diabetes[2]. Obesity has increased dramatically worldwide over the last 30 years, and current estimates suggest that at least 35% of adults in the United States are obese[3]. A series of studies on twins have revealed that the variation in body weight is 50-90% genetic, a factor underappreciated by the general public[4]. Nevertheless, there is a continual increase in average BMI and obesity, implying that environmental factors must also play a role. Thus, obesity is a result of genetic susceptibility, coupled with an "obesigenic" environment in which inexpensive, high calorie, palatable foods are readily available[5]. An understanding of these genetic and environmental factors, and the development of effective interventions to control them, is of paramount importance for public health in the 21st century.

The role of the hypothalamus in body weight and energy homeostasis has been known since the 1940's. Bilateral lesions introduced in rats in the lateral hypothalamus completely inhibited food intake to the point that the animals die of starvation[6]. Conversely, lesions in the ventromedial nucleus of the hypothalamus cause hyperphagia. Based on these observations, Kennedy proposed the existence of a circulating factor which could signal the level of fat to the hypothalamus[7]. The spontaneously occurring obese mouse mutants *ob* and *db* (named for obese and diabetes) provided additional clues about the nature of these factors. By fusing the circulatory systems of *ob* and wild type animals (parabiosis), the obese phenotype of the *ob* animal could be abrogated[8]. By contrast, the *db* mouse did not lose weight when parabiosed with the wild type animal. In fact, the animal fused to the *db* mouse lost weight and eventually died of starvation[9]. Furthermore, when the *ob* and *db* animals were fused, the *ob* animal lost weight, while the *db* did not. Collectively, these experiments suggested that the *ob* mouse was lacking Kennedy's circulating satiety factor, and that the *db* animal was lacking a receptor for a satiety factor. However, without a molecular mechanism to explain these observations, little advance could be made in understanding the basic organization of fat metabolism.

The positional cloning of the *ob* gene in 1994 by Friedman and co workers ushered in a new era in which rapid progress could be made in unraveling the regulation of fat and energy homeostasis[10]. The Ob gene encodes a 167 amino acid protein, termed leptin (after the Greek "leptos" for thin), which, following processing of the signal sequence and secretion, circulates as a 146 amino acid protein of approximately 16 kDa. Several lines of evidence rapidly established that leptin could serve as Kennedy's satiety factor: leptin is expressed in adipose tissue[11,12], its expression is correlated with fat mass

in rodents and BMI in humans[13], and treatment of the *ob* mouse with leptin rapidly corrects the obese phenotype[14]. Shortly thereafter, the leptin receptor (ObR) was cloned from a cDNA library from choroid plexus and was found to be contained within the *db* locus[15]. Subsequent studies demonstrated that ObR is expressed in the hypothalamus (among many other tissues)[16], that leptin is transported into the brain by a saturable mechanism[17], and that deletion of the gene in neurons was sufficient to generate an obese phenotype[18]. Thus, leptin is a circulating factor, produced by adipose tissue in proportion to lipid mass, which can signal the level of fat stores in the body and produce a compensatory response[19].

A human pedigree of individuals with an inactivating mutation in the leptin gene causing morbid obesity was described in 1997 by O'Rahilly and co-workers[20], confirming that leptin is essential for normal energy homeostasis in humans. These individuals display a complex syndrome of obesity, hyperphagia, diabetes, central hypogonadism, abnormalities of T-cell number and function, hypothyroidism, and other endocrine abnormalities, which is corrected by replacement therapy with the hormone[21]. A similar syndrome is observed in individuals with loss of function mutations in ObR[22]. Several other genetic abnormalities of signaling downstream of leptin which cause morbid obesity have been described in humans, and these relatively rare occurrences have helped identify the roles played by these mediators in normal fat homeostasis[23,24].

Leptin's mechanism of action suggested that it could function as an obesity drug. However, the weight loss induced by the hormone was less profound than expected, suggesting that obese humans were resistant to its actions[25]. The mechanism of leptin resistance in humans remains unclear, but it is likely that several factors play a role.

Obese humans have high circulating levels of leptin, but the high peripheral level is not necessarily reflected in the CNS, where the crucial hypothalamic leptin receptors are located[26]. Thus, transport of leptin into the brain may be reduced in obese individuals. Central leptin resistance may also play a role, as leptin signaling in the CNS also appears to be attenuated in various models of obesity[27]. Additionally, signaling pathways in neural or peripheral tissues downstream of leptin may be affected.

The mechanism of leptin resistance in humans remains cryptic, but recently described combination therapies with the peptide amylin are promising for the treatment of obesity[28,29]. Additionally, leptin is used in the clinic for treatment of the fat deficiency seen in lipodistrophy, and may potentially be used for hypothalamic amenorrhea[30,31]. Further understanding of leptin physiology and resistance may help in the development of novel therapeutics. Thus, a more thorough characterization of the physiology of leptin production, biodistribution, and function is of central importance to the understanding of fat homeostasis and obesity in modern man.

1.2 Leptin and Leptin Receptors (ObR)

Leptin circulates in mice and humans as a 146 amino acid protein of approximately 16 kDa[32]. The crystal structure of leptin revealed that it is a four-helix bundle with structural homology to long chain cytokines such as LIF, IL-6, and hGH (Figure 1)[33]. The lone post-translational modification is a disulfide bond between C96 and C146. Although no high-resolution structure of leptin receptor has yet been reported, its extracellular domain is a class I cytokine receptor, with sequence homology to the extracellular gp130 subunits of the IL-6, G-CSF, and LIF receptors. The extracellular

portion of leptin receptor is common to all isoforms, and consists of two cytokine receptor homologous domains (CRH1), an IgD like domain, and two fibronectin type III domains (Figure 2). Based on extensive mutagenesis and homology modeling, Peelman et al. have proposed a plausible model of leptin binding to leptin receptor in which signaling is activated in a 2:4 leptin:leptin receptor complex[34]. However, not all evidence supports this model[35], and in the absence of further structural information the true mechanism of leptin:leptin receptor binding will remain obscure.

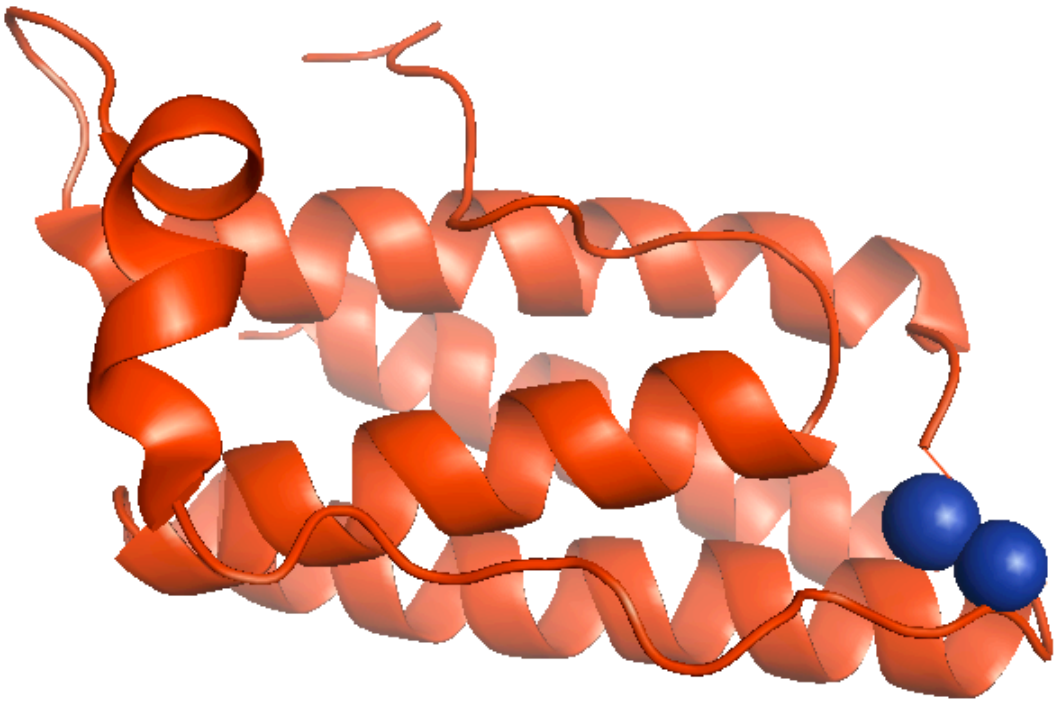

Figure 1. The crystal structure of leptin. The disulfide bond between C96 and C146 is indicated in blue. The protein is a four helix bundle with homology to other cytokines such as IL-6.

Leptin receptor is expressed as several different isoforms, with varying transmembrane and intracellular domains (Figure 2). By far the best characterized is ObRb, which is the longest of the isoforms, and is abundantly expressed in the hypothalamus. Abnormal splicing of the intracellular domain, causing a functional replacement of ObRa for ObRb, is the mutation underlying the obesity seen in the *db* mouse[16]. ObRb has a juxtamembrane segment which binds the JAK2 kinase, and two tyrosine residues (985 and 1138) which can be phosphorylated by this kinase (Figure 2). ObRb also activates STAT3, MAPK, PI3K, and AMPK downstream of JAK2[36]. The short isoforms, ObRa, ObRc, ObRd, and ObRf, lack the full signaling capacity of this receptor[37,38]. ObRa and ObRc are highly expressed in choroid plexus and cerebral microvessels, suggesting that they may function in transporting leptin into the CNS, although this has not been proven[39,40]. ObRe lacks a transmembrane domain altogether, and circulates in the bloodstream where it binds to leptin, possibly modulating the half life of the hormone[41-43].

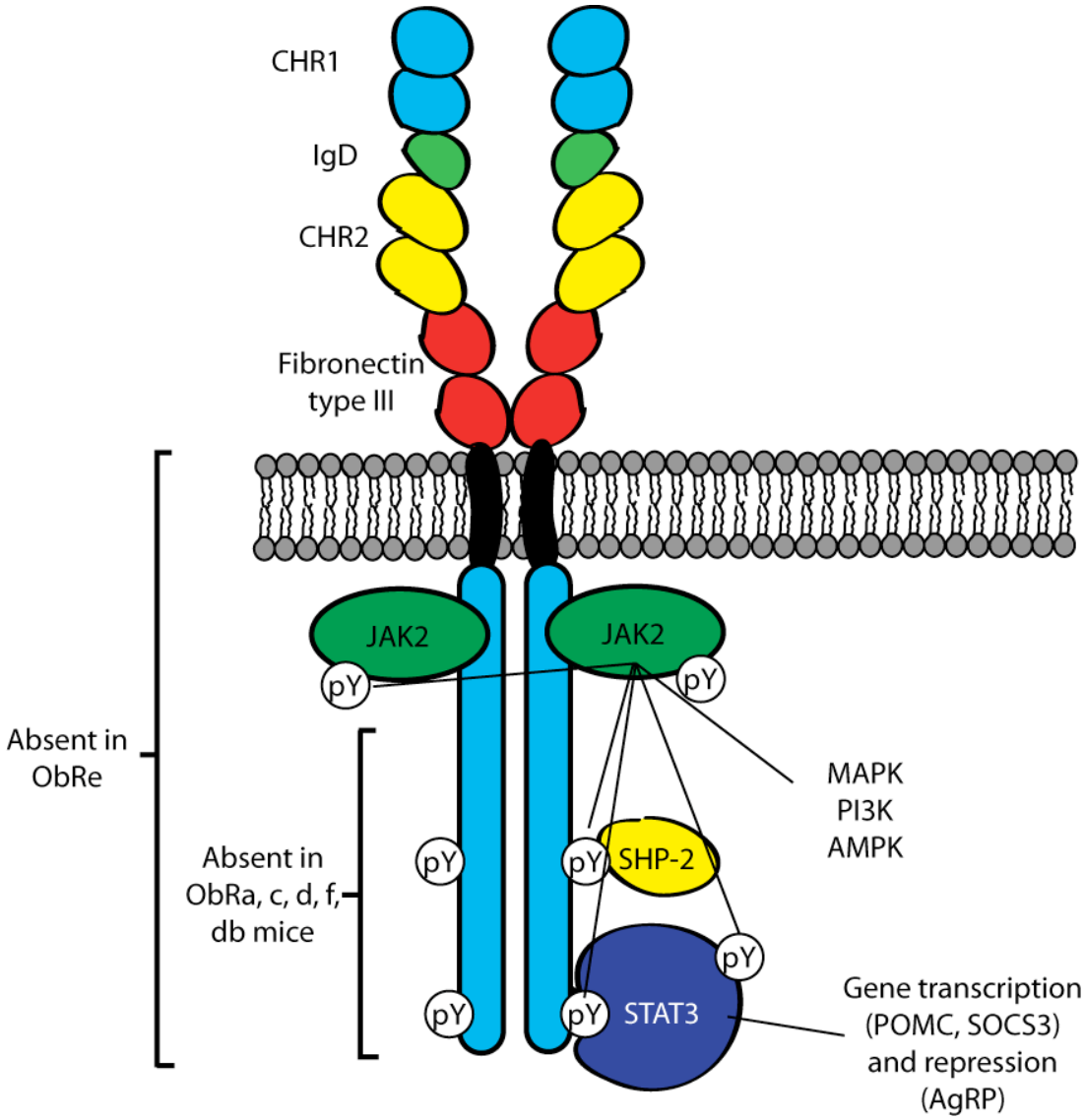

Figure 2. Simplified diagram of leptin receptor, long isoform (ObRb). Leptin binding to the IgD and CHR2 domains of the extracellular portion of the receptor drives recruitment of JAK2 to the juxtamembrane segment of the receptor. JAK2 then trans-phosphorylates the JAK2 associated with another receptor subunit, as well as STAT3, SHP-2, and other substrates. Engagement of the receptor by leptin drives gene transcription and repression via STAT3 and also activates MAPK, PI3K, and AMPK pathways. The figure represents full length ObRb, while ObRa, c, d and f lack the intracellular domain (with the exception of the JAK2 juxtamembrane binding segment), and ObRe lacks both the transmembrane and intracellular regions.

A variety of other non-ObR leptin-binding proteins have been described. For example, leptin binds to siglec-6, a sialic acid binding lectin abundantly expressed on the

placenta[44]. Additionally, leptin may bind to and be inactivated by C-reactive protein (CRP)[45], although the results and conclusions of this study are controversial[46-48]. Leptin also binds to α-2 macroglobulin, an abundant serum protein, with an apparent affinity of 2 μM[49]. Finally, leptin binds to megalin, a receptor abundantly expressed on kidney tubules[50]. Remarkably, the physiological significance of these binding partners, as well as most of the isoforms of the leptin receptor, remains unknown.

1.3 Leptin action and binding in the CNS and in the periphery

Several lines of evidence support the concept that leptin signaling in the CNS is both required and sufficient to produce many of leptin's effects[51]. Firstly, an ObR gene deletion in neurons in mice was sufficient to produce a syndrome nearly identical to that of total leptin receptor deficiency[18]. Secondly, the reintroduction of ObRb in neurons rescues the obese phenotype seen in *db* mice.[52] Thirdly, direct injection of leptin into the CNS is much more potent at inducing its effects than peripheral injection[53]. Fourthly, lesions of the hypothalamus are sufficient to produce syndromes of hyperphagia and obesity[54]. Finally, many leptin resistant animal models have defective leptin signaling in the hypothalamus[27].

There are two well-characterized populations of leptin-responsive neurons in the arcuate nucleus of the hypothalamus. The first produces two potent orexigenic peptides, agouti-related peptide (AgRP) and neuropeptide Y (NPY). These AgRP neurons are inhibited by leptin, and ablation of this population causes life threatening hypophagia[55]. The other population of neurons, which produce pro-opiomelanocortin (POMC), is activated by leptin. POMC is cleaved by proteases to generate a variety of peptides

termed melanocortins[56]. These POMC-derived melanocortins are agonists for melanocortin G-protein coupled receptors (principally MC3R and MC4R in the CNS), while AgRP is an antagonist at these receptors[57]. The AgRP and POMC neurons project to neurons expressing MC3R and MC4R in the lateral hypothalamus and paraventricular nucleus, which in turn produce a variety of downstream mediators of leptin action. Thus, leptin acts simultaneously on two populations of neurons, activating AgRP neurons, while inhibiting POMC neurons. The net effect of this program is to activate the central melanocortin signaling system, which causes anorexia and energy expenditure[19,56,58].

While the direct action of leptin on the CNS is clearly required for its physiological outputs, strong evidence for direct peripheral actions of leptin has also accumulated (fig 3). ObRb mRNA is transcribed in several peripheral tissues, including pancreas[59], lung[37], kidney[37,60], placenta[61], adrenal glands[60], T lymphocytes[62], hematopoietic stem cells[63], endothelial cells[64], fat[65], and bone[65]. Furthermore, leptin administration in rats induces STAT3 phosphorylation in fat, muscle, and liver[66]. However, these data must be approached with caution as they do not exclude an indirect effect through the CNS, acting through similar downstream signaling mediators. Nevertheless, the presence of leptin receptor RNA, coupled with evidence of activation of signaling downstream of this receptor, strongly suggests that leptin acts directly on peripheral tissues.

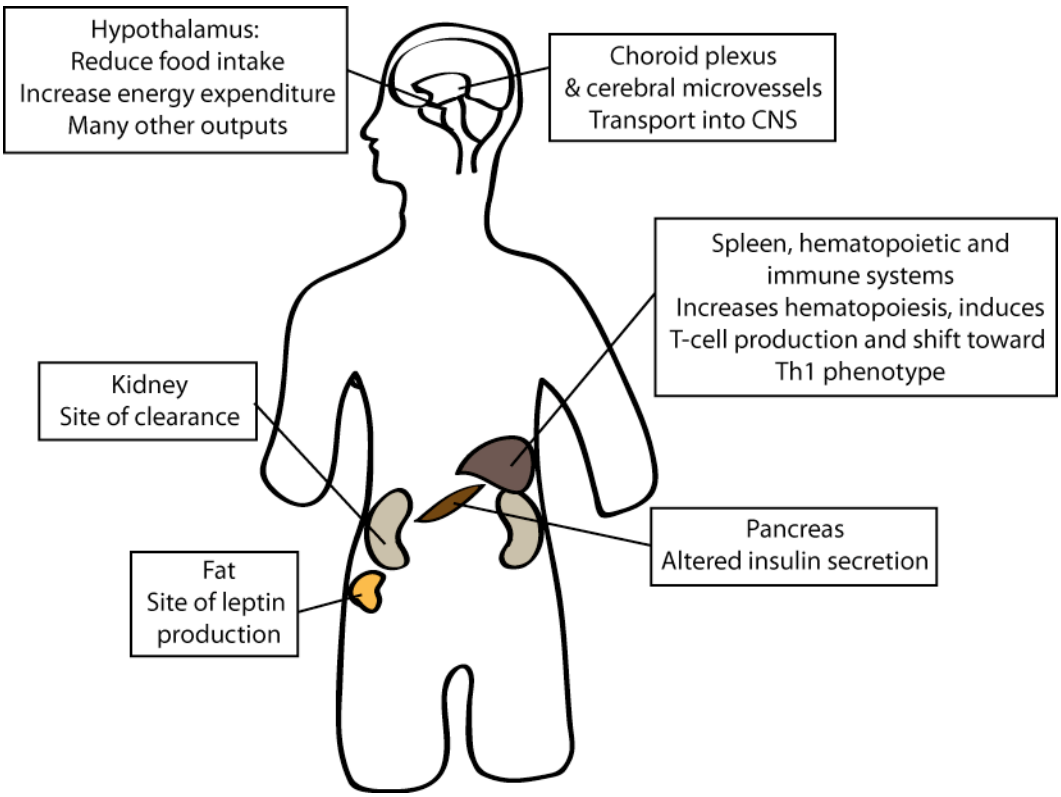

Figure 3. A simplified summary of peripheral and central actions of leptin.

The specific physiological effects of leptin on peripheral tissues have also been investigated (Figure 3). A tissue specific gene deletion of leptin receptor in the pancreas resulted in enhanced early phase insulin secretion, which was attenuated by high fat diet, suggesting that leptin modulates islet β-cell function[67]. Leptin also has direct effects on immune cells *in vitro*: it shifts T-cells towards a Th1 phenotype[62] and stimulates T-cell proliferation[68]. Ob mice are resistant to the development of autoimmune disease[69], and have defective cell mediated immune systems[62], suggesting that leptin plays a permissive role in regulating the immune system *in vivo*. Furthermore, leptin, acting in concert with parathyroid hormone, may stimulate fetal lung to produce surfactant[70]. In adipose tissue, leptin may signal in a paracrine manner, which is suppressed in leptin resistant diet

induced obese mice[71,72]. The physiological function of leptin signaling in adipose tissue is not yet understood, but may include increased lipolysis and glucose utilization[73]. In the placenta, which is itself a source of leptin, the hormone induces the release of pro-inflammatory cytokines[74]. In muscle, leptin stimulates the phosphorylation of AMPK, increasing fatty acid oxidation, an effect that may be mediated in part by direct action on the muscle tissue[75]. Leptin may also act as an angiogenic factor *in vivo* by directly activating the proliferation of endothelial cells[64]. Thus, it is clear that in addition to the well established role of leptin in regulating food intake and energy expenditure in the hypothalamus, the hormone also directly modulates the physiology of peripheral organs. Collectively, leptin appears to signal the nutritional and energy status of the organism to peripheral tissues. A reduction of leptin, such as would be seen during starvation, alters the function of peripheral organs so as to conserve energy, and downregulates non-essential functions.

The binding of leptin to sites in the CNS and in the periphery has also been studied extensively. In this analysis, animals are sacrificed, and tissue sections are prepared. Radiolabeled leptin can then be bound to the sections, and visualized using autoradiography. Due to the fixation process, this analysis allows for visualization of both extracellular and intracellular leptin receptors. The initial cloning of leptin receptor was accomplished following autoradiographic localization of leptin binding in the choroid plexus, and subsequent expression cloning from a choroid plexus cDNA library[15]. This binding pattern was subsequently replicated by several other groups[76-78]. In the brain, leptin binds to various nuclei in the hypothalamus, including the arcuate, paraventricular, and ventromedial nuclei[79,80]. High affinity binding sites in the medulla of the kidney have

also been identified[81]. Leptin binding sites were also identified in the adrenal medulla[82]. In a particularly thorough study, Dal Farra et al. characterized leptin binding sites in mice at several stages of development[83]. Binding was found in the lung, digestive tract, liver, kidney, cartilage, spleen, and in the choroid plexus. Taken together, these experiments show that leptin binds to ObR in peripheral and central tissues, where it activates signaling, producing a diversity of outputs to regulate energy homeostasis, as well as to conserve energy in times of starvation.

1.4 The application biodistribution studies to leptin

One approach to integrate the enormous amount of data on the divergent functions of leptin would be to study the biodistribution of the hormone in live animals. This methodology could confirm the validity of studies of leptin activity and ex vivo binding in various peripheral or central tissues, as well as discovering new functions of the hormone in an unbiased approach. Additionally, specific hypotheses about the molecular identity of leptin binding partners or transporters could be assessed using appropriate animal models.

Before the development of high resolution *in vivo* imaging technology, the method traditionally used to assess these parameters was biodistribution analysis. In this technique, a radiolabeled tracer is injected into an animal, and after a predetermined period of time, the animal is sacrificed, and the radioactivity in various tissues counted. These data complement tissue binding and mRNA expression data (section 1.3), as they account for a physiological pattern of cell surface receptor expression. By far the most commonly used tracer for this purpose is ^{125}I-leptin. ^{125}I-leptin has been used for the

purpose of studying leptin half-life and clearance in mice, rats, and rhesus monkeys. The half-life of leptin has been found to follow bi-exponential decay, which presumably represents rapidly cleared free leptin, and more slowly cleared leptin bound to circulating receptors (mainly ObRe). The first phase half-life is very fast, under 10 minutes in rats, while the second phase is about one hour[84-86]. These and other studies also revealed that leptin was cleared from the circulation by the kidney, as expected for small polypeptides[50,87-90]. This is consistent with the fact that human patients with end-stage renal disease have relative hyperleptinemia when the values are corrected for their BMI[91]. In addition to binding in the kidney and choroid plexus, one study also suggested that leptin was taken up in the bone marrow in mice[92].

Leptin transport into the CNS has also been extensively studied using biodistribution methodology. A saturable, low capacity transport system into the CNS has been defined in cerebral microvessels by using ^{125}I leptin[17]. However, the transporter responsible for this phenomenon has not yet been identified. While ObRa is abundantly expressed at the capillary endothelium and choroid plexus[78], and is able to transcytose leptin in cell lines[93], isolated brain preparations from rats lacking ObR have identical transport rates compared to normal rats and mice[40,94] . Thus, the commonly cited observation that mice and rats lacking ObR have reduced transport of leptin into the brain is likely an artifact of the compensatory high levels of leptin in these animals[39,95]. The identity of this molecular transporter is crucial to understanding leptin resistance, as reduced transport of leptin into the CNS has been proposed to underlie leptin resistance seen in obese humans[26].

1.5 *In vivo* imaging methodologies and application to leptin

A live animal imaging approach has advantages over the classical biodistribution approach in studying leptin biology. In particular, quantitative kinetic information of uptake in various organs can be readily obtained, and probes can be readily translated into studies in nonhuman primates and into the clinic. To date there have been two live animal imaging studies of leptin biodistribution, in different contexts. Karonen et al. studied the biodistribution of ^{123}I labeled leptin in rabbits using dynamic gamma imaging[96]. In this study, the authors saw uptake in the lungs, kidney, liver, and choroid plexus. However, the relatively low resolution of the images makes the conclusions difficult to verify and interpret. McCarthy et al. labeled leptin with the positron emitting isotope ^{68}Ga using the chelator diethylene triamine pentaacetic acid (DTPA)[97]. They subsequently imaged the biodistribution of leptin when injected into the intrathecal space in baboons using positron emission tomography (PET). In this study the authors found that the intrathecally injected leptin moved rostrally to the cranium, but that there was considerable variation in the three animals tested. Thus, to date there has been no comprehensive study of leptin biodistribution using *in vivo* imaging technologies.

Several live animal imaging approaches could be used to study leptin biology. In principle, fluorescence, bioluminescence, magnetic resonance imaging (MRI), and positron emission tomography (PET) could readily be applied to studying leptin biology. For example, a fluorescently labeled leptin derivative could be imaged *in vivo* or a leptin derivative labeled with gadolinium could be imaged using MRI. However, in comparing the available imaging technologies for this purpose, positron emission tomography (PET) has several advantages (table 1)[98]. It has the highest sensitivity of currently available

imaging techniques, while still retaining excellent spatial resolution, and ease of quantification. Additionally, PET can be readily translated into large animal systems and into the clinic. Thus, we chose to study leptin biodistribution using PET.

Imaging modality	Form of energy	Spatial resolution	Sensitivity	Quantification	Organism
Fluorescence	Visible/NIR	2-10 mm	+++	low	mouse
Magnetic resonance (MRI)	Radio wave	sub mm	+	medium	mouse, primate, human
Bioluminescence imaging	Visible/NIR	3-10 mm	variable	low	mouse
Positron emission tomography (PET)	Annihilation photons	1-10 mm	++++	high	mouse, primate, human

Table 1. A comparison of live animal imaging techniques. Adapted from Levin, C.S., *Eur. J. Nucl Med. Mol. Imaging*[98].

1.6 Technical aspects of PET tracer development: Isotopes, labeling chemistries

Positron emission tomography requires that the tracer of interest be labeled with a positron emitting isotope. Positron emitting isotopes, such as ^{18}F or ^{64}Cu, are intrinsically unstable and decay, producing positrons, which travel a short distance in tissue before finding their antiparticle, the electron. When positron/electron pair collide, they annihilate, producing two antiparallel photons of 511 keV. These photons are subsequently counted by a detector. Following various corrections to account for scattering effects, an image can be reconstructed with excellent spatial resolution (in the 1-2 mm range). Careful design of a tracer is crucial to obtaining high-resolution images that correspond to the authentic biodistribution[99].

Probably the single most important decision regarding PET tracer development is isotope selection. An variety of isotopes are currently available (table 2) with differing properties[100]. The half-life of an isotope is an important parameter, as in practice any labeling technique which cannot be accomplished in 3 half-lives of the isotope is unlikely to be successful. Thus, very short -lived isotopes such as ^{15}O and ^{13}N are not used frequently. A second important feature is the percentage of positrons emitted by an isotope: other modes of decay can confound the imaging results and produce undesirable radiation exposure. Additionally, the energy of the positron emitted (Bmax) limits the resolution of the image obtained, as high energy positrons undergo various scattering events prior to annhilation[101]. The final factor regarding isotope selection is the method of generation, either via cyclotron, generator, or reactor. Cyclotrons are relatively common in nuclear medicine, radiology, and oncology departments due to the popularity of ^{18}F -fluorodeoxyglucose (FDG), the most commonly used PET tracer. Nuclear reactors will remain rare due to safety considerations. A generator is a smaller device containing a fixed amount of a parent isotope, which decays continually, to a positron emitting isotope of shorter half-life. Thus, the generator produces a constant supply of a desired isotope, which can be used approximately every 3-4 half-lives. Based on the considerations of half -life, resolution, and method of production, ^{18}F has emerged as the leading isotope for PET, with ^{11}C being nearly as widely used for small molecule tracers. Other isotopes are more commonly used for specialized applications- for example radiometals are widely used for peptide and protein labeling (see below)[102].

Isotope	Half-life	Bmax (positron energy, MeV)	Percent positron emission	Production method
11C	20.5 min	0.96	100	cyclotron
13N	9.97 min	1.2	100	cyclotron
15O	122.2 sec	1.73	100	cyclotron
18F	109.8 min	0.63	99	cyclotron
64Cu	12.8 hours	0.65	18	cyclotron
68Ga	68.3 min	1.92	89	generator
76Br	15.9 hours	3.94	54	cyclotron
86Y	14.7 hours	3.14	34	cyclotron
124I	4.17 days	2.14	23	cyclotron

Table 2. Commonly used positron emitting isotopes.

PET radiochemistry is fundamentally similar to organic/inorganic chemistry, but has several key differences. Firstly, owing to the short half-life of the isotopes, the labeling must be performed rapidly. Secondly, the reactions must be performed at trace or "no-carrier added" level: 10 MBq of ^{18}F, a typical dose injected into a mouse in a PET experiment, is only 200 fmol of the isotope. Thus, in practice not all reactions are applicable to PET radiolabeling. Finally, positrons produce highly energetic, penetrating gamma rays, which for safety reasons require extensive shielding and precautions.

The generation of a high quality PET tracer requires that several design considerations be observed. Firstly, the tracer itself must be chemically and biologically similar to the normal, unmodified molecule which it is attempting to mimic. Frequently, for small molecular tracers, it is possible to generate a tracer with no changes made to the intact structure of the molecule. However, this is not always possible, and the case of

peptide and protein labeling, nonnative prosthetic reactive groups must be installed[103]. Therefore, it is crucial to test if a modified tracer retains its biological activity. This is generally accomplished by generating a "cold" version of the molecule in which the positron-emitting isotope is replaced with the naturally occurring one, and testing its activity in various biological assays. Finally, the specific activity (defined as the amount of radioactivity in Curies or Becquerels per mole) determines which interactions can be visualized. If the tracer has low specific activity, a large molar amount of tracer must be used to enable visualization, potentially saturating the binding sites which are to be studied[104]. However, with careful selection of isotope, labeling site, conjugation chemistry, and technique, high quality, high specific activity positron emitting tracers can, in principle, be generated with biological activity intact.

1.7 Chemical and radiochemical aspects of protein labeling for PET imaging

Proteins are both particularly desirable and challenging targets for labeling with positron emitting isotopes. The challenge of labeling them arises from the fact that there is no generally applicable method for radio-conjugation without destroying their activity, and that since they generally produce their effect *in vivo* with high affinity (typically low nanomolar), the labeled tracer must have very high specific activity. Furthermore, proteins can not generally be exposed to extreme conditions, such as high temperature, microwave heating, or treatment with organic solvents since these will denature them. Thus, protein labeling with positron emitting isotopes is generally accomplished with robust reactions which can proceed at lower temperatures.

The most commonly used technique for labeling proteins with positron emitting isotopes is the chelation of radiometals, such as ^{68}Ga and ^{64}Cu[102,105]. This can be accomplished by appending a chelator to the protein and subsequently complexing the modified protein with the radiometal of interest. By far the most commonly used chelator for this purpose is 1,4,7,10-tetraazacyclododecane-1,4,7,10-tetraacetic acid (DOTA)[106]. A wide variety of metals, such as the postiron emitting ^{64}Cu or ^{68}Ga, can be incorporated, and the metal complexes formed with this chelator are stable over the course of days in live animals. Furthermore, DOTA derivatives for labeling lysine and cysteine side chains are commercially available. Thus, DOTA, and other metal chelators such as diethylene triamine pentaacetic acid (DTPA) are widely used for protein labeling with positron emitting isotopes.

Radiohalogens are the second most frequently used nuclides for postiron emitting isotope labeling of proteins. ^{124}I, ^{75}Br, ^{76}Br, and ^{18}F are all positron emitters with useful half lives. Iodine and bromine isotopes can be installed using conventional radiohalogenation chemistry, for example using Chloramine-T, Iodogen, or enzymatic peroxidases[107]. However, the low percentage of positrons emitted and high energy of those positrons emitted by these isotopes (table 2) results in low quality images in a micro-PET setting. Owing to the favorable imaging properties of the isotope, ^{18}F labeling of peptides and proteins is particularly desirable. However, standard radiohalogenation chemistry is not applicable, as synthesis of ^{18}F-F_2 can only be accomplished in the presence of carrier, resulting in very low specific activity. Nucleophilic $^{18}F^-$ is highly unreactive in water due to solvation, and thus cannot be directly installed on proteins via currently available techniques. Recently, promising methods for one step labeling of

small molecules and peptides have been developed based on the incorporation of boronic acids or organosilicon, and treatment with fluoride anion in organic solvents[108,109]. At present, these techniques are not applicable to protein labeling due to the requirement for organic solvents[109], or very high concentrations of the reactive precursor[108]. Thus, ^{18}F is currently conjugated to proteins using multistep reactions, in which ^{18}F is first introduced into an organic reactive group which is subsequently conjugated to the protein of interest[110,111]. Due to the optimal imaging properties of ^{18}F these labeling methodologies are an area of intense interest in the field of radiochemistry. The currently available techniques for peptide and protein radiofluorination, as well as our own developments in this area will be covered in chapter 2.

Chapter 2. Design, synthesis and characterization of ^{18}F and ^{68}Ga labeled leptin tracers

2.1 Labeling of proteins for PET and design considerations for isotopic labeling of leptin

PET has emerged as a powerful tool for *in vivo* imaging in clinical medicine as well as in basic research. PET imaging is complementary to other *in vivo* imaging techniques such as single photon emission computed tomography (SPECT), fluorescence imaging, bioluminescence imaging, and magnetic resonance imaging (MRI), and in particular it offers good resolution, high sensitivity, ready translation to clinical studies, and ease of quantification[98,99,112]. PET requires that a probe of interest be labeled with a positron emitting nuclide, such as ^{18}F, ^{11}C, or ^{68}Ga[100]. ^{18}F is a particularly desirable radionuclide for PET imaging owing to its intermediate half-life of 109.7 minutes, its routine availability by biomedical cyclotron production, and the high resolution of images obtained. Proteins and peptides are widely used tracers in PET and a variety of techniques, principally based on the incorporation of radiometals, have been developed to label them[102]. The interest in peptide imaging and the superior imaging properties of ^{18}F has led to the development of several approaches for labeling synthetic peptides with this isotope[109-111,113-121]. Protein labeling using ^{18}F synthons targeting lysine[122-125] residues has also been developed and applied to a variety of substrates. However, in contrast to the aforementioned peptide labeling approaches, these protein labeling techniques give rise to a variety of labeled products, and it is difficult to characterize the structure or function

of the tracer. Site-specific labeling of proteins is particularly desirable as it allows unambiguous biophysical and activity-based characterization of a homogeneous product, leading to reproducibility in labeling and imaging[126,127]. Accordingly, the generation of site-specifically labeled proteins for molecular imaging has become an area of active research[126]. Recently, site-specific ^{18}F labeling of proteins on unique cysteine residues has also been described[128-132]. These site-specifically radiolabeled proteins are promising reagents for molecular imaging for biodistribution studies in model animals as well as in the clinic.

In order to study leptin biodistribution using PET, we developed two complementary labeled tracers, which we term ^{18}F-FBA-leptin and ^{68}Ga-DOTA-leptin. While no high resolution crystal structure of a leptin-leptin receptor complex has been reported, mutagenesis studies have established the residues of leptin which are required for both receptor binding and activation[34,133,134]. The lysine residues of the protein, and both the C and N termini of the molecule, are mainly distributed elsewhere on the structure from the receptor binding region[33,135]. We therefore rationalized that either an amine-directed or a site-specific C-terminal labeling strategy would produce a labeled leptin derivative with unaltered bioactivity (Figure 4). Thus, we have developed an amine-directed labeling method for ^{68}Ga labeling using the chelator DOTA, and a site-specific ^{18}F labeling method using a two step expressed protein ligation/oximation protocol.

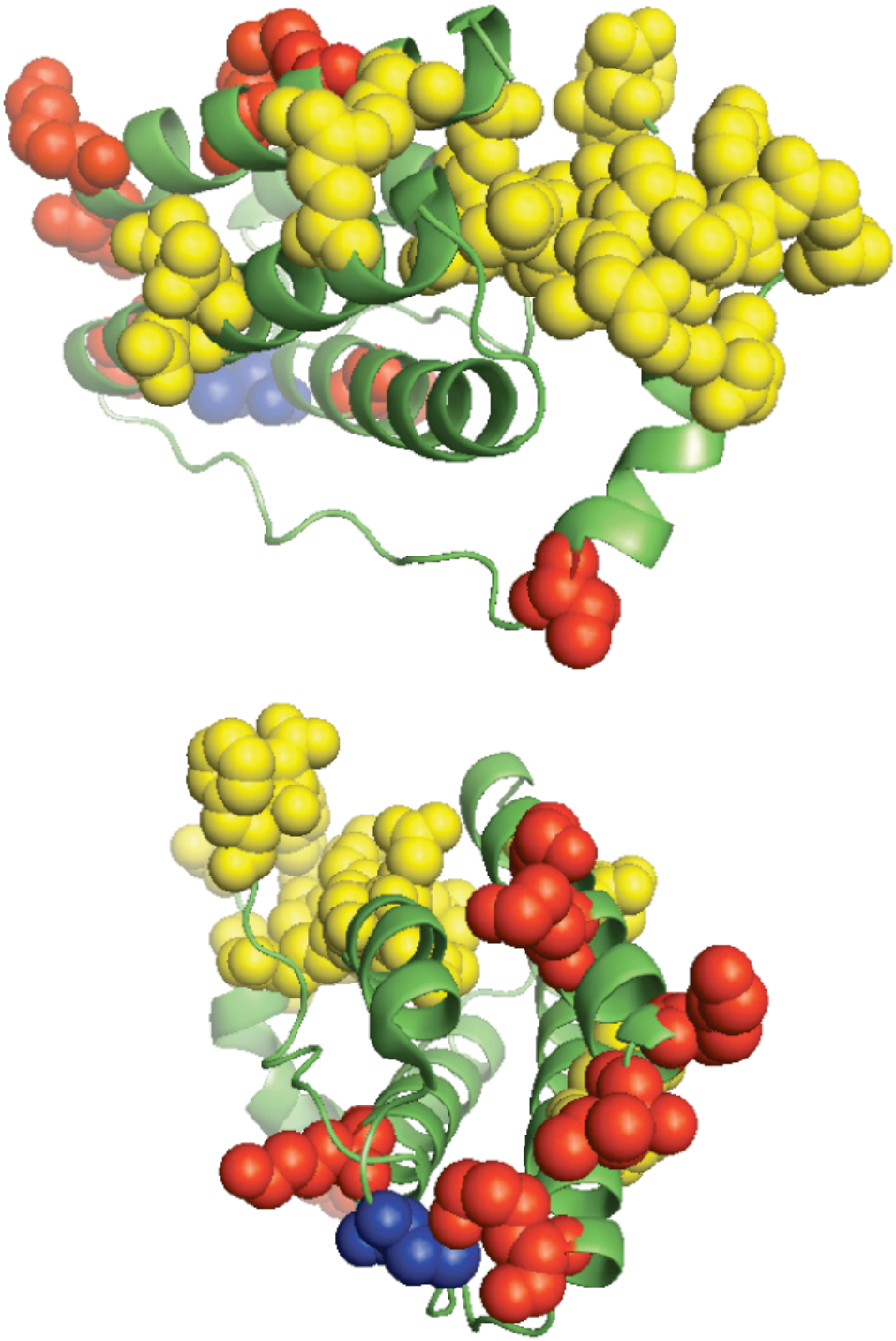

Fig 4. Design, synthesis, and biological activity of the tracers ^{18}F-FBA-leptin and ^{68}Ga-DOTA-leptin. Two views of the structure of leptin (PDBID 1AX8), with side chains rendered as spheres for residues which are known to be required for ObR binding (yellow). The potential labeling sites for ^{68}Ga-DOTA-leptin (lysine side chains and the N-terminus) are rendered as red spheres, while the C-terminus, the labeling site of ^{18}F-FBA-leptin, is rendered as a blue sphere.

2.2 Development of ^{68}Ga-DOTA-leptin

Radiometallation of proteins is a widely used technique in radiochemistry, with ^{68}Ga and ^{64}Cu being the most commonly used postiron emitting isotopes for labeling[102]. ^{68}Ga is obtained from a ^{68}Ge generator, making it an attractive method for labeling. ^{68}Ga labeling of a protein was first reported in 1975 with an albumin labeling strategy[136], and the key findings of this study remain the crucial guidelines for ^{68}Ga labeling today - ^{68}Ga labeling is optimal at acidic pH (2.5-4.5) due to the formation of insoluble $Ga(OH)_3$ complexes at higher pH, and must be accomplished rapidly due to the short 68 minute half life. The development of the high affinity chelators diethylene triamine pentaacetic acid (DTPA) and 1,4,7,10 tetraazacyclododecane-1,4,7,10-tetraacetic acid (DOTA) allowed more practical and extensive use of this isotope, owing to the inertness and stability of the chelated metal complexes[106,137,138]. DOTA chelates gallium via a hexadentate interaction in which the metal is coordinated axially by two nitrogens and two opposite carboxylates, and equatorially by the remaining two nitrogens[139]. Recently ^{68}Ga-DOTA labeled peptides have become popular for use in PET and biodistribution studies, and are promising reagents for use in clinical diagnosis[104,140-143].

Thus, in order to study leptin biodistribution, we developed a lysine directed labeling approach to conjugate the isotope ^{68}Ga to leptin using the metal chelator DOTA (Figure 7a). Using DOTA-NHS, we found that the level of labeling of the protein could be controlled by varying the molar excess of DOTA-NHS used in the reaction (Figure 5). Out of eight possible labeling sites (seven lysines plus the N-terminus), we found that we could conjugate and average of one to four copies of DOTA to leptin by varying the

reaction conditions. In preliminary studies, we found that radiolabeling was most efficient using the most heavily modified tracer (data not shown). Thus, we pursued this compound, with an average of four copies of DOTA per leptin molecule (figure 7b) for use as a tracer in studying leptin biodistribution.

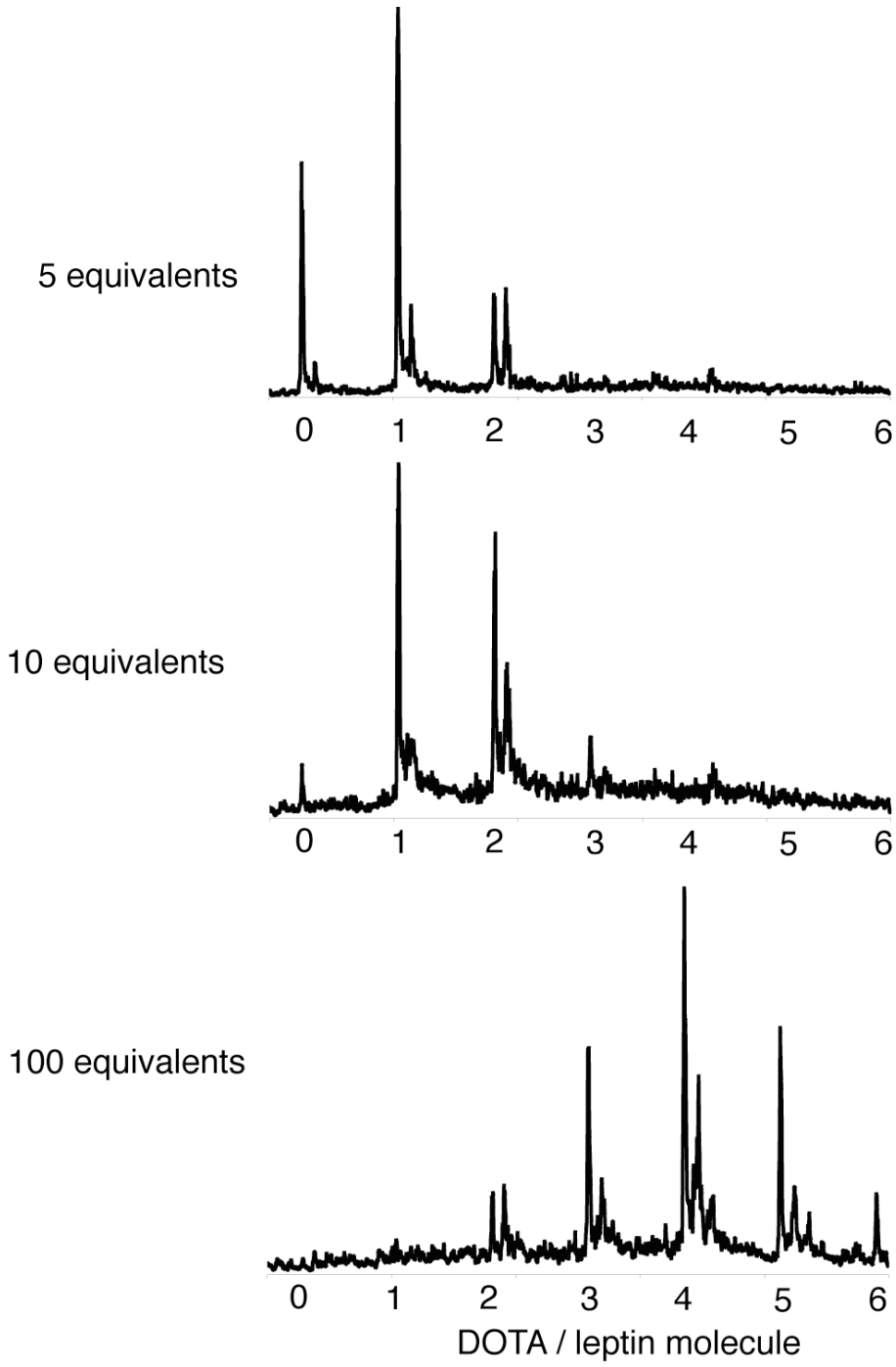

Figure 5. ESI-MS reconstructs of DOTA-NHS : Leptin conjugation reactions. All reactions were performed at pH 7.5, 5 mg/mL leptin, with the indicated number of equivalents of DOTA-NHS.

In order to verify the bioactivity of our DOTA-modified protein, its activity was tested in several assays. A cell-based assay was developed using a 293 cell line stably transfected with ObRb, and luciferase under the control of a STAT3-dependant element (Figure 6). As expected based on the design considerations (Figure 4), the ability of the modified protein to activate leptin receptor STAT3-dependant signaling was unaltered in this cell line (Figure 7c). Additionally, the ability of DOTA-leptin to induce weight loss in leptin deficient (Ob/Ob*)* mice was identical to unmodified recombinant leptin over a period of 9 days, when administered via subcutaneous osmotic pumps (Figure 7d). Thus, labeling leptin with DOTA using an amine directed labeling strategy does not alter its bioactivity.

Radiolabeling of the protein using ^{68}Ga proceeded in good yield (decay corrected yield of 25.7% ± 4.9% s.d., n = 30, specific activity of 5.5 – 11 GBq/μmol, scheme 1), affording a product that was always greater than 90% pure (Figure 7e). As expected based on the extraordinary inertness of DOTA-metal complexes, the tracer was stable *in vivo* as assessed by HPLC analysis of the serum recovered from a mouse injected with ^{68}Ga-DOTA-leptin 30' prior (Figure 7e). Finally, the ^{68}Ga labeling procedure did not abrogate receptor-binding activity, as the labeled protein bound to the aforementioned cell line expressing ObR, and the binding could be displaced by excess competing cold leptin (Figure 7f). Thus, leptin can be labeled with ^{68}Ga, preserving the biological activity of the hormone.

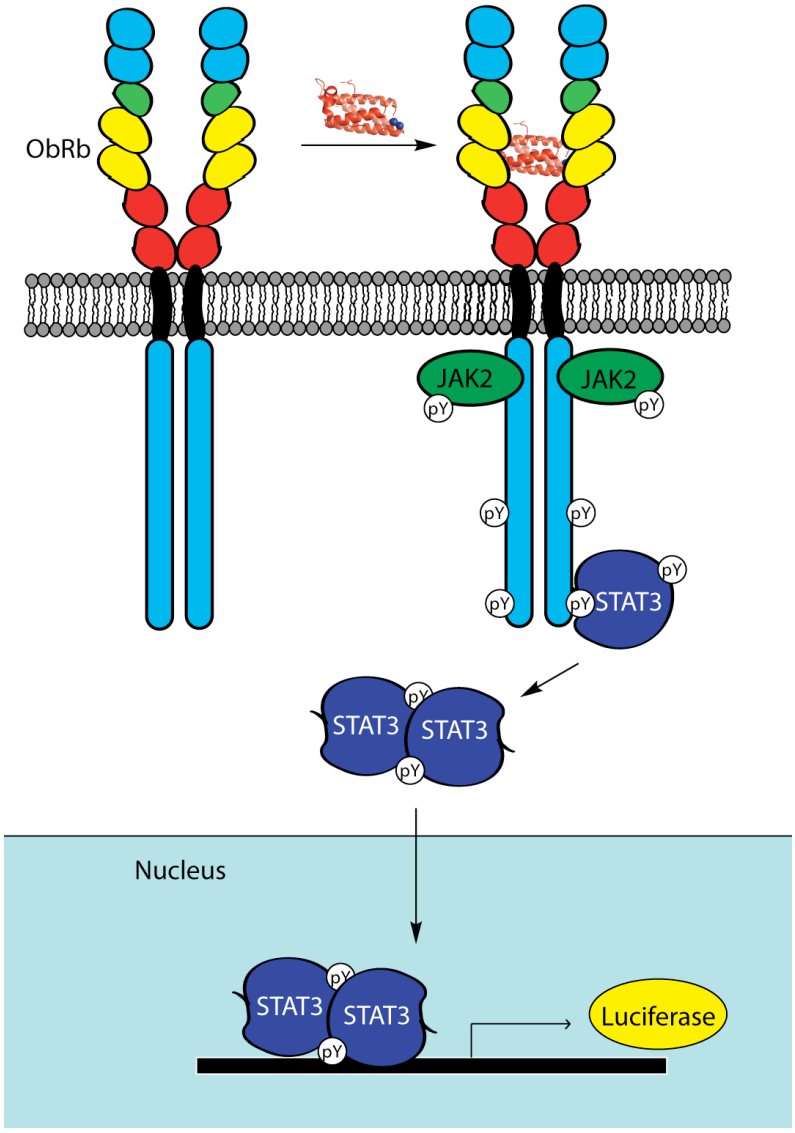

Figure 6. Schematic of ObRb-STAT3-Luciferase assay. A 293 cell line is stably transfected with ObRb and luciferase under the control of a STAT3 dependant element. In this cell line, leptin binds to and activates ObRb, which recruits JAK2 to the receptor. Phosphorylated leptin receptor subsequently recruits STAT3, which is phosphorylated by receptor-bound JAK2. Phosphorylated STAT3 dissociates from the receptor, translocates to the nucleus, where it activates luciferase gene transcription. Luciferase activity can then be quantified using a luminometer. Thus, luciferase is produced in a leptin dose-dependant manner.

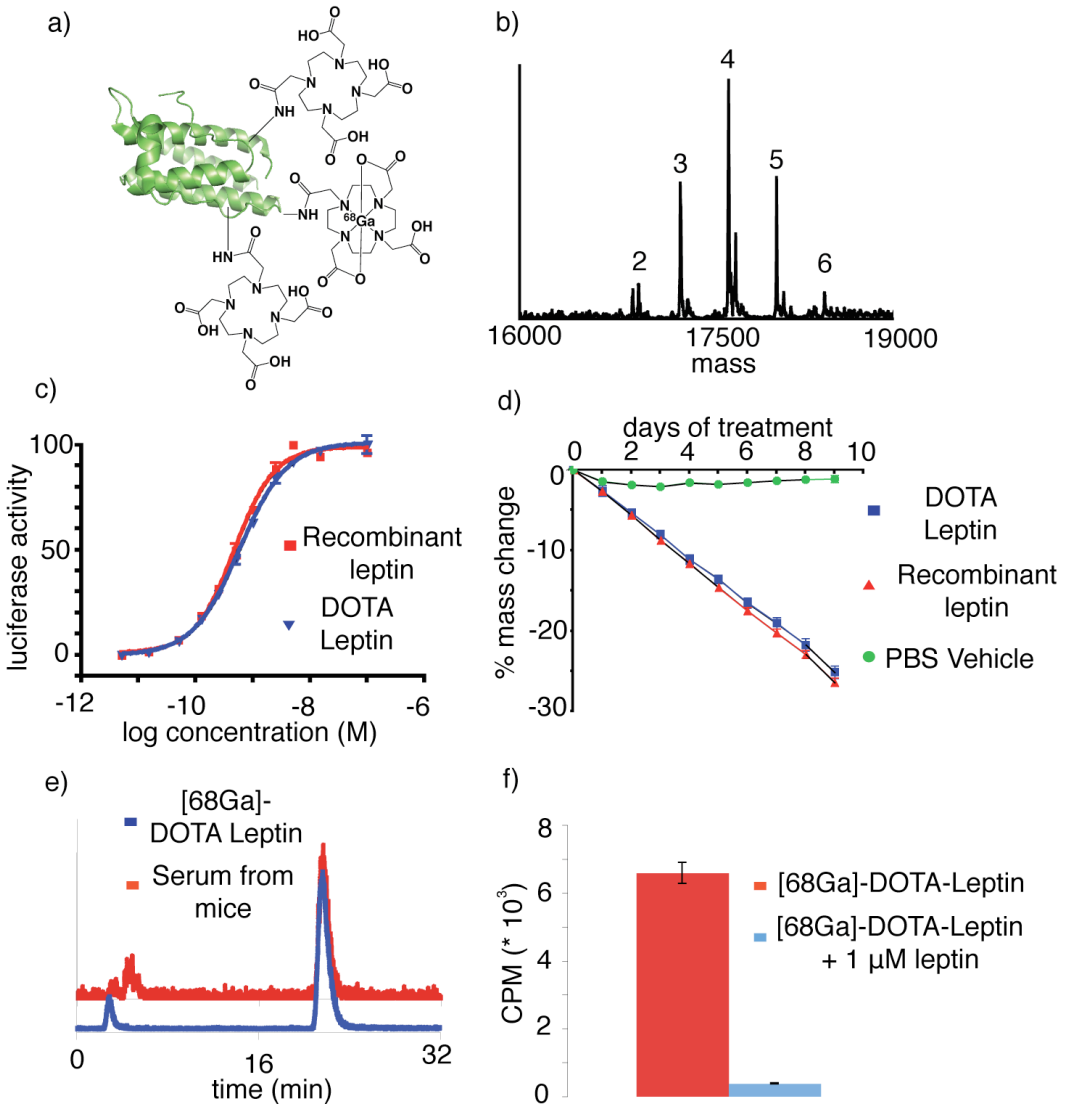

Figure 7. a) Schematic of ^{68}Ga-DOTA-leptin tracer. b) ESI-MS of DOTA-leptin revealing an average of 4 copies of DOTA per leptin molecule. c) *in vitro* bioactivity of DOTA-leptin was compared to recombinant leptin using a 293 cell line stably expressing leptin receptor (ObRb) and a luciferase reporter under STAT3 responsive element. The EC_{50} for activation was 0.42 to 0.55 nM for recombinant leptin and 0.54 to 0.66 nM (95% confidence intervals, n=2 ± s.d.) for DOTA-leptin. d) DOTA-leptin induces weight loss to a similar extent as recombinant leptin in ob/ob mice (n=4 ± s.e.m., dose = 450 ng/hr). e) Radiochemical HPLC analysis of purified ^{68}Ga-DOTA-leptin (blue) and serum recovered from a mouse 30 minutes post injection with ^{68}Ga-DOTA-leptin, demonstrating the stability of the tracer *in vivo*. f) Cell binding assay of ^{68}Ga-DOTA-leptin using a 293 cell line overexpressing ObRb, in the presence or absence of 1 µM competing recombinant leptin (n=3, ± s.d.).

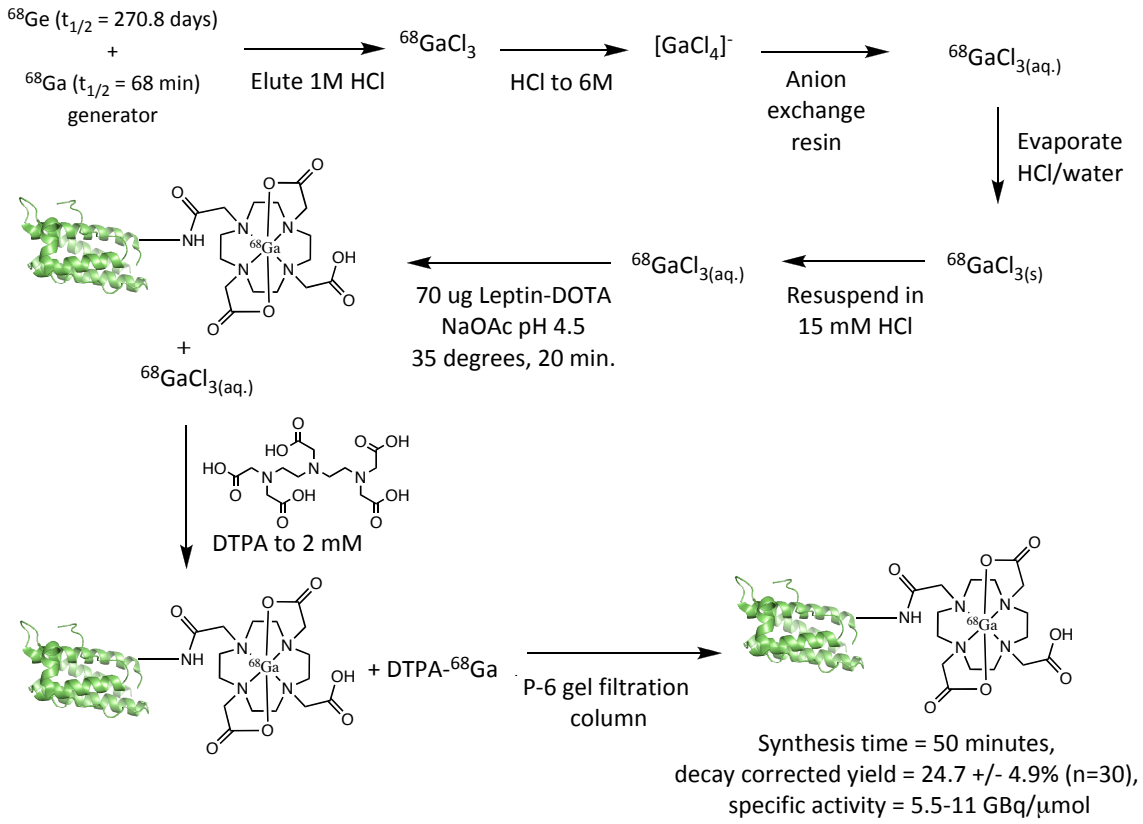

Scheme 1. Schematic of method used to label DOTA-leptin with ^{68}Ga.

2.3. Development of expressed protein ligation to site-specifically label the C-terminus of leptin

In designing a site-specific leptin ^{18}F labeling protocol, various options were considered. While in principle a cysteine directed labeling approach could produce site specifically ^{18}F labeled leptin, we found that the introduction of additional cysteines in the protein led to difficulties in refolding and protein purification (data not shown). Fortunately, the C-terminal amino acid of leptin is cysteine, which in principle would allow for direct modification of the protein using expressed protein ligation (EPL)[144]. EPL is a semisynthetic technique based on the earlier development of native chemical

ligation, in which a recombinantly expressed protein α-thioester is fused to any peptide containing an N-terminal cysteine. In native chemical ligation, an unprotected peptide with an N-terminal cysteine can react with a second peptide with a C-terminal α-thioester to form a peptide bond (Figure 8a)[145,146]. The fusion of a recombinant protein α-thioester with a synthetic N-terminal cysteine peptide was accomplished by re-engineering the process of protein splicing. In protein splicing, a protein segment termed an intein is excised out of two flanking sequences, named exteins, in a process analogous to the splicing of RNA introns (Figure 8b)[147]. This fascinating autocatalytic process has been exploited for many different purposes by our group and others. However, one of the simplest uses of protein splicing has proven to be the most versatile: by mutating the intein to prevent the formation or breakdown of the branched intermediate, the protein can be trapped in equilibrium between the α-thioester and amide forms. The mutated intein can then be cleaved by treatment with thiols, generating a recombinant protein α-thioester. The ligation of the recombinant protein α-thioester with a synthetic N-terminal cysteine peptide was first reported in 1998 (Figure 8c)[148-150], and has been termed expressed protein ligation (EPL) or, less frequently, intein-mediated protein ligation.

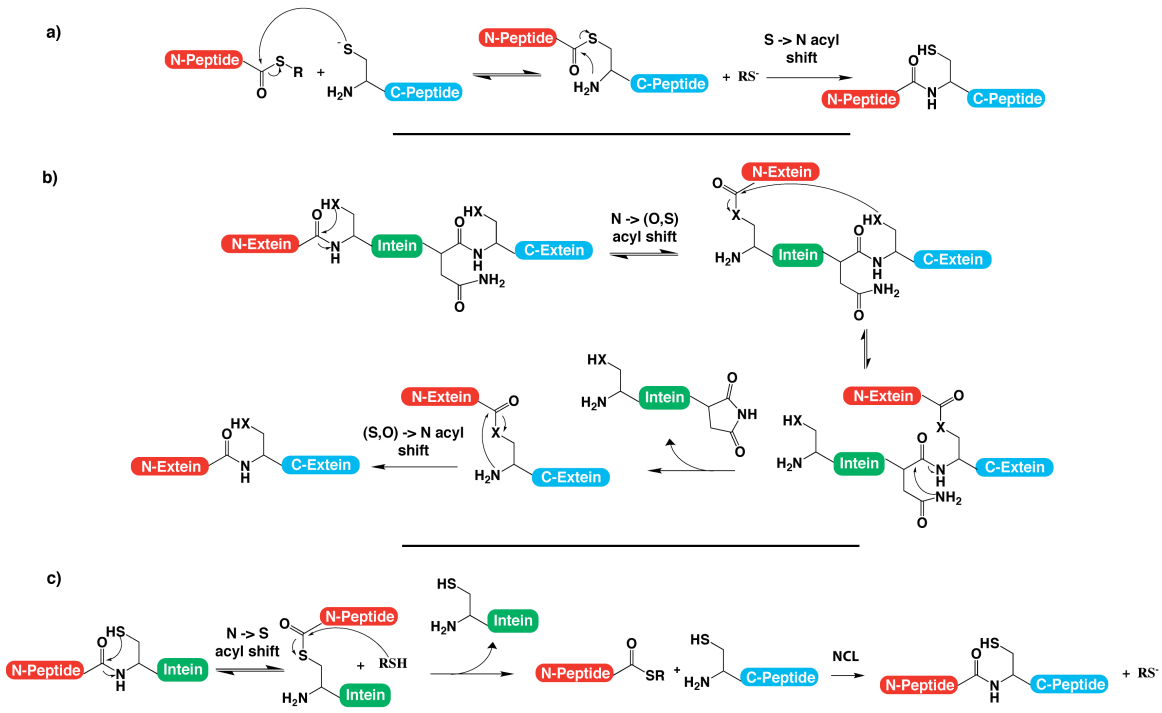

Figure 8. Mechanism of native chemical ligation (NCL) (a). In NCL, trans-thioesterification by the N-terminal cysteine is followed by an S->N acyl shift, generating a native peptide bond. Mechanism of protein splicing (b). In protein splicing, an N -> S or O acyl shift at the N-terminal residue of the intein is followed by trans(thio)-esterification to the residue C-terminal to the intein, generating a branched intermediate. The C-terminal Asn of the intein then cleaves the C-terminal intein-extein bond, generating a succinimide product, and the fused exteins undergo an (S,O)-> N acyl shift to create a native peptide bond. Mechanism of EPL (c). In EPL, a thiol is used to generate a α-thioester from a mutated intein. The α-thioester can then react by NCL with an N-terminal cysteine peptide. R = alkyl, phenyl, benzyl, $CH_2CH_2SO_3Na$. X = O, S.

Heterologous expression of leptin in *E. coli* generally requires isolation from inclusion bodies[151]. Thus, in order to generate an active intein fusion protein, we fused leptin to the GyrA intein, which can be refolded from bacterial inclusion bodies using conditions previously developed in our laboratory[152]. Unfortunately, these refolding conditions resulted in precipitation of the leptin-GyrA fusion. Thus, we tested the ability of the intein to cleave in the presence of various additives, including detergents, small

molecule additives, and chaotropes. We found that 4M urea was most effective in promoting the cleavage of the intein (Figure 9). Upon refolding in 4M urea, intein cleavage with sodium-2-mercaptoethanesulfonate allowed the preparation of the corresponding α-thioester (Figure 10). Following EPL of the α-thioester with cysteine to reconstitute full-length leptin (Figure 11a), and refolding to form the disulfide bond between Cys97 and Cys147 using reduced and oxidized glutathione as a redox couple, leptin with activity identical to recombinant commercial leptin could be produced (Figure 11b). These optimized protocols were subsequently applied to the generation of a site specifically ^{18}F labeled protein (see section 2.4).

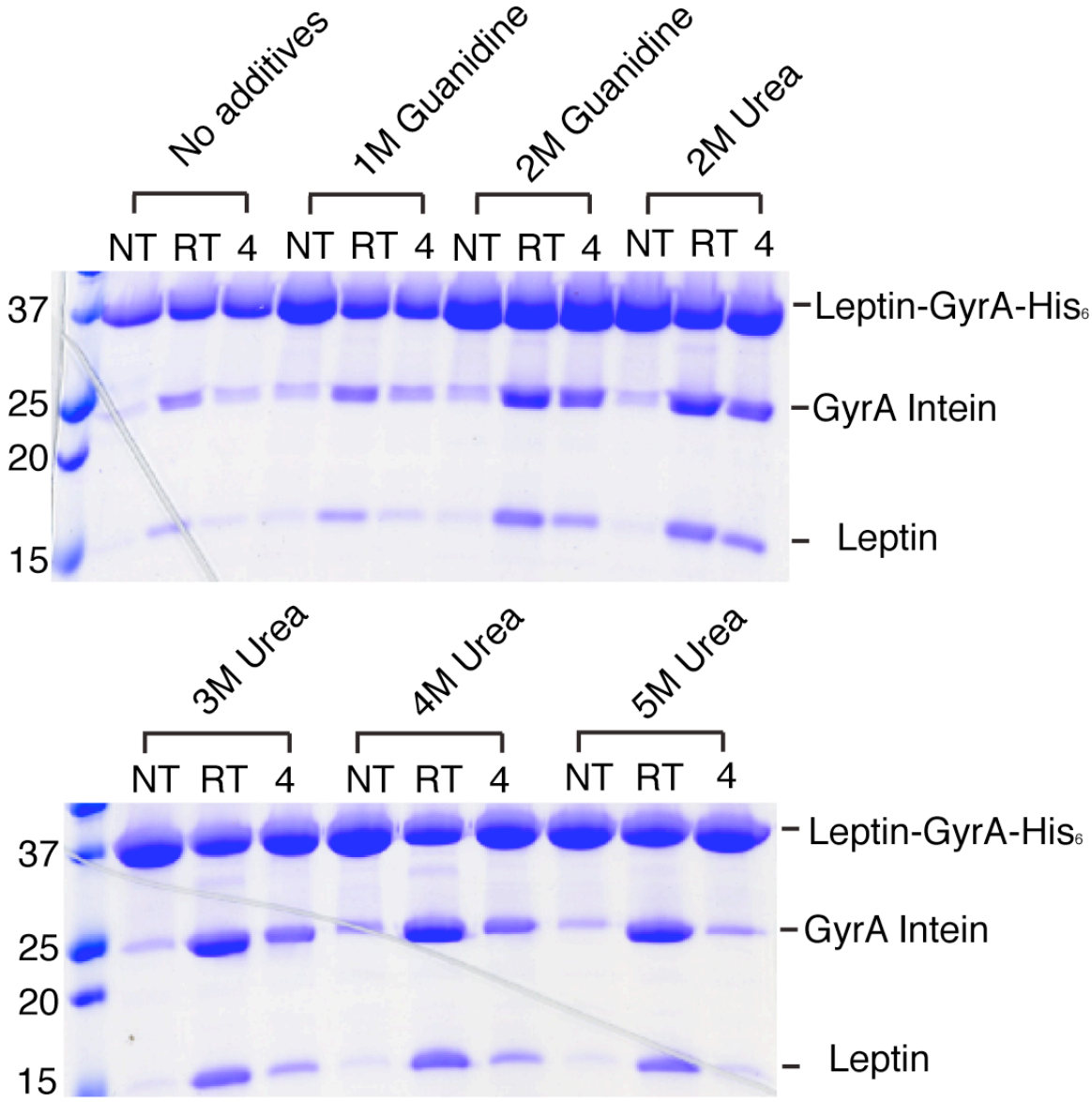

Figure 9. Optimization of leptin intein-cleavage conditions. Leptin-GyrA-His_6 was refolded into pH 7 buffer containing the indicated additives and cleaved with 3% ethanethiol overnight at room temperature (RT) or 4° C (NT= no thiol).

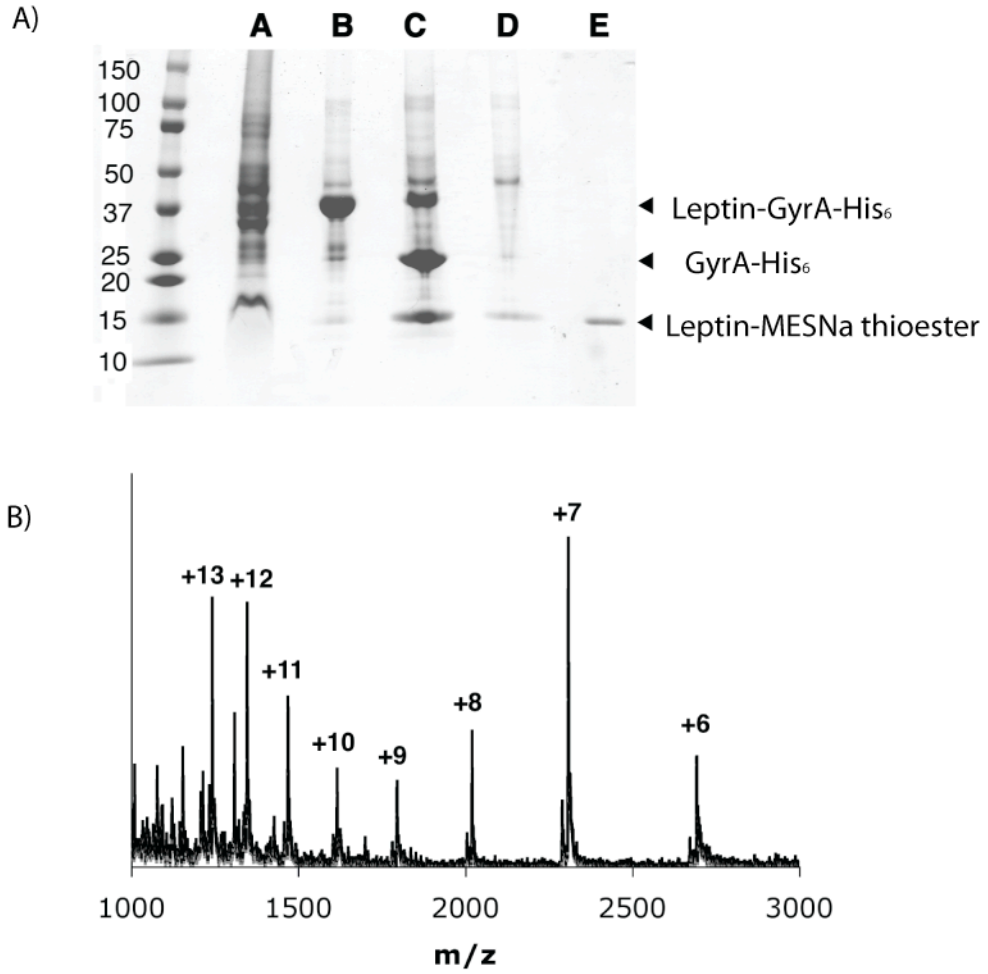

Figure 10. A) Expression and purification of leptin α-thioester **1**. Coomassie stained 4-20% gradient SDS-PAGE analysis of leptin purification fractions. A: Crude insoluble fraction from cell lysate. B: Leptin-GyrA-His_6 purified on a Ni-NTA column. C: Cleavage of leptin-GyrA-His_6 using 100 mM MESNa. D: Eluate of leptin α-thioester **1** from the Ni-NTA column, E: Purified leptin α-thioester **1**. B) ESI-MS of leptin-MESNa α-thioester **1** (calculated mass 16156.2 Da, obtained 16157.2 ± 3.0 Da). Charge states are indicated. The smaller peaks represent the hydrolyzed thioester.

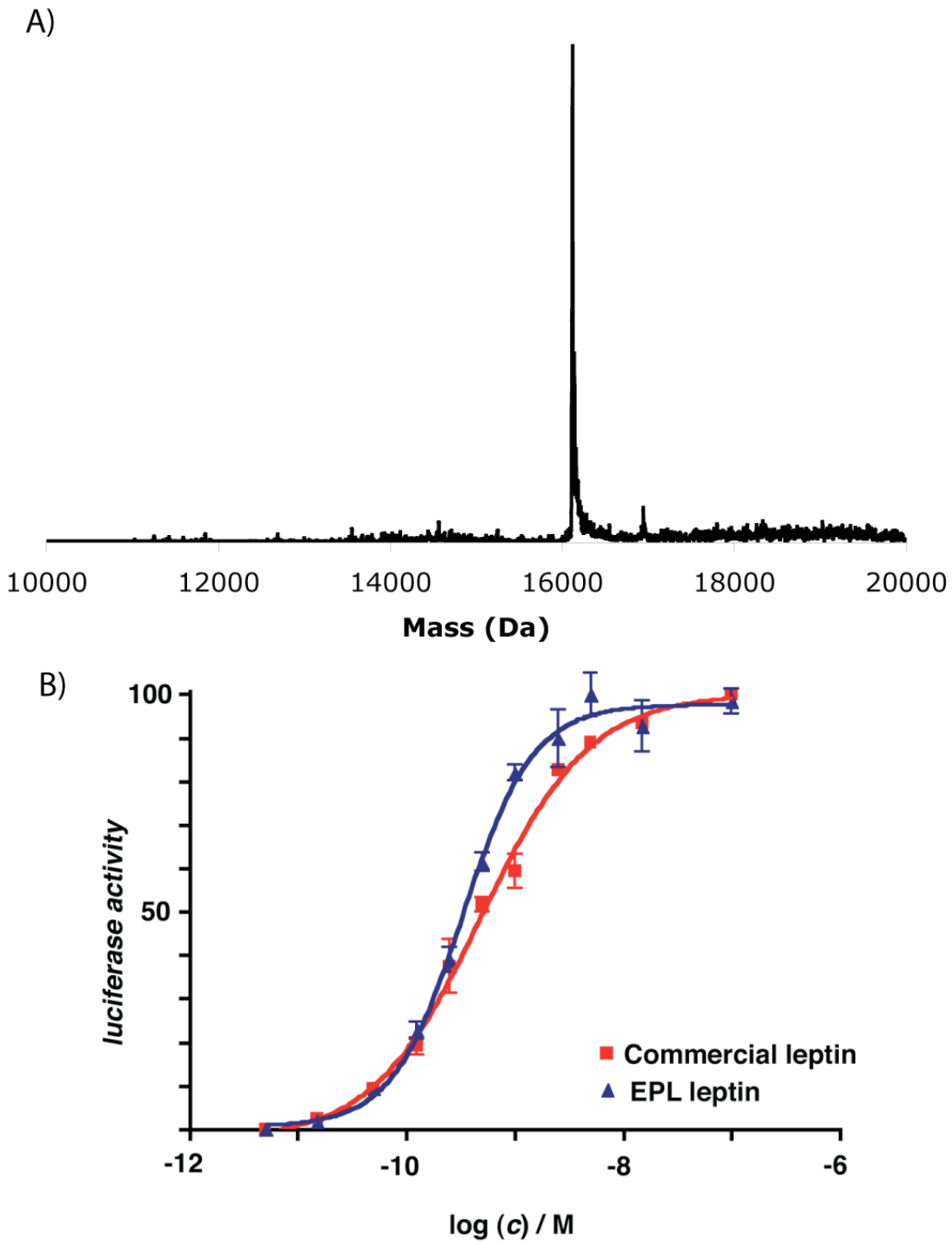

Figure 11. A) ESI-MS reconstruct of murine leptin produced in an EPL protocol (calculated mass 16135.6, obtained 16134.6 ± 2.5). B) Leptin receptor-STAT3 dependant luciferase assay comparing the activity of recombinant leptin produced by an EPL protocol and recombinant leptin obtained from a commercial source. EC_{50} for recombinant leptin = 0.49 nM (95% confidence intervals 0.39-0.61 nM). EC_{50} for semisynthetic leptin = 0.31 nM (95% confidence intervals 0.25-0.38 nM)

2.4 Synthesis of ^{18}F-FBA-leptin

As mentioned above (see section 1.7, 2.1), several methods for protein labeling with the isotope ^{18}F have been described. While a one step radiochemical labeling strategy, in which aqueous ^{18}F could be directly appended to leptin, would be optimal, current methods are not applicable to protein labeling due to the very low specific activity of the resulting products[108], or the requirement for organic solvents[109]. Thus, a two-step methodology was required. We were attracted to the use of ^{18}F-4-fluorobenzaldehyde (FBA), owing to its previous use in chemoselective ligations with synthetic peptides[114]. We rationalized that leptin could be radiolabeled using this synthon, if the protein were labeled site-specifically with an aminooxy functional group. Thus, we developed an EPL strategy for labeling leptin site-specifically at its C-terminus with an aminooxy functional group for the purpose of site-specific oximation with ^{18}F-FBA. Again, this strategy exploits the fact that leptin has a cysteine at its N-terminus, allowing for the facile incorporation of modifications using EPL.

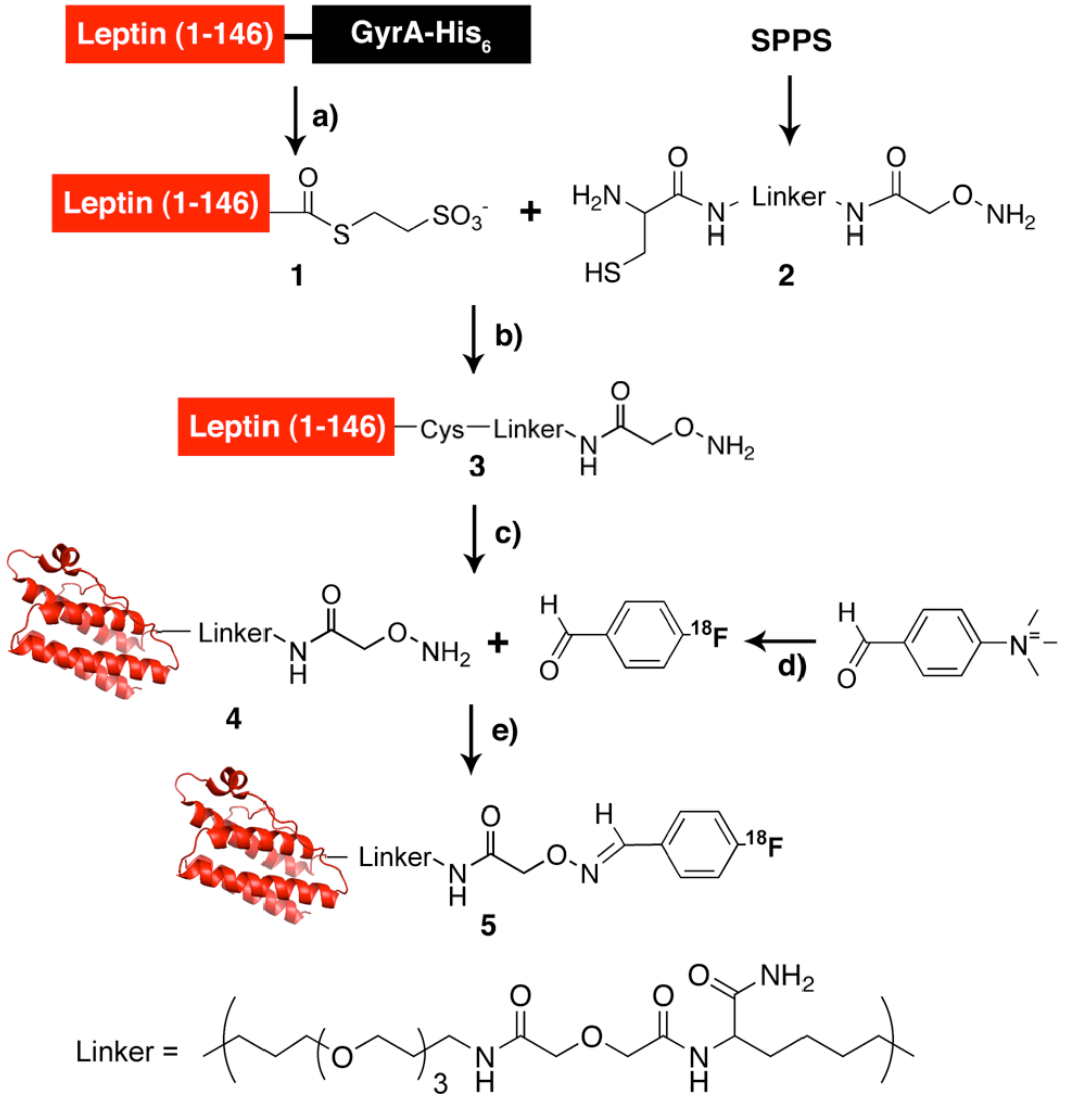

Scheme 2: Synthesis of ^{18}F-FBA-leptin **5**. Reaction conditions: **a)** 100 mM mercaptoethanesulfonic acid, 4M urea, 150 mM NaCl, 100 mM sodium phosphate pH 7.0, 4 °C, 2 days. **b)** 20 mg/mL **1**, 10 mg/mL **2**, 100 mM mercaptoethanesulfonic acid, 6M Gn-HCl, 150 mM NaCl, pH 7.2, 1 day. **c)** Refolding by stepwise dialysis and disulfide exchange. **d)** 20 mg kryptofix, 2 mg potassium carbonate, 1-2 mg (4-formylphenyl)trimethylammonium trifluoromethanesulfonate and K^{18}F in DMSO, 120 °C, 8 minutes. **e)** 30 nmol **4**, 100 mM anilinium acetate pH 4.5, 15 minutes, 0° C.

An overview of the synthetic strategy to generate ^{18}F-FBA-leptin is depicted on Scheme 2. Leptin α-thioester **1** was prepared as described in section 2.3 and ligated to

cysteine derivative **2** to give leptin analog **3** (Scheme 2). Compound **2** was synthesized by solid phase methods and contains two reactive moieties, namely a cysteine and an aminooxy group, separated by a short PEG spacer (Scheme 3, Figure 12). In preliminary studies, we found the PEG spacer was required to maintain native-like solubility of the final folded product. We anticipated that at pH 7 the α-thioester in protein **1** would react preferentially with the cysteinyl group in **2**, via native chemical ligation, due to the relatively slow rates of hydroxymate formation under these conditions[153,154]. The EPL reaction between **1** and **2** was complete after 24 hours at which point the crude ligation mixture was refolded as described above. The refolded aminooxy-leptin analog **4** was then purified by RP-HPLC (Figure 13a, b). Aminooxy-leptin analog **4** gave an identical tryptic digestion pattern to commercially available recombinant leptin as determined by LCMS (Figure 13c). As expected for natively folded leptin, the two C-terminal tryptic peptides in **4** were found to be linked by a disulfide bond, while no reduced tryptic peptides could be found. Interestingly, the mass spectrum of this disulfide-linked C-terminal tryptic peptide contained a peak of mass consistent with loss of aminooxy-acetate. The presence of this fragment, which may have been produced either by trypsinolysis of the aminooxyacetate, or by gas phase fragmentation, provides evidence that protein **4** contains the desired amide bond at the ligation site, since aminooxy-acetate could not be lost from a hydroxymate-containing ligation side-product.

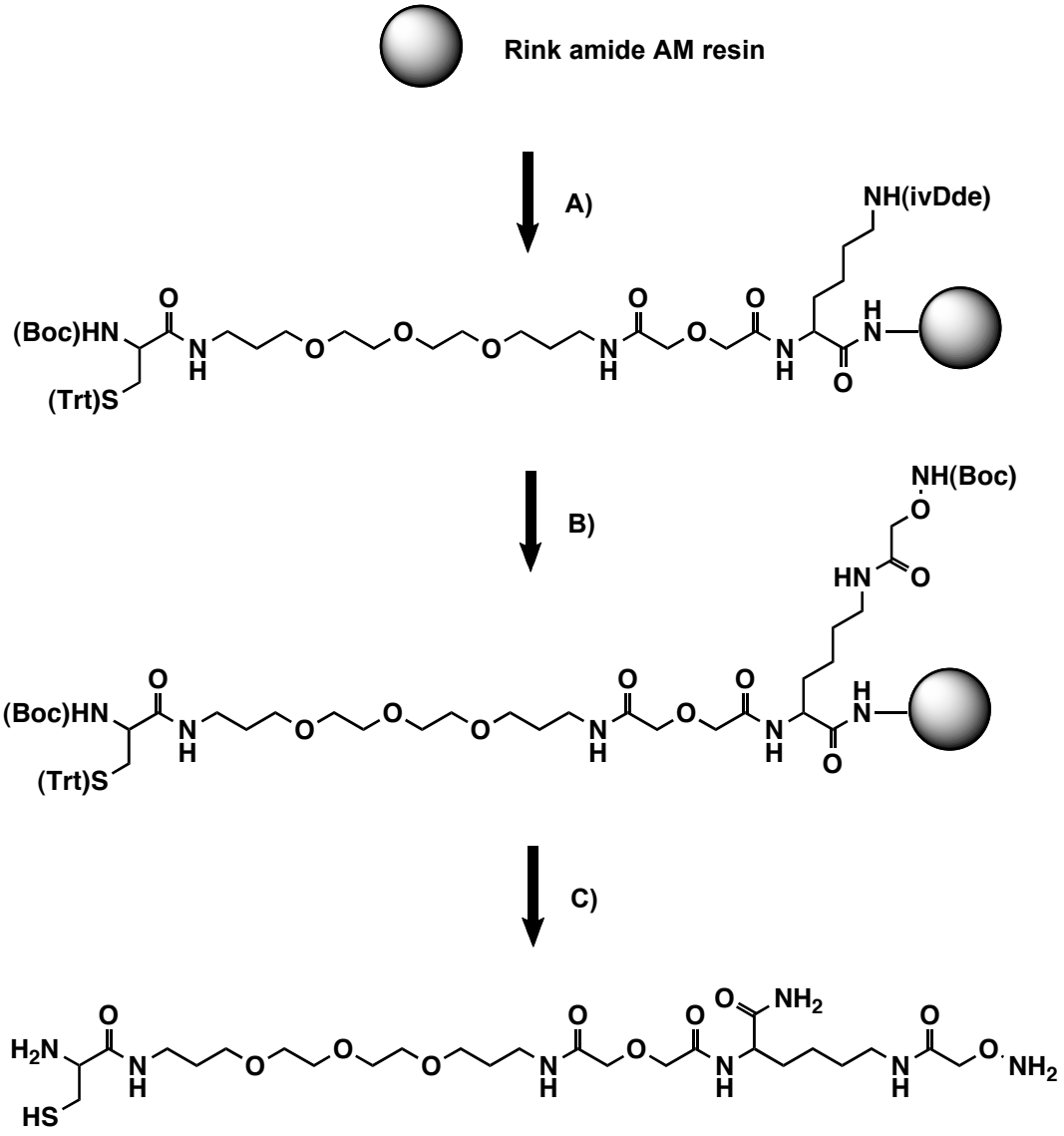

Scheme 3. Solid phase synthesis of peptide **2**. Reaction conditions: A) Standard Fmoc-SPPS. B) 2% Hydrazine in DMF followed by 8 equivalents of Boc-aminooxyacetic acid activated with diisopropylcarbodiimide. C) 1% triisopropyl silane, 2.5% ethanedithiol, 2.5% water in trifluoroacetic acid, 1 h.

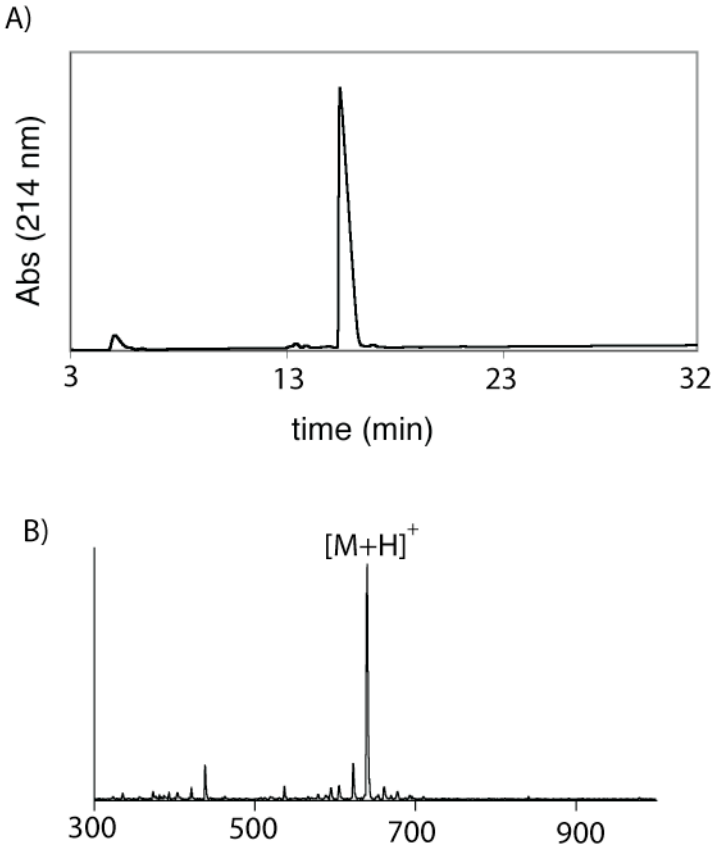

Figure 12. A) C18 analytical RP-HPLC chromatogram of purified peptide **2** on a 5-20% B gradient. B) ESI-MS of peptide **2** (calculated mass 639.8 Da, obtained $[M+H]^+$ = 641.0 Da).

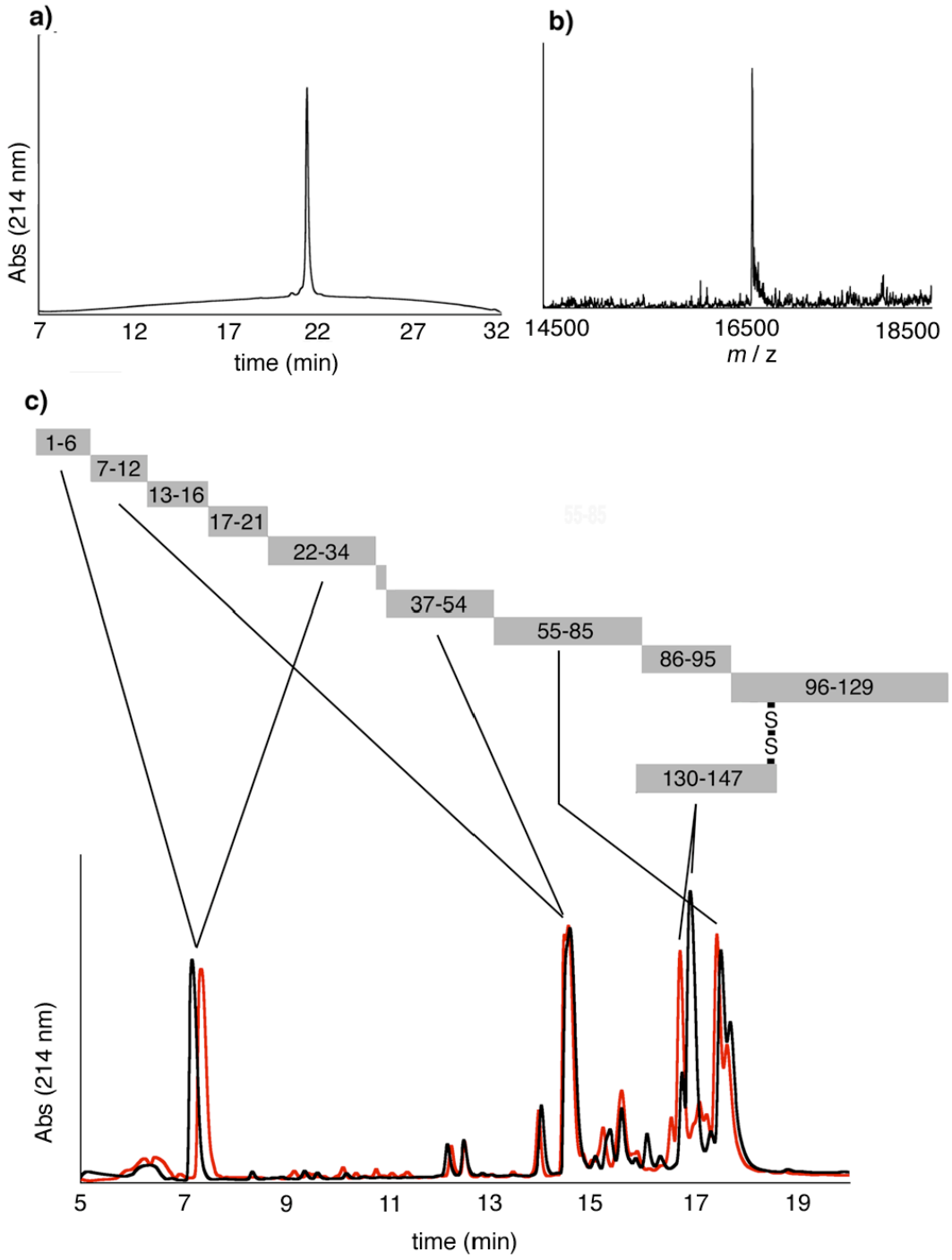

Figure 13. Synthesis and characterization of AOA-leptin **4**. a) RP-HPLC chromatogram of **4** on a 0-100% B gradient on a C4 analytical column. b) ESI-MS reconstruct of AOA-leptin **4** (calculated mass 16652.2 Da, obtained 16652.2 ± 3.3 Da). c) Trypsinization HPLC/MS analysis of commercial recombinant leptin (black) and AOA leptin **4** (red). The indicated peaks connected by a line were identified as the corresponding tryptic peptides by ESI-MS. The disulfide bond between C97 and C147 is indicated.

Cold FBA-leptin derivative **5** was generated by overnight treatment of **4** with 1 mM 4-fluorobenzaldehyde at 4 °C in 100 mM sodium acetate buffer, pH 4.5. No side reactions were detected, and the resulting oxime-containing product was purified by RP-HPLC and the identity confirmed by ESI-MS (Figure 14a). FBA-leptin **5** was then tested for its ability to activate leptin receptor signaling using the aforementioned ObRb-STAT3-luciferase assay (Figure 6). In this assay, **5** induced leptin receptor signaling to a similar extent as commercial recombinant leptin, with a slightly increased EC_{50} (95% confidence intervals 0.26-0.34 nM for recombinant leptin and 1.0-2.0 nM for **5**, Figure 14b). This subtle reduction in potency observed for **5** was not due to the ligation or refolding procedures employed in its preparation as unmodified leptin generated via a similar EPL procedure had an identical EC_{50} compared to commercial recombinant leptin in this assay (Figure 11b). Importantly, when administered to ob/ob mice via subcutaneous osmotic pumps, FBA-leptin **5** had identical ability to induce weight loss over a 24 hour period as commercial recombinant leptin (Figure 14c). We conclude that FBA-leptin **5** is able to bind and activate the leptin receptor, and that it is able to induce weight loss in mice, the hallmark of leptin bioactivity.

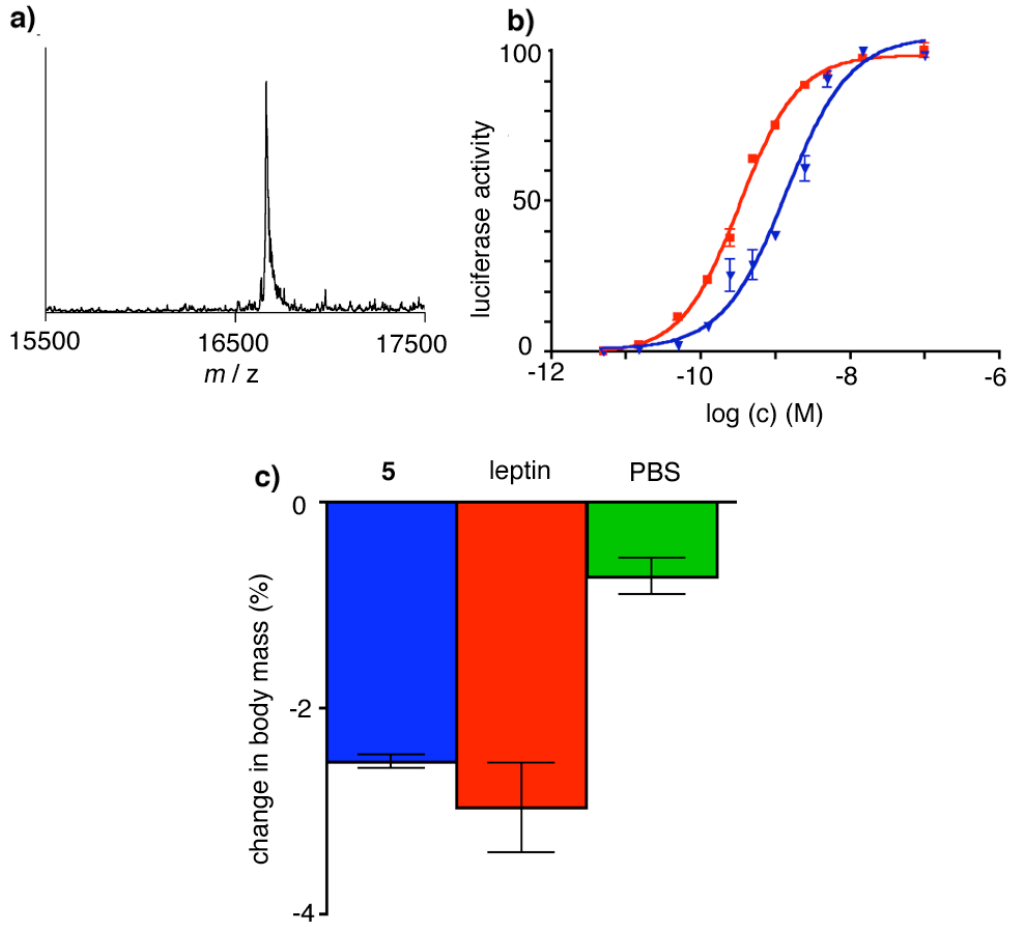

Figure 14. Characterization and biological activity of FBA-leptin **5**. a) ESI-MS reconstruct of FBA-leptin **5** (calculated MS 16758.3, obtained 16760.9 ± 3.5). b) ObR-STAT3 dependant luciferase assay comparing the activity of FBA-leptin **5** (blue triangles) and recombinant leptin (red squares), n = 2 ± s.d.. c) Comparison of the weight loss induced by FBA-leptin **5**, recombinant leptin, and PBS vehicle in ob/ob mice. Samples were infused at a constant rate of 450 ng/hr. The weight of the animals was recorded after 24 hours (n = 4 ± s.e.m).

Synthesis of ^{18}F-FBA was accomplished as previously described[155], with minor modifications, using the precursor (4-formylphenyl)trimethylammonium trifluoromethanesulfonate. Initial attempts towards oximation of ^{18}F-FBA with leptin analog **4** failed owing to precipitation of the protein at elevated temperatures required to allow the reaction to proceed in good yield[114,115]. Jencks and co-workers described catalysis of semicarbazone formation between 4-chlorobenzaldehyde and semicarbazide

by aniline and substituted derivatives thereof, and recently Dawson and co-workers found that aniline acts as a catalyst in peptide oxime ligations[156,157]. Thus, we reasoned that aniline should catalyze the radiochemical oximation of ^{18}F-FBA with aminooxy-leptin **4**. Comparison of the rate of oximation of aminooxy-leptin **4** in 100 mM sodium acetate or anilinium acetate at 4 °C revealed that aniline dramatically accelerates the reaction (Figure 15a). Notably, aniline catalysis allows the reaction to proceed in good yield at lower concentration of the aminooxy precursor, and at lower temperature than previously described for this radiolabeling reaction[114,115].

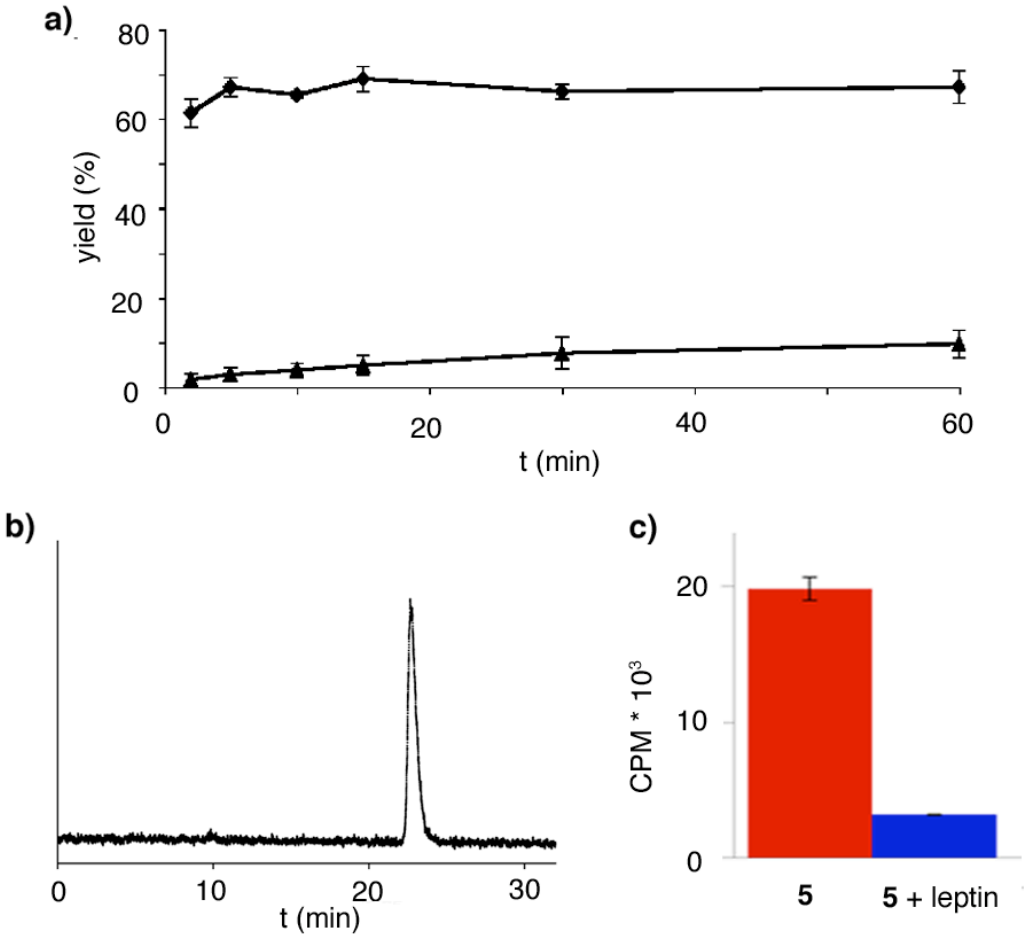

Figure 15. Catalysis of radiochemical oximation of AOA-leptin **4** with ^{18}F-FBA by aniline and characterization of the ^{18}F-FBA-leptin **5**. a) Catalysis of the oximation reaction by aniline. 125 uM **4** was incubated with ^{18}F-FBA in the presence of either 100 mM sodium acetate pH 4.5 (triangles) or 100 mM anilinium acetate (diamonds) at pH 4.5 on ice. The radiochemical yield was quantified by TLC and confirmed by RP-HPLC. The results are an average ± standard deviation of four experiments. b) Radiochemical HPLC of ^{18}F-FBA-leptin **5**, on a C4 analytical column. c) ^{18}FBA-leptin **5** was incubated with a cell line overexpressing ObRb in the presence or absence of 5 μM competing leptin (average of 2 experiments).

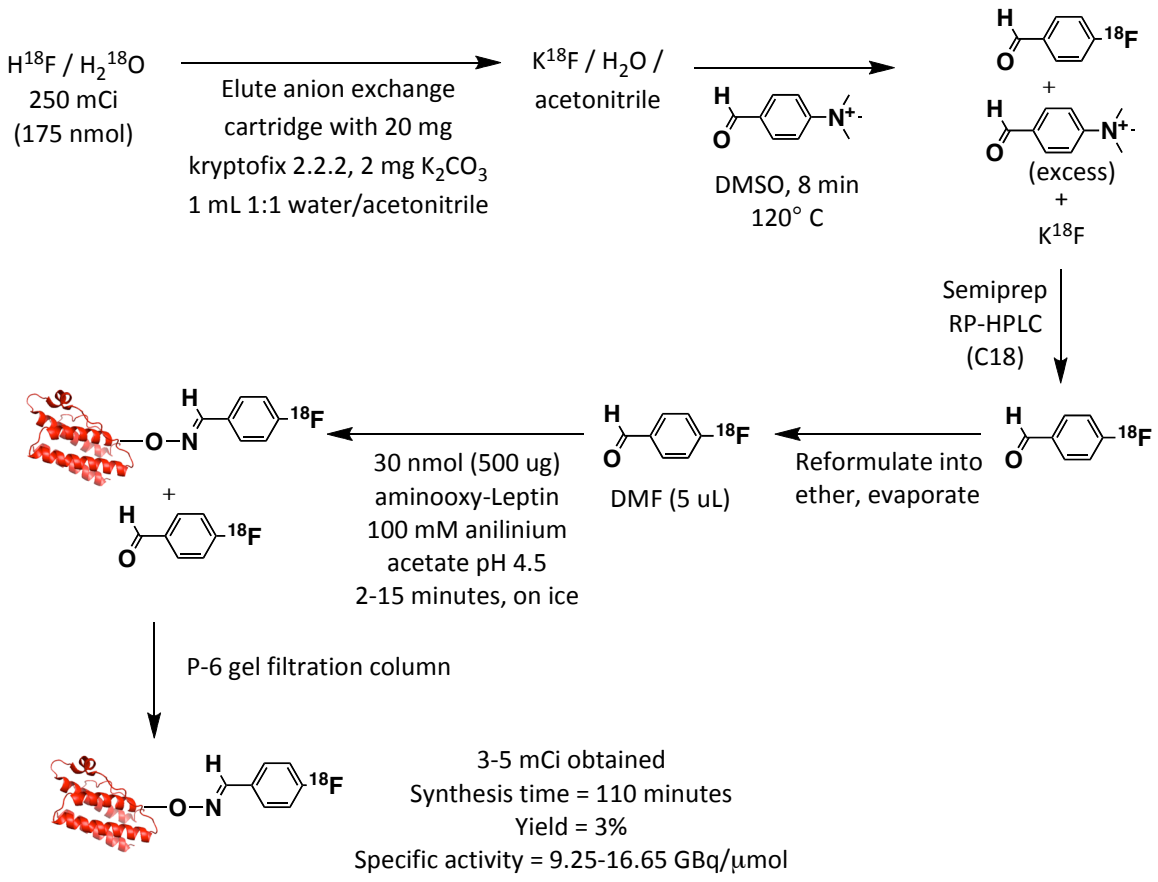

Scheme 4. Overview of method to label aminooxy-leptin **4** with ^{18}F-FBA.

The method for preparative-scale labeling of aminooxy-leptin **4** with ^{18}F-FBA is depicted on Scheme 4. Preparative scale ^{18}F labeling of aminooxy-leptin **4** was accomplished by treatment with ^{18}F-FBA in 100 mM anilinium acetate on ice for 15 minutes, and purification of the resulting mixture on a P-6 gel filtration column. Using this method, 74-185 MBq (2.5-5.0 mCi) of ^{18}F-FBA-leptin **5** could be recovered starting from 7.4-11.1 GBq of ^{18}F, with a total synthesis time of ~120 minutes (n=4). The specific activity of the protein varied from 9.25-16.65 GBq/μmol, and the radiochemical purity of the protein was greater than 95% as judged by iTLC and HPLC (Figure 15b). The ability

of ^{18}F-FBA-leptin **5** to bind to the aforementioned cell line expressing ObRb was tested. We found that the labeled protein bound to the cells when incubated together at room temperature, and that binding could be blocked by the addition of an excess of unmodified recombinant leptin (Figure 15c). Additionally, the presence of the toxic catalyst aniline could not be detected in the final preparation of leptin by RP-HPLC.

The stability of the ^{18}F-FBA-leptin **5** was tested both *in vitro* and *in vivo*. Over the course of an hour, the protein was stable in PBS (10 mM sodium phosphate, 140 mM sodium chloride, pH 7.4), 100 mM sodium acetate, pH 4.5, and mouse serum *in vitro* as determined by HPLC analysis (Figure 16b-d). Finally, the stability was tested *in vivo*. In blood recovered from mice, greater than 95% of the radioactivity detected corresponded to intact ^{18}F-FBA-leptin **5** (Figure 16a). Thus, the stability of the protein is sufficient for studies both *in vitro* and *in vivo*. Importantly, this synthesis provides sufficient highly stable radiolabeled protein in good specific activity for studies in small and large animals, as well as in humans, with the biological activity of the protein intact.

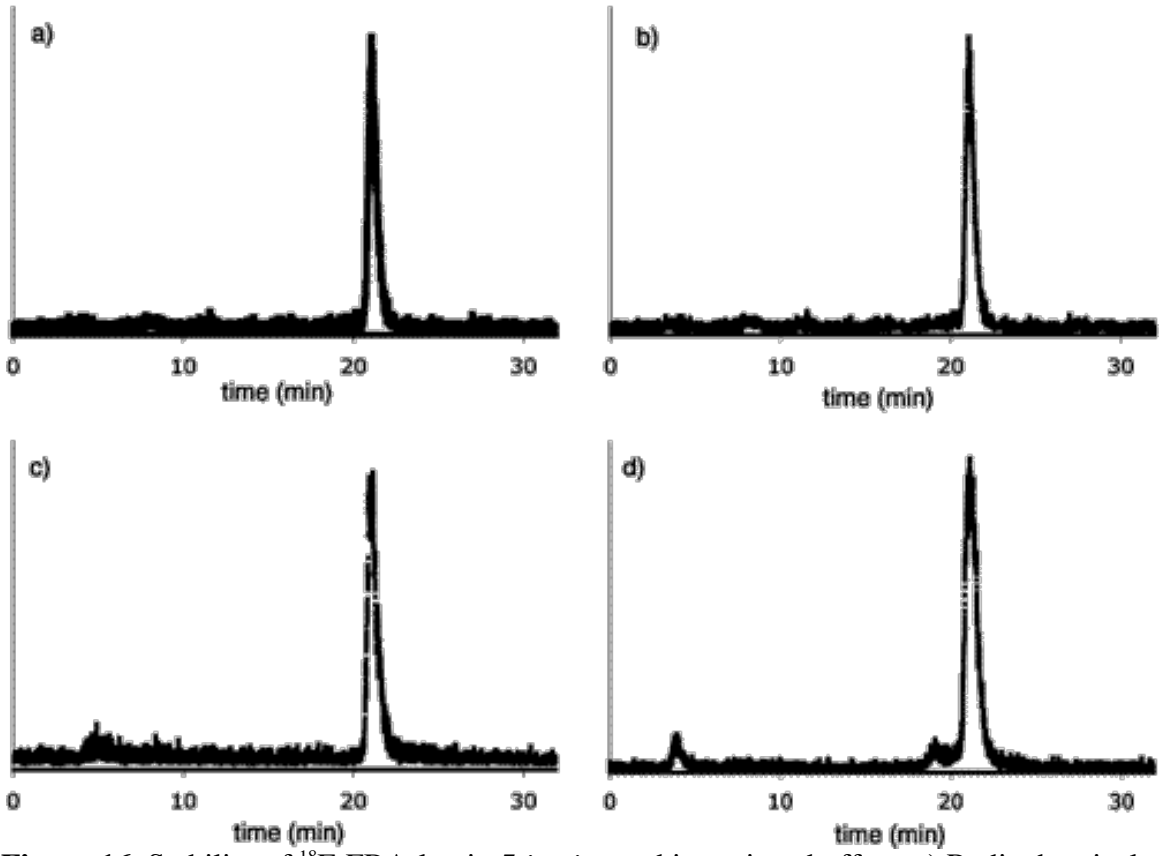

Figure 16. Stability of ^{18}F-FBA-leptin **5** *in vivo* and in various buffers. a) Radiochemical RP-HPLC of serum recovered from wild type mice injected with ^{18}F-FBA-leptin **5** 30 minutes prior. Similar results were obtained from *ob*/*ob* mice. b-d) Radiochemical HPLC of ^{18}F-FBA-leptin after incubation for 60 minutes in PBS, 100 mM sodium acetate pH 4.5, or mouse serum, respectively. Stability in PBS and sodium acetate was greater than 95% while in serum it was 93% stable. The initial purity of the labeled product in this experiment was 96%.

We next performed preliminary PET imaging experiments in mice. ^{18}F-FBA-leptin **5** (3.7-5.55 MBq) was injected in ob/ob mice, and they were immediately imaged in a micro-PET scanner. We found that most of the protein rapidly accumulated in the kidneys (Figure 17a) in agreement with previous biodistribution studies[84,96,158]. A key advantage of ^{18}F over other nuclides is the improved resolution of the PET images obtained, up to five fold[101]. To illustrate this, we compared images obtained using ^{68}Ga-

DOTA-leptin against those obtained with ^{18}F-FBA-leptin. As expected, the resolution of the micro-PET images obtained with ^{18}F-FBA-leptin was substantially improved over images produced with ^{68}Ga-DOTA-leptin. Thus, while imaging ^{68}Ga-DOTA-leptin demonstrated binding to the kidney in mice (Figure 17b), imaging using ^{18}F-FBA-leptin **5** clearly reveals binding specifically in the cortex of the kidney, with less binding in other regions (Figure 17a). This pattern is consistent with the uptake of the hormone in the cortex of the kidney, in agreement with previous results[50].

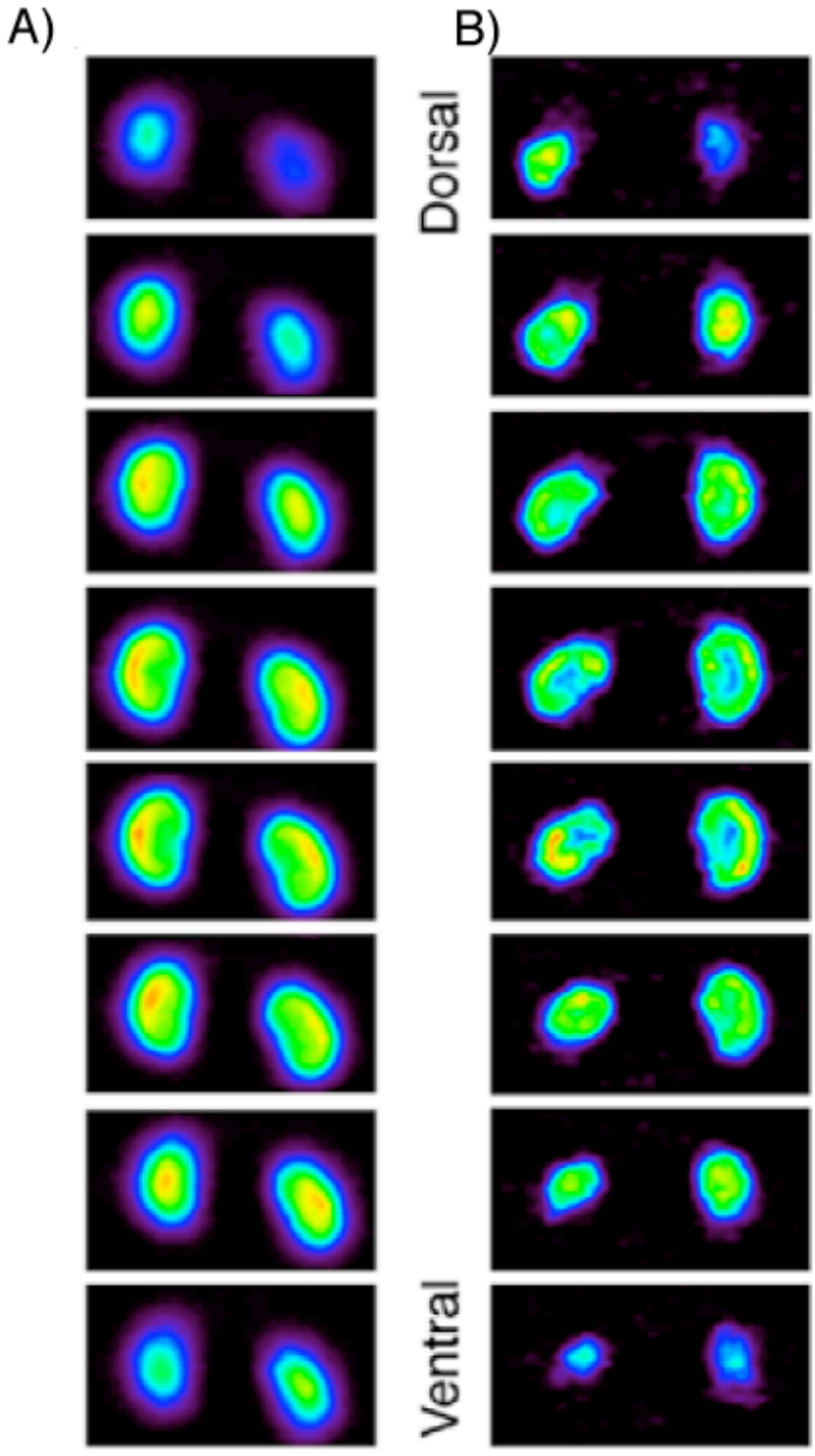

Figure 17. a) Serial coronal PET images of ob/ob mouse kidneys, injected with ^{68}Ga-DOTA-leptin. b) Serial coronal PET images of ob/ob mouse kidneys, injected with ^{18}F-FBA-leptin **5**.

2.5 Toward ^{18}F-labeling of lysine residues using aminooxyacetic acid-modified side chains

One alternative approach to ^{18}F-labeling of leptin would be to adopt a lysine side-chain modification technique, similar to the DOTA modification method (Section 2.2). Lysine directed side-chain modification using ^{18}F has been previously described using 18F-fluorobenzoic acid, succinimide ester (FSB), and applied to a variety of substrates[122,159]. Similarly, Chang et al. labeled the side chains of albumin with hydrazinonicotinic acid, succinimide ester, and subsequently conjugated ^{18}F-FBA to generate a hydrazone product[125]. We were attracted to the latter technique, owing to our experience with ^{18}F-FBA, and the finding that aniline catalyzes reactions of this type[156,157,160]. However, we were concerned that the stability of a hydrazone containing conjugate would be insufficient for the study of leptin biodistribution of leptin *in vivo*, based on previous reports revealing degradation of ^{18}F-FBA labeled hydrazone conjugates in mildly acidic solution[118]. Although, to our knowledge no direct comparison has been made between the stability of oxime and hydrazone conjugates *in vivo*, a recent model study revealed greater stability of oximes as compared to hydrazones in aqueous buffers[161]. Thus, we envisioned a leptin labeling approach in which aminooxy groups could be installed on lysine side chains, which could be subsequently derivitized with ^{18}F-FBA, to generate the stable oxime linkage.

A method to generate aminooxy-derivitized proteins by native chemical ligation was developed by Shao et al., who found that 1M methoxylamine could be used to deprotect an isopropylidene protecting group on an aminooxyacetic acid moiety in the context of a small protein, CCL-5 (RANTES)[162]. Thus, we devised a synthetic strategy in

which the lysine side chains and N-terminus of leptin could be modified using isopropylidene-aminooxyacetic acid, succinimide ester (**6**), deprotected using methoxylamine, and finally labeled with ^{18}F-FBA (Figure 18). We synthesized **6** using the method depicted on Figure 19a in two steps in 52% overall yield. We then conjugated the reagent to leptin. Similar to leptin labeling with DOTA-NHS, we found that the stoichiometry of **6** to leptin determined the degree of leptin labeling (Figure 19b). Importantly, treatment with 500 mM methoxylamine on ice overnight removed all of the isopropylidene protecting groups following conjugation with **6** in a one pot reaction, in 70% yield (Figure 19c, d). In preliminary experiments, we found that this aminooxy-leptin derivative could be labeled with ^{18}F-FBA, in similar yield to aminooxy-leptin **4** (data not shown). Thus, this technique allows for lysine side-chain modification of proteins with aminooxyacetic acid, and is a promising technique for generating ^{18}F-labeled protein tracers.

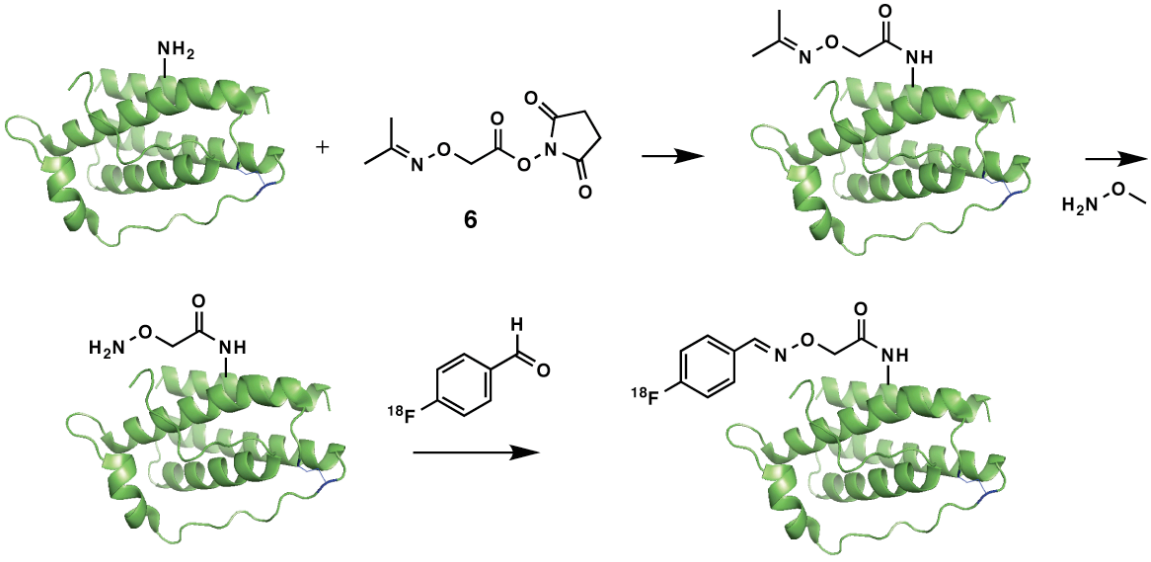

Figure 18. Schematic of lysine chain modification strategy to generate aminooxy leptin.

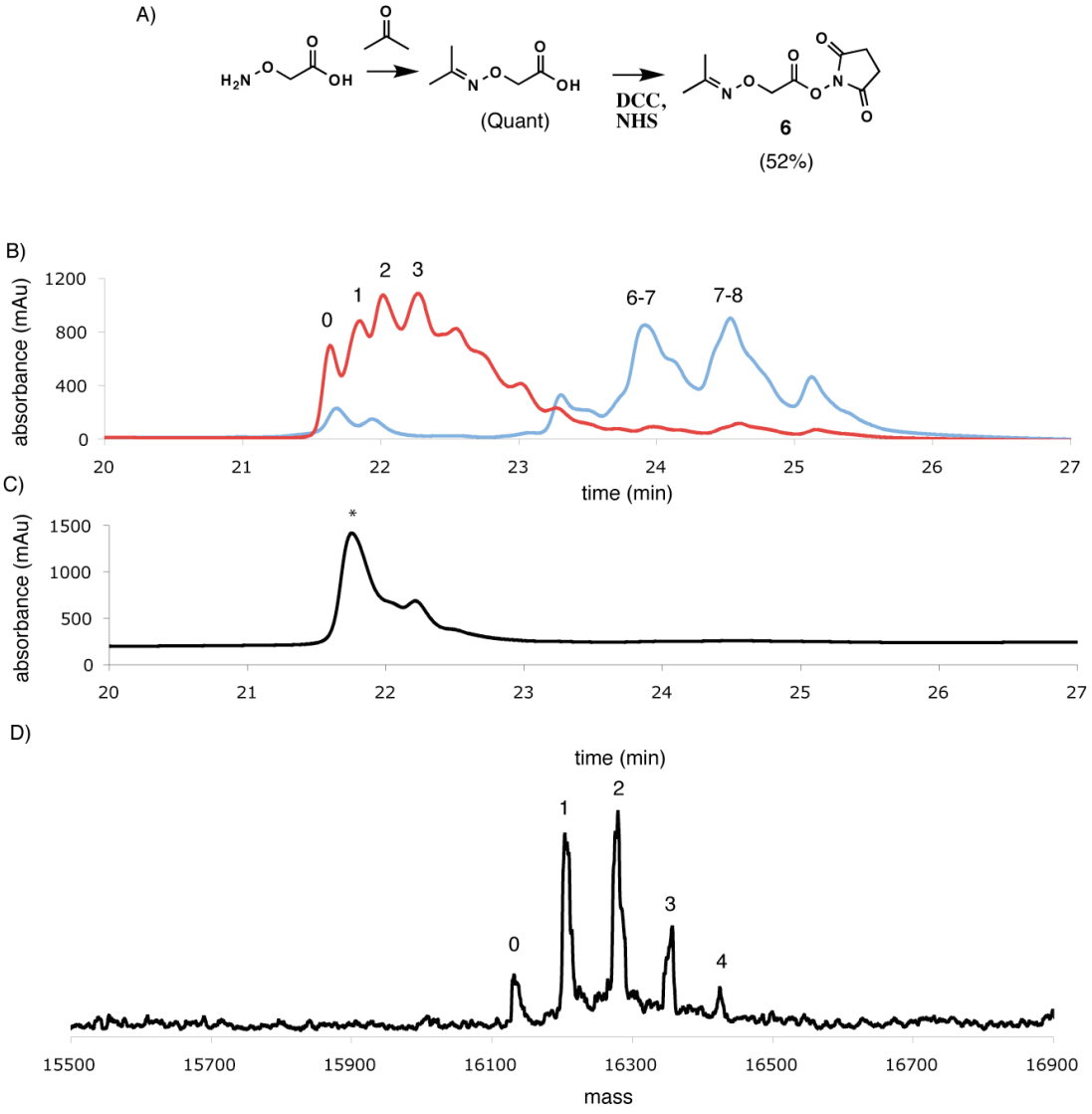

Figure 19. Preparation of aminooxy-leptin by modification of lysine side chains. A) Synthetic scheme to generate isopropylidene-aminooxyacetic acid-ONHS (**6**). B) RP-HPLC of leptin labeled with **6**, on the same 0-100% B gradient on a C4 analytical column. Four equivalents were used for the red trace, and 20 for the blue trace. The number of equivalents of **6** per leptin molecule is indicated above each HPLC peak. C) HPLC of deprotected aminooxyacetic acid-leptin following the conjugation with four equivalents of **6** (i.e. the red trace from B). D) ESI-MS of the product of the deprotection reaction (i.e. the starred peak from panel C) The number of amionooxyacetic acid labels per leptin molecule is indicated.

2.6 Summary of tracer development

In conclusion, we have developed two complementary radiolabeled tracers, which we term ^{68}Ga-DOTA-leptin, and ^{18}F-FBA-leptin. DOTA labeling of leptin was accomplished in an amine directed manner using DOTA-NHS, incorporating an average of 4 chelators per protein molecule (fig 7b). DOTA-leptin could readily be labeled with ^{68}Ga in good yield. A site-specific ^{18}F-labeling strategy was developed, in which an aminooxy functional group was first installed on the C-terminus of leptin using EPL, which was subsequently derivitized in an aniline accelerated oximation reaction with ^{18}F-FBA (Scheme 2)[163]. Thus, the ^{18}F labeling method we have developed is intrinsically site-specific, and should be readily applicable to other substrates. Furthermore, both tracers preserve the ability to bind to and activate ObRb and induce STAT3 signaling, and to induce weight loss in ob mice. A comparison of the imaging properties of the two tracers revealed that ^{18}F-FBA-leptin has higher resolution compared to ^{68}Ga-DOTA-leptin, allowing for the uptake of the tracer in the cortex of the kidney to be visualized (Figure 17). Additionally, a lysine directed labeling strategy to generate ^{18}F-FBA-modified leptin, based on the conjugation of aminooxyacetic acid to lysine side chains, was developed. The use of these tracers to interrogate leptin biology in model systems in rodents and primates is discussed in chapters 3 & 4, and an extensive comparison of our tracers to others in the literature is presented in section 5.1.

Chapter 3. Imaging leptin biodistribution by PET reveals clearance of the hormone by Megalin in the cortex of the kidney

The work described in this chapter was performed in close collaboration with G. Ceccarini (Friedman lab)

Section 3.1. Leptin half life, clearance, and biodistribution.

Leptin is a 16 kDa protein hormone, produced and secreted into the circulation by adipocytes, which regulates body weight homeostasis by reducing food intake and increasing energy expenditure[19,24]. Leptin also signals nutritional status to several other physiological systems and modulates their function. Plasma leptin levels are directly proportional to the amount of adipose tissue mass[13], and its major site of action is in the hypothalamus, where it binds and activates the leptin receptor (ObR). In addition, a number of non-ObR binding partners interacting with leptin have been identified, but their physiological significance is unknown[44,45,49,50]. Leptin action in the central nervous system is both necessary[18] and sufficient[52] to generate many of the effects of the hormone. Additionally, the hormone has direct effects on some peripheral tissues, modulating their function (see section 1.3)[62,64,67,75]. In particular, leptin has a short half-life which follows biphasic kinetics[84-87]. All available evidence suggests that leptin is cleared by the kidney, as would be expected based on its small size[84,87,89-91,158,164,165]. However, the molecular mechanism underlying this uptake remains unclear. The kidney expresses both ObR and the multiligand endocytic receptor megalin[50,166,167]. Recently, leptin was found to bind to an L2 yolk sac tumor cell line expressing megalin. Furthermore, purified megalin binds

to leptin with an apparent K_d of 200 nM as revealed by quartz crystal microbalance (QCM) analysis[50], a technique analogous to surface plasmon resonance which allows the monitoring of protein-protein interactions on surfaces[168]. Thus, both megalin and ObR are candidate receptors for leptin uptake in the kidney.

In vivo imaging of leptin biodistribution could be used to characterize the molecular mechanism of leptin uptake in various organs in animal models. Positron emission tomography (PET) is well suited for this purpose due to mm scale resolution, high sensitivity, and ease of quantification[112]. Furthermore, by using the appropriate genetically modified animals, the role of various receptors in regulating biodistribution can be determined. Herein we describe the application of two tracers, ^{18}F-FBA-leptin[163] and ^{68}Ga-DOTA-leptin (see chapter 2), to micro-PET imaging in various rodent and primate models. We found that leptin was rapidly taken up in a saturable manner in the kidney, and that this uptake was dependant on the multiligand endocytic receptor megalin.

Section 3.2 Whole body PET scans in rodents and rhesus macaques using ^{18}F-FBA-leptin and ^{68}Ga-DOTA-leptin

Firstly, we analyzed the biodistribution of leptin in normal mice and rats. In Figure 20a we show a typical whole body image of a leptin deficient (ob/ob) mouse injected with ^{68}Ga-DOTA-leptin, imaged by micro-PET for an hour. The tracer accumulates principally in the kidneys, but also in other visceral organs such as liver and spleen, and in the head. The tracer was largely absent from fat and brain. The low level of uptake in the bladder (2.2% of total injected dose) likely represents ^{68}Ga-DTPA, an

impurity of the radiochemical synthesis, which is known to be rapidly cleared to the urine[169]. Similar results were obtained with the ^{18}F-FBA-leptin tracer as shown in Figure 20b. The improved anatomical definition of ^{18}F compared to ^{68}Ga allowed us to observe the specific accumulation of the tracer in the periphery of the kidney (cortex) rather than the inner portion of the organ (medulla, Figures 18, 19b, e). This finding was confirmed using the ^{68}Ga-DOTA-leptin tracer in a rat model, where the larger size of the animal permits visualization of the cortex, despite the lower resolution of the ^{68}Ga isotope (Figure 20c). Uptake in the proximal femur was also observed in the rat images, suggesting uptake in bone marrow. To test if a similar biodistribution pattern could be also observed in primates, we imaged rhesus macaques using ^{68}Ga-DOTA-leptin as a tracer. The high definition of the PET-CT scan confirmed the renal cortical uptake of the tracer (Fig 19d). The fact that both ^{68}Ga-DOTA-leptin and ^{18}F-FBA-leptin provide similar images, that these patterns of distribution are consistent with previous biodistribution studies[92,96], and are consistent between species, strongly suggests that the pattern of radioactivity observed in these images coincides with the authentic biodistribution of leptin.

Urine formation occurs in the renal tubules, which travel from the cortex of the kidney (proximal convoluted tubules) deep into the medulla (loop of Henle), and return to the cortex (distal convoluted tubules, Figure 20e, f). A previous study, in which ^{125}I leptin was injected into mice, and the biodistribution subsequently analyzed ex-vivo by autoradiography, suggested that leptin is taken up in the proximal convoluted tubule[50]. Taken together with these previous results, our data suggest that leptin is taken up by the proximal convoluted tubule within the cortex of the kidney.

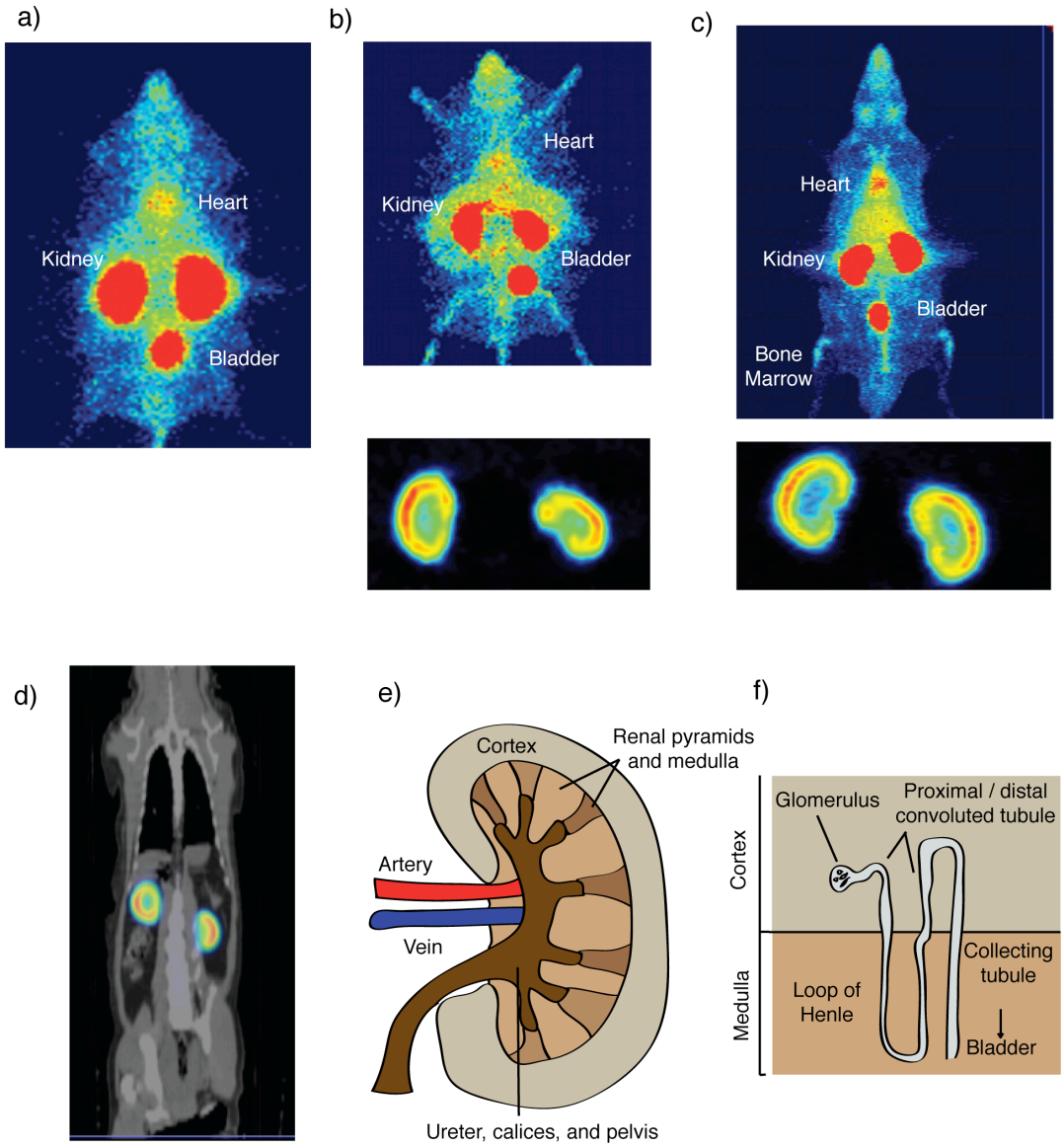

Figure 20. Whole body PET images of mice, rats, and rhesus macaques reveal that leptin is taken up in the cortex of the kidney in mammals. The images are overexposed to reveal areas with a lower level of uptake. a) Whole body PET maximum intensity projection (MIP) image of a leptin deficient (ob/ob) mouse injected with ^{68}Ga-DOTA-leptin. Renal uptake of leptin in ob/ob mice is 65.1% ± 3.5% while the bladder is only 2.2 ± 0.2% over 30 min. Uptake in other organs is lower than this per volume. b) Whole body PET coronal MIP image of an ob/ob mouse injected with ^{18}F-FBA-leptin, with inset of kidneys with lowered contrast, revealing uptake of the hormone in the cortex of the kidney. c) Whole body PET coronal MIP of a Sprague-Dawley rat injected with ^{18}F-FBA-leptin, with inset with lowered contrast, revealing uptake of the hormone in the cortex of the kidney. d) Coronal section of a PET-CT fusion image of a rhesus monkey injected with ^{68}Ga-DOTA-leptin, revealing uptake of the hormone in the cortex of the kidney e, f) Simplified diagram of kidney and renal tubular anatomy.

Section 3.3. Quantitative analysis of renal uptake of leptin

One of the strengths of PET imaging is quantitative kinetic analysis of uptake in organs. We therefore generated time vs. activity curves in the kidney and bladder by drawing regions of interest on the aforementioned anatomical regions of the micro-PET images. First, we compared the performance of our two tracers. We found that ^{18}F-FBA-leptin accumulated rapidly in the kidneys, but then the kidney radioactivity began to decrease and move to the bladder as time progressed (Figure 21a). In contrast, ^{68}Ga-DOTA-leptin uptake increased continually in the kidney over the course of the scan, while the level in the bladder remained consistently low (Figure 21a). Radiochemical HPLC analysis of the urine of the ^{18}F-FBA-leptin injected animals revealed that the tracer had been metabolized to uncharacterized byproducts (Figure 21b). Since ^{18}F-FBA-leptin is stable in serum *in vitro*, and *in vivo* (Figure 16a, c), this metabolite is probably formed following endocytosis of leptin by proximal convoluted tubule cells, where it diffuses out into the urine. It is interesting to note that a similar phenomenon was observed in the hepatobiliary clearance of ^{18}F-FBA labeled LDL particles[128]. Previous analysis of ^{111}In-DOTA labeled antibody fragments has demonstrated that the final product of intracellular metabolism is ^{111}In-DOTA-lysine, which is retained in lysosomes[170]. Thus, it is likely that ^{68}Ga-DOTA-leptin is similarly degraded to ^{68}Ga-DOTA-lysine. Tracers which are retained intracellularly following degradation are termed "residualizing tracers[171]." Thus, we used ^{68}Ga-DOTA-leptin for all further quantitative analysis, as the fact that it is residualizing tracer allows for the accurate quantitation of tissue uptake.

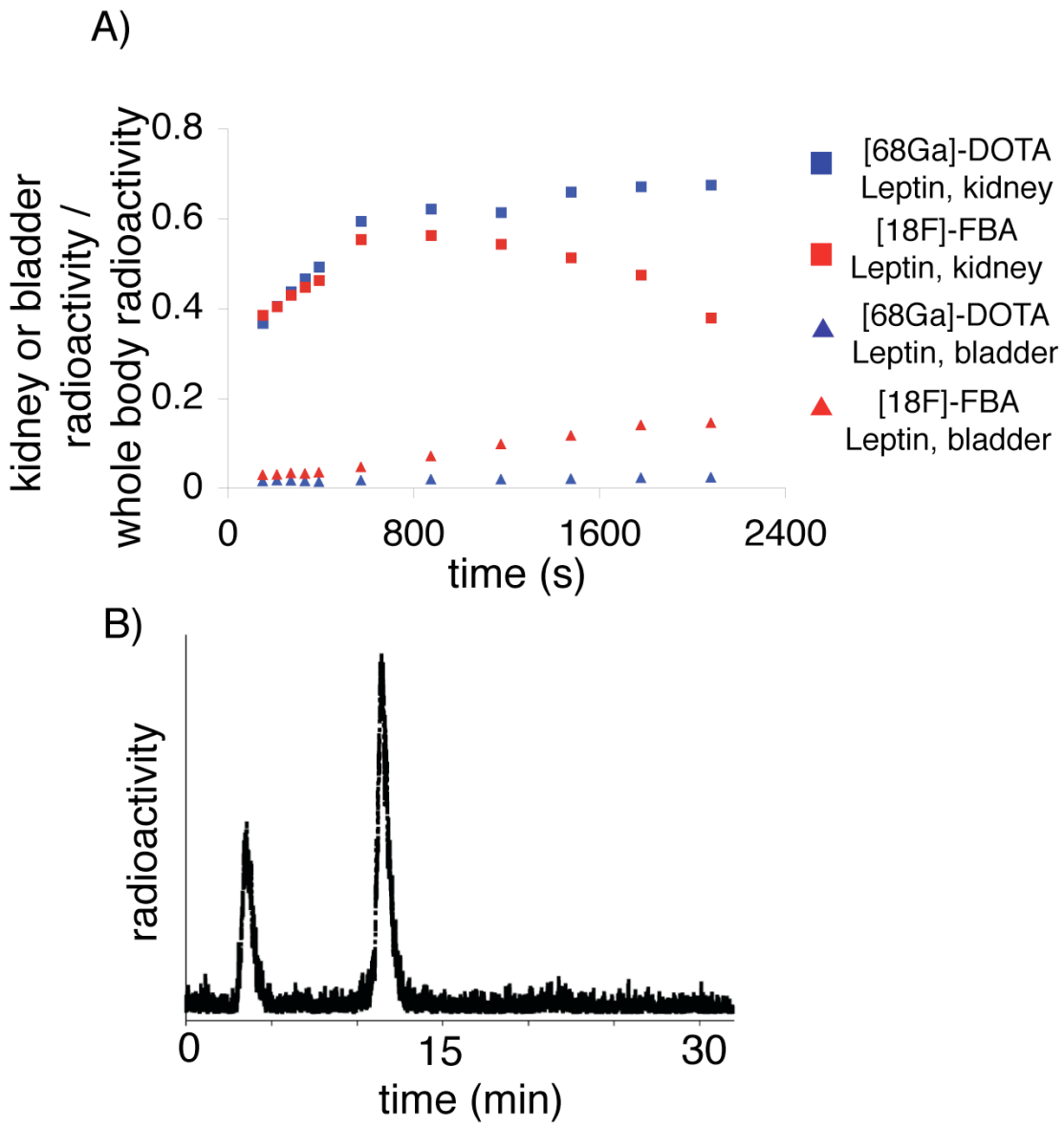

Figure 21. ^{68}Ga-DOTA-leptin is a residualizing tracer, while ^{18}F-FBA-leptin is not. A) Representative time activity curves of organ uptake of ^{68}Ga-DOTA-leptin and ^{18}F-FBA leptin in mouse kidneys and urinary tract. Organ uptake is defined as the total activity quantified in an organ, divided by total body radioactivity, with both quantified by region of interest (ROI) analysis of PET scans. B) Radiochemical HPLC analysis of urine from a mouse injected with ^{18}F-FBA-leptin indicating degradation of the tracer after one hour. For reference HPLCs of intact ^{18}F-FBA-leptin on the same gradient see figures 15b, 16.

Three wild type C57BL/6J mice were scanned after injection of ^{68}Ga-DOTA-leptin, and quantification of kidney and bladder uptake on the resulting micro-PET images revealed that 68.2 ± 1.5% and 3.1% ± 0.6% of the tracer was taken up over 30 minutes, respectively (Figure 22a, e). Radiochemical HPLC analysis of kidney extracts isolated from mice, which had been injected with the tracer, revealed only a peak at 3 min, indicating that the leptin had been degraded at later time points (presumably to ^{68}Ga-DOTA-lysine, see above). When co-injected with a 30 fold excess of cold ligand, 23.7 ± 2.2% of the leptin was displaced from the kidney to the bladder, with 47.3 ± 2.0% retained in the kidney (Figure 22c, e). Radiochemical HPLC analysis of the urine of these animals revealed a peak at 21.6 min, the characteristic retention time of leptin on this gradient, indicating that intact leptin is displaced from the kidney receptors (Figure 22d). Thus, micro-PET imaging of ^{68}Ga-DOTA-leptin biodistribution in mice reveals the presence of a saturable uptake system in the cortex of the kidney.

We then confirmed these results using ex-vivo biodistribution analysis. In these experiments, a radiotracer is injected (in this case ^{68}Ga-DOTA-leptin or commercially available ^{125}I-leptin), and following a period of time, the animals are sacrificed, and the radioactivity in the corresponding tissues counted. Thus, these experiments are analogous to PET imaging experiments, with only one time point - when the animal is sacrificed. The advantage of this technique is that a smaller radioactive dose need be injected to quantify tissue uptake (under 10 ng vs. 20 μg in a PET experiment), potentially minimizing effects of receptor saturation. In contrast to PET imaging experiments, the addition of competing cold leptin increases the amount of protein accumulating in the kidney in this analysis (Figure 23a). This is probably due to the fact that peripheral

receptors only become saturated when cold leptin is co-injected. When peripheral receptors are saturated, a much higher level of protein is delivered to the kidney, probably explaining the paradoxical increase seen in Figure 23a. A similar phenomenon was observed in PET imaging experiments in rhesus macaques (see section 4.4, Table 4, Figure 34). In order to exclude the contribution of increased protein delivery to the kidney resulting from saturation of peripheral ObR, we present the biodistribution on Figures 22b and c as a ratio of (urinary leptin / kidney leptin + urinary leptin). This analysis excludes the contribution of increased delivery of leptin to the kidney via the bloodstream, and instead quantifies only binding within the tubules of the kidney. When analyzed in this manner, biodistribution experiments performed ex-vivo using ^{68}Ga-DOTA-leptin and ^{125}I-leptin similarly confirmed that kidney binding can be partially displaced to the urine (Figure 23b, c). These results mimic the pattern observed via PET imaging. Therefore, uptake of leptin in the tubules of the kidney is partially saturable in rodents, as revealed by both PET imaging and biodistribution analysis.

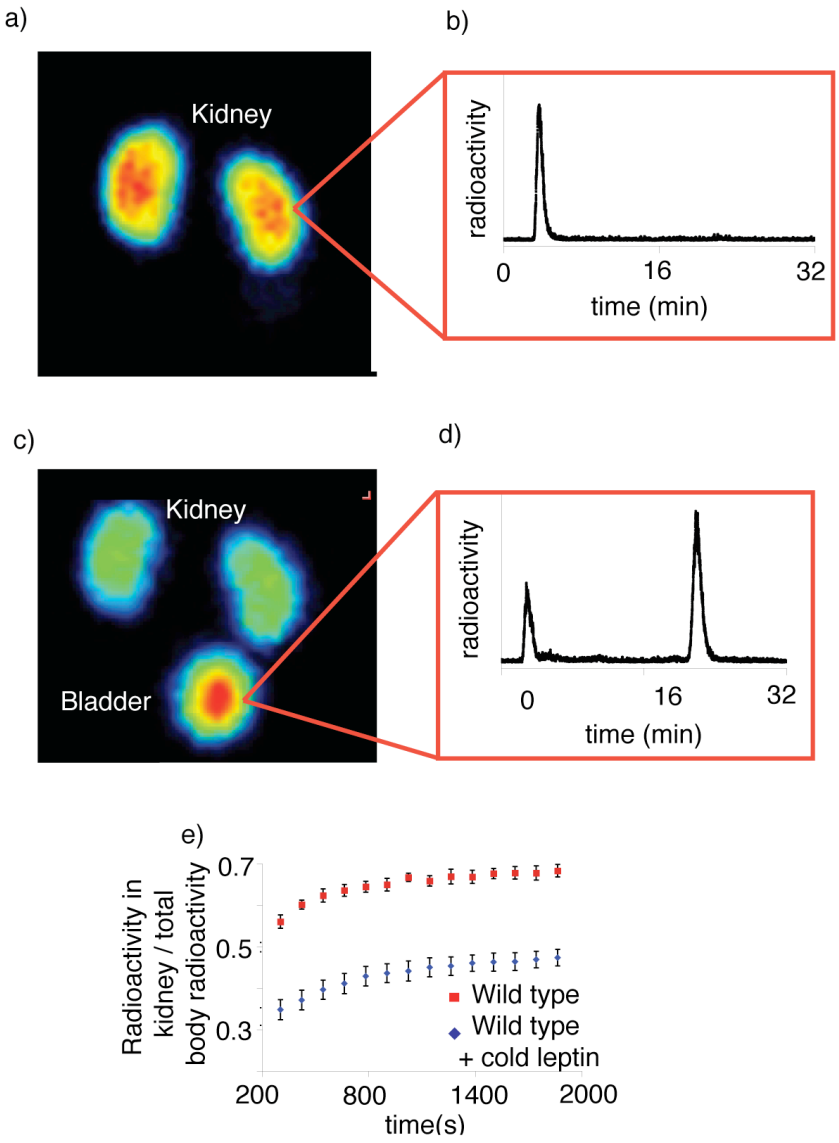

Figure 22. Leptin uptake in the kidney is partially saturable in mice as detected by PET imaging. a) Coronal maximum intensity projection (MIP) of a C57Bl6 wild type mouse injected with ^{68}Ga-DOTA-leptin, with inset of radiochemical HPLC analysis (b) of homogenized kidneys one hour post injection with ^{68}Ga-DOTA-leptin c) Coronal MIP of a C57Bl6 wild type mouse co-injected with ^{68}Ga-DOTA-leptin and 650 μg leptin, with inset of a radiochemical HPLC analysis of the urine 30 minutes post injection (d). e) Time activity curves of the kidney of C57Bl6 wild type mice injected with ^{68}Ga-DOTA-leptin in the presence or absence of 650 μg leptin. Kidney uptake on the Y-axis is defined as the total radioactivity quantified in the kidney, divided by total body radioactivity, with both quantified by region of interest (ROI) analysis. All data are reported as means (n=3) ± s.e.m. Statistical significance of the difference between the two groups was assessed by Student's T-test, $p < 0.01$.

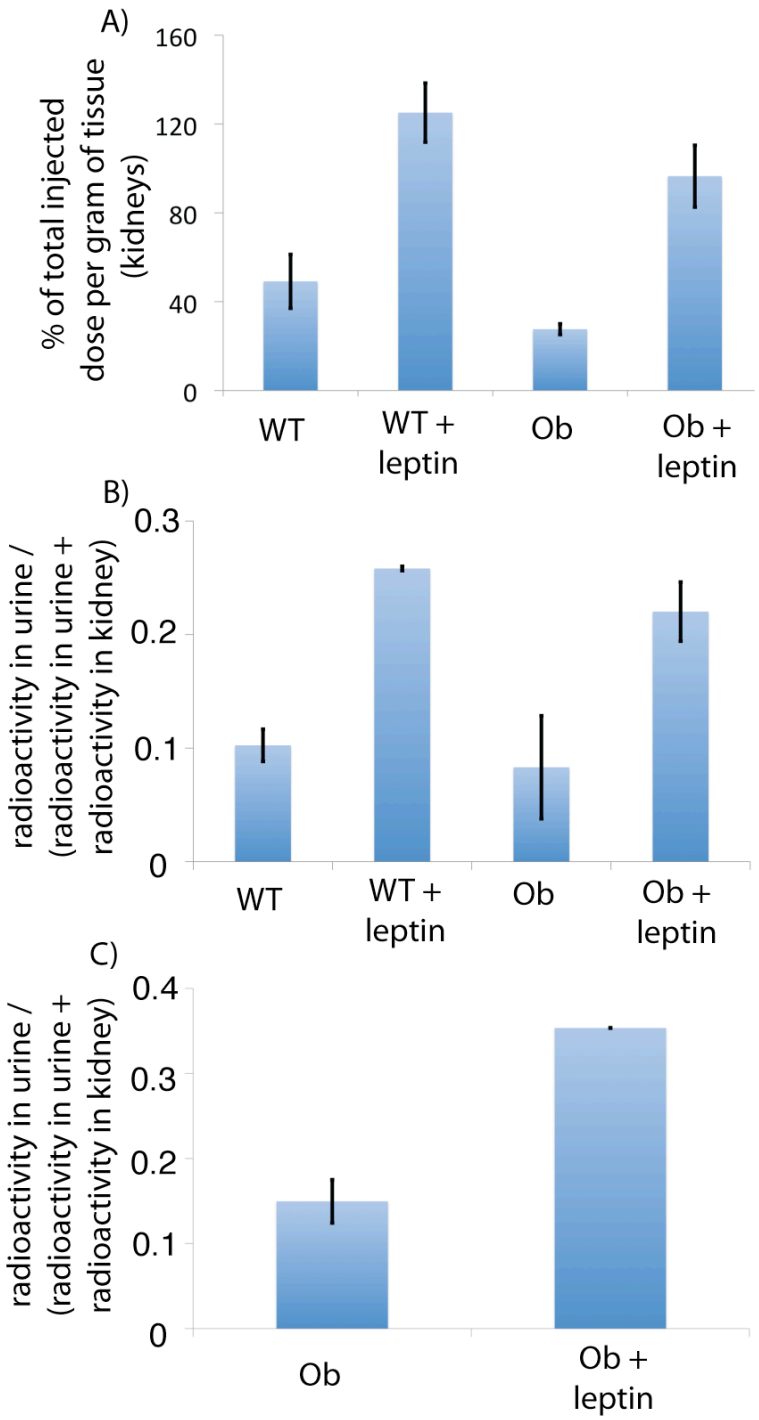

Figure 23. Ex-vivo biodistribution analysis reveals saturable uptake in the kidneys of ob and wild type mice. A) Ex vivo biodistribution analysis of ^{125}I leptin in wild type and ob/ob mice reveals an increase in accumulation of leptin in the kidney when coinjected with cold leptin. B, C) Ex vivo biodistribution results of ^{125}I-leptin (B) or ^{68}Ga-DOTA-leptin (C) in ob/ob and wild type C57Bl6 mice. The fraction of radioactivity appearing in the urine divided by the activity in the kidney plus urine is represented on the Y-axis. n= 2-3 ± S.E.M.

Section 3.4. Comparison of kidney uptake of leptin in ob/ob and ObRΔ/ob/ob mice

In order to test if the ObR is required for the uptake of leptin in the kidney, we compared wild type mice, leptin deficient (ob/ob) and leptin/leptin receptor deficient mice (ObRΔ/ob/ob). ObRΔ/ob/ob mice have a functional knock out for all the isoforms of ObRs and are also leptin deficient. This model allows us to dissect the role of ObRs without the potential confounding factor of elevated leptin levels associated with the receptor deletion. Results from ObRΔ/ob/ob can therefore be directly compared to those obtained in ob/ob littermates. Time activity curves, obtained by ROI analysis of PET images of renal uptake in the three experimental groups are superimposable, suggesting either that ObR mediated uptake is saturated in this model, or that ObR mediated uptake is very low in this organ (Figure 24a).

In order to exclude the possibility that saturation of ObR is responsible for the identical levels of uptake in the kidney in PET imaging, biodistribution experiments were performed in the same animal strains using ^{125}I-leptin. In this assay, substantially less leptin accumulates in the kidneys, owing to the fact that there is no saturation of ObR dependant binding sites, as is the case in micro-PET imaging experiments (e.g. compare Figure 24a, b). There is no statistically significant difference in the uptake of ^{125}I-leptin in the kidney in wild type, ob/ob, and ObRΔ/ob/ob mice as assayed by ex vivo biodistribution analysis (Figure 24b). However, when corrected for the slightly higher blood levels of ^{125}I-leptin in ObRΔ/ob/ob mice (see chapter 4 for a full discussion of this analysis), there is a trend of reduced uptake in the kidneys of ObRΔ/ob/ob vs ob/ob mice (Figure 24c, not statistically significant by Student's one-tailed t test, p value of 0.054). This suggests that there may be a low level of ObR mediated uptake in the kidneys of

mice, which is less than that mediated by other mechanisms. However, ObR mRNA could not be detected in the kidney in rhesus macaques by northern blotting[172], suggesting that ObR could not be involved in the uptake of leptin of the kidney in rhesus macaques. Taken together, our data indicate that ObR mediated uptake is insufficient to account for the very high level of uptake of leptin in the kidney, and another mechanism must underlie this phenomenon.

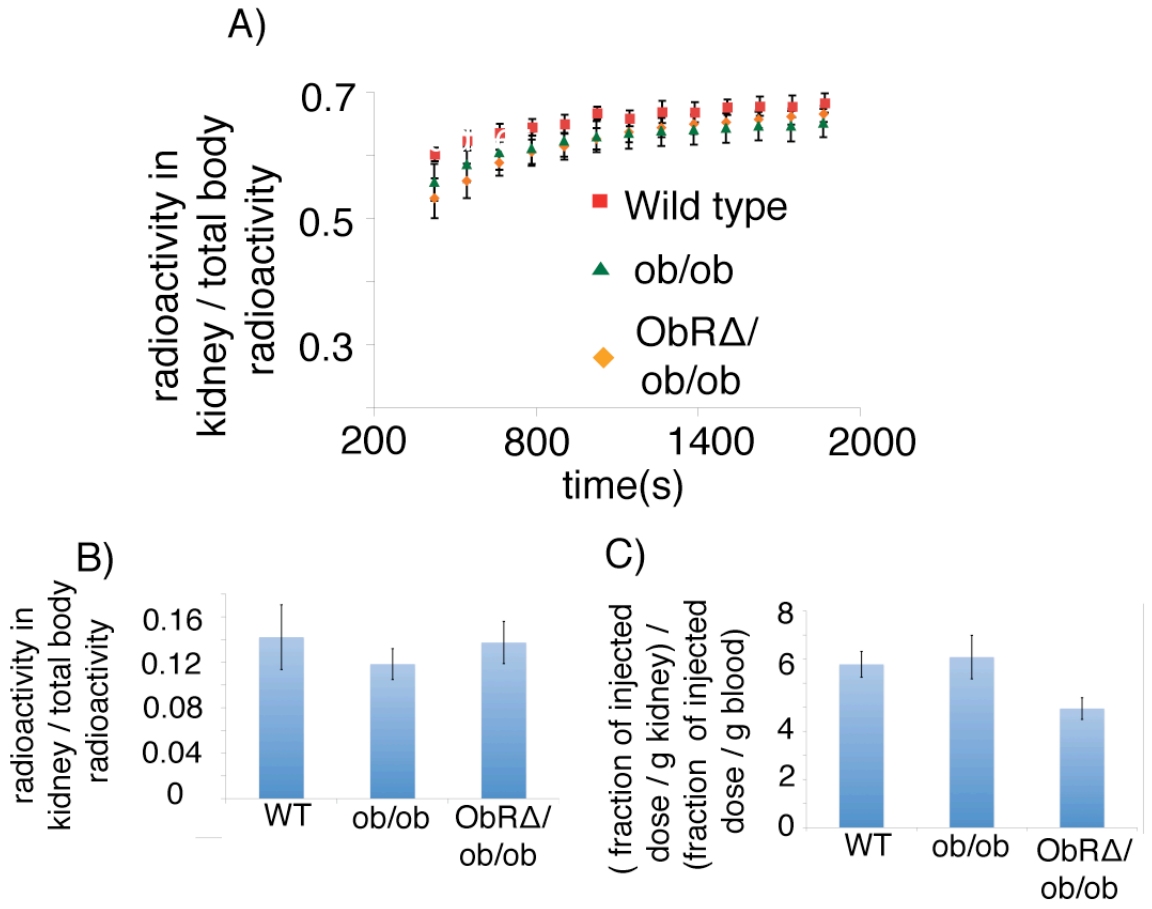

Figure 24. ObR does not mediate the majority of leptin uptake in the kidney. A) A comparison of the uptake of ^{68}Ga-DOTA-leptin in the kidneys of wild type C57Bl6, ob/ob, and ObRΔ/ob/ob mice as judged by micro-PET imaging. Kidney uptake on the Y-axis is defined as the total radioactivity in the kidney, divided by total body radioactivity, with both quantified by region of interest (ROI) analysis. B) A comparison of the uptake of ^{125}I-leptin in the kidneys of wild type C57Bl6, ob/ob, and ObRΔ/ob/ob mice as judged by biodistribution analysis. Kidney uptake on the Y-axis is defined as the total radioactivity quantified in the kidney, divided by total body radioactivity (n = 3-4 ± s.e.m.) C) A comparison of the uptake of ^{125}I-leptin in the kidneys of wild type C57Bl6, ob/ob, and ObRΔ/ob/ob mice as judged by biodistribution analysis, following correction for blood radioactivity. Kidney uptake on the Y-axis is a dimensionless variable, defined as the total radioactivity quantified in the kidney divided by the mass of the kidney, divided by the fraction of injected dose per gram of blood (i.e., the standard uptake value of leptin in the kidney when compared against the reference of radioactivity in the blood, n = 3-4 ± s.e.m).

Section 3.5 Quantitative analysis of renal uptake and metabolism of leptin in megalin knockout mice

We then tested the role of megalin (gp330/LRP2) in the kidney uptake of leptin. Megalin is a 600 kDa type I glycoprotein receptor, which is expressed is various tissues in mammals including the proximal convoluted tubule of the kidney, the choroid plexus, and other sites[167]. Megalin has a similar domain organization to the LDL receptor, with an extracellular domain consisting of four clusters of cysteine rich LDL receptor type A repeats, which are believed to mediate ligand binding, separated by seventeen EGF-type repeats each. Megalin is known to bind to a variety of ligands, including albumin, apolipoproteins, various vitamin and hormone carrying proteins such as thyroglobulin and vitamin-D binding protein, and low molecular weight hormones such as insulin, prolactin, and parathyroid hormone, and mediate their clearance in the proximal convoluted tubule of the kidney[166,167]. Leptin had been previously shown to be endocytosed and degraded by the yolk sac L2 tumor cell line (which expresses megalin[173]) and to bind to megalin *in vitro* using QCM analysis[50]. Additionally, antibodies against megalin were able to co-immunoprecipitate exogenously added leptin from a choroid plexus cell line, and siRNA directed against megalin reduced uptake of leptin into the brain in mice[174]. Taken together, these results suggest that leptin binds to megalin in L2 and choroid plexus cells. Furthermore, these studies suggest the hypothesis that leptin clearance may be mediated by megalin in the proximal convoluted tubule of the kidney, and that leptin transport into the CSF may be mediated by megalin.

In order to test if megalin was responsible for the kidney uptake of leptin *in vivo*, we obtained mice with a kidney specific gene deletion of the receptor megalin (termed

megalin$^{lox/lox}$, ApoE^{cre}, kind gift of T. Willnow, Max-Delbrueck-Center for Molecular Medicine, Berlin)[175]. In this model, cre recombinase expression in the kidney is driven by a fragment of the human apolipoprotein promoter E (apoE) and megalin expression is reduced to 10% of normal levels[175]. We measured leptin levels in urine of megalin$^{lox/lox}$, ApoE^{cre} mice by an Enzyme-Linked ImmunoSorbent Assay (ELISA). Leptin levels are undetectable in the urine of rodents[158] but in megalin$^{lox/lox}$, ApoE^{cre} mice levels are 16.7 ± 2.9 ng/mL (SEM, n=4) indicating a significant leptin loss in urine (Figure 25a). In the urine of the megalin$^{lox/lox}$, ApoE^{cre} mice, leptin is intact as confirmed by western blotting (Figure 25b). These results strongly suggest that megalin is required for the reuptake of leptin in the proximal convoluted tubule of the kidney.

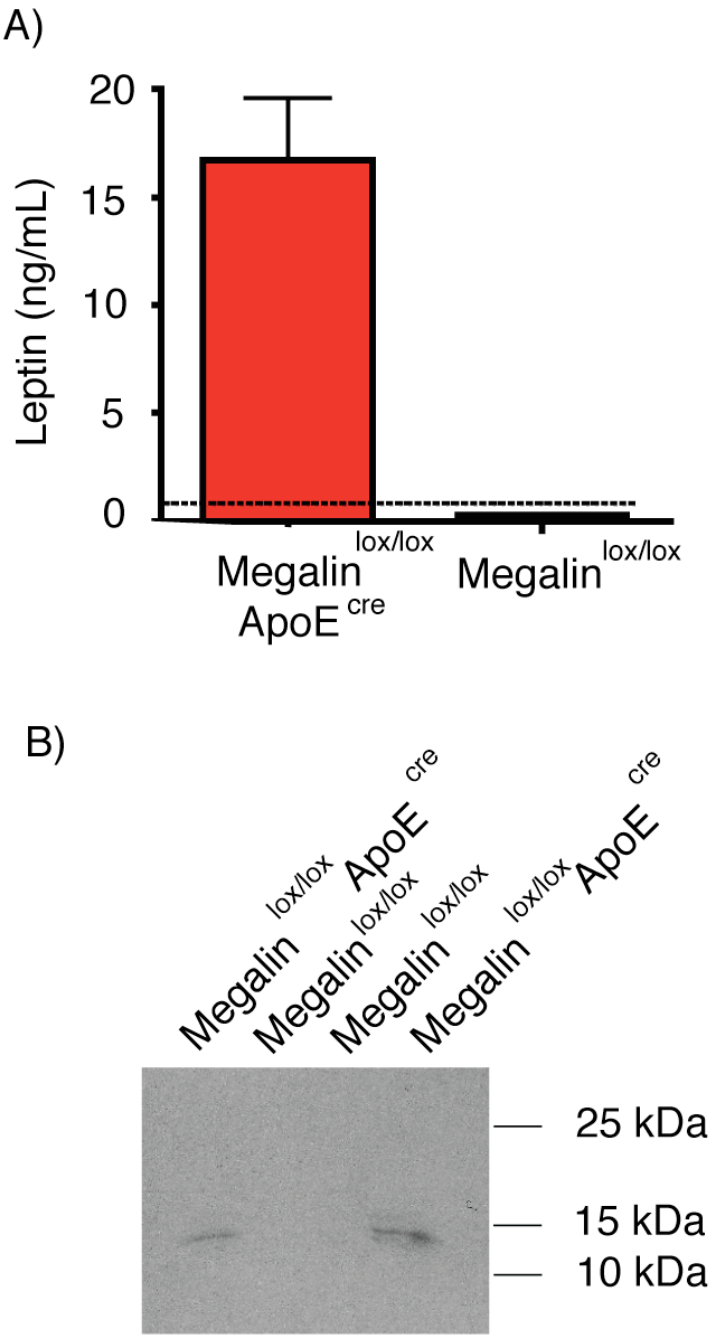

Figure 25. Leptin is released intact in the urine of Megalin$^{lox/lox}$ApoE^{Cre} mice. A) Enzyme-Linked ImmunoSorbent Assay (ELISA) of leptin in the urine of the indicated mouse strains. The dotted line represents the limit of detection (n=3 ± s.e.m., statistical significance of difference between Megalin$^{lox/lox}$ApoE^{Cre} and Megalin$^{lox/lox}$: $p<0.001$). B) Western blot of leptin levels in the urine of megalin$^{lox/lox}$ ApoE^{cre} and megalin$^{lox/lox}$ controls.

We confirmed this hypothesis using PET imaging in the same mouse model. Megalin$^{lox/lox}$, ApoE^{cre} mice were imaged using ^{68}Ga-DOTA-leptin together with their littermate megalin$^{lox/lox}$controls. Our results show that in the basal condition, megalin$^{lox/lox}$, ApoE^{cre} mice have a pattern of distribution of ^{68}Ga-DOTA-leptin in the urinary tract that is similar to one observed when wild type mice are co-injected with cold leptin (Figure 26a,b, compare to 21a, c). Accumulation of ^{68}Ga-DOTA-leptin in the bladder is greatly increased (18.7 vs. 3.5% $p< 0.01$) and in the kidney significantly reduced (54.5 vs. 63.7%, $p<0.05$) when compared to controls (Figure 26d, e). Radiochemical HPLC analysis of the urine from a megalin$^{lox/lox}$, ApoE^{cre} mouse revealed the characteristic 21.6 min peak corresponding to intact leptin (Figure 26c). An ^{18}F-FBA-leptin scan of the same mouse model revealed that the residual uptake in the kidney is still concentrated in the cortex (Figure 27a), suggesting that the remaining uptake in the kidney is either due to the residual megalin expression, or to binding to a second receptor in the cortex of the kidney, rather than binding to other locations in the kidney.

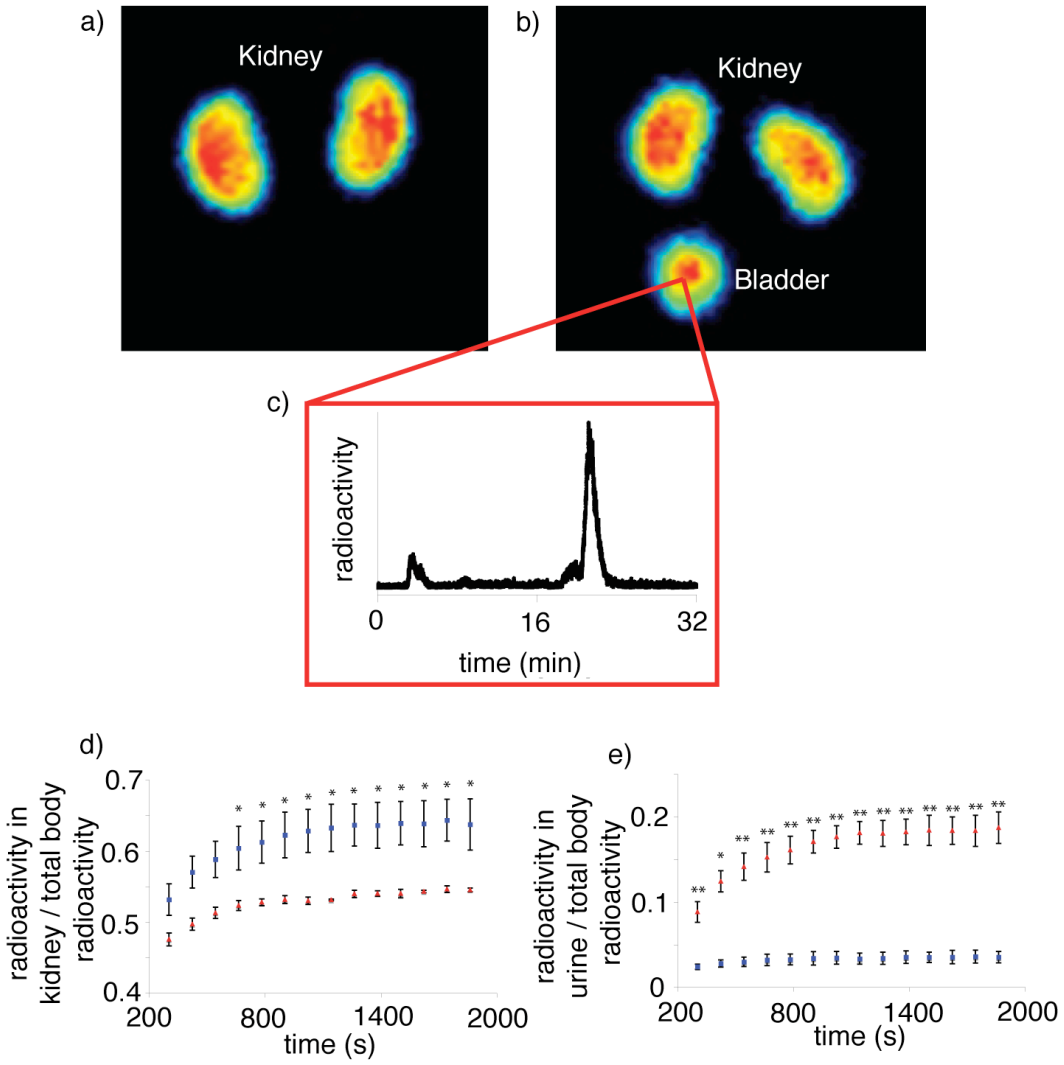

Figure 26. Megalin is required for the uptake of leptin in the kidney *in vivo*. Coronal MIP of a megalin$^{lox/lox}$ control mouse (a) injected with ^{68}Ga-DOTA-leptin and of a megalin$^{lox/lox}$ ApoE^{cre} mouse (b) injected with ^{68}Ga-DOTA-leptin. c) Radiochemical HPLC analysis of urine recovered from a megalin$^{lox/lox}$ ApoE^{cre} mouse, which was injected with ^{68}Ga-DOTA-leptin. d, e) Time activity curves of the uptake in the kidney (d) and bladder (e) of ^{68}Ga-DOTA-leptin in megalin$^{lox/lox}$ ApoE^{cre} (red triangles) and megalin$^{lox/lox}$ (blue squares) mice. Kidney or urinary uptake on the Y-axis is defined as the total radioactivity quantified in the kidney or bladder plus spilt urine, divided by total body radioactivity, with both quantified by region of interest (ROI) analysis. All data are reported as mean ± s.e.m. (n=3). Statistical significance of megalin kidney KO versus lox controls: * $p < 0.05$, ** $p < 0.01$.

The addition of a 30-fold excess of competing leptin during micro-PET imaging led to a further displacement of leptin from the kidney to the urine (Figure 27b, c). A comparison of Megalin$^{lox/lox}$, ApoE^{cre} mice vs. littermate lox controls, imaged using ^{68}Ga-DOTA-leptin, with co-injection of a 30 fold excess of cold leptin, reveals that the pattern of uptake in the kidney and bladder are similar over the first 10 minutes of the scan (Figure 27b). However, in the last 20 minutes of the scan, the lox control animals began to again to take up leptin in the cortex of the kidney, while Megalin$^{lox/lox}$, ApoE^{cre} mice do not. These results show that the reuptake process in the cortex of the kidney in Megalin$^{lox/lox}$, ApoE^{cre} is exhausted following challenge with competing leptin and unable to recover over the course of the scan. These results are consistent with the dramatically reduced expression of megalin in the kidneys of Megalin$^{lox/lox}$, ApoE^{cre} mice. Collectively, these data support a model of leptin renal metabolism in which leptin is freely filtered by the glomerulus in the kidney and subsequently reabsorbed in the proximal convoluted tubule by megalin.

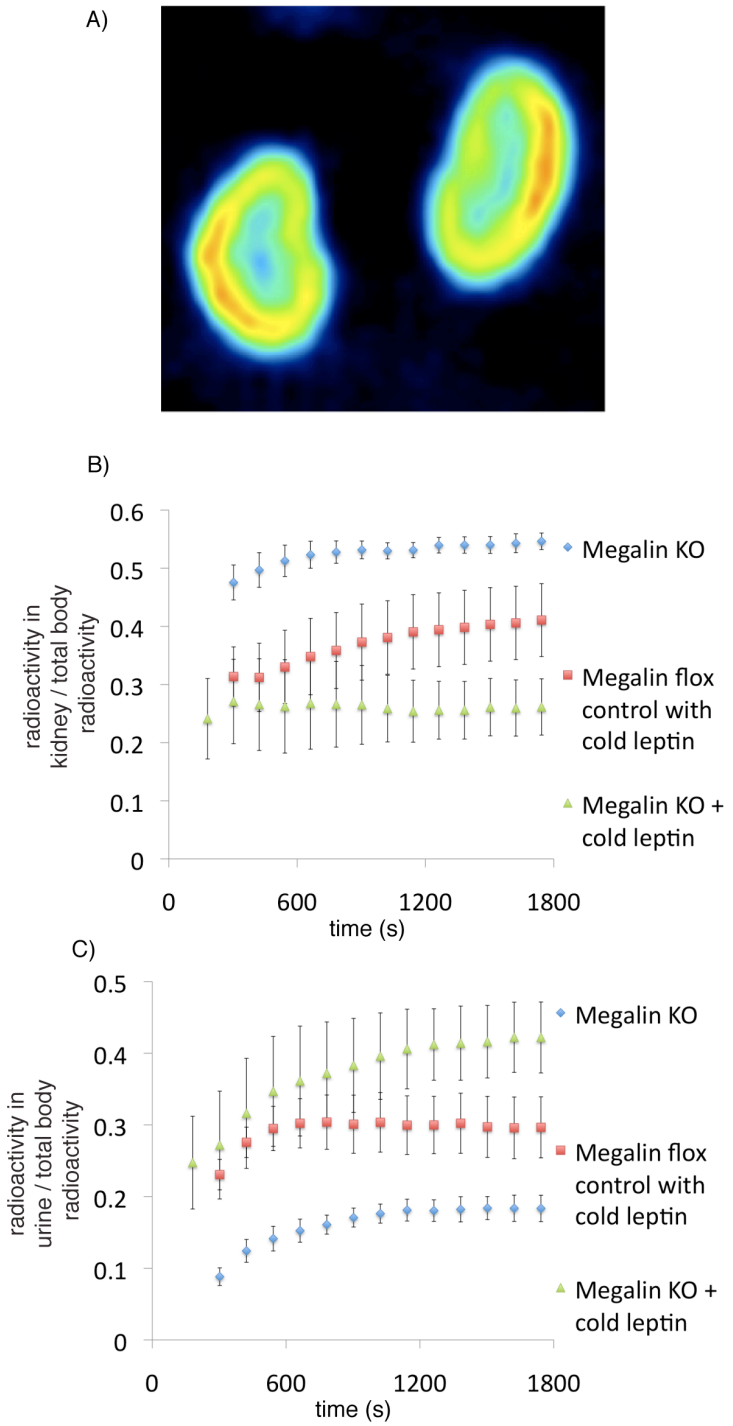

Figure 27. A) ^{18}F-FBA-leptin scan of megalin$^{lox/lox}$, ApoE^{cre} mice reveals that leptin uptake remains restricted to the cortex of the kidneys. B, C) Time activity curves of the uptake in the kidney (B) and urine (C) of ^{68}Ga-DOTA-leptin in megalin$^{lox/lox}$ ApoE^{cre} (red triangles) and megalin$^{lox/lox}$ (blue squares) mice, when the tracer is injected with a 30 fold excess of competing leptin. Kidney or urinary uptake on the Y-axis is defined as the total radioactivity quantified in the kidney or bladder plus spilt urine, divided by total body radioactivity, with both quantified by region of interest (ROI) analysis. All data are reported as mean ± s.e.m. (n=3).

Section 3.6. Megalin mediates the uptake and clearance of leptin in the proximal tubules of kidney

We have described the application of two complementary tracers, ^{18}F-FBA-leptin and ^{68}Ga-DOTA-leptin to micro-PET imaging in mice. Imaging in wild type mice and rats revealed rapid uptake in the cortex of the kidney. Additionally, lower levels of uptake were observed in the visceral organs, head, and bone marrow. Unfortunately, probably due to the relatively large molar quantity of tracer that had to be injected in mice, peripheral ObR receptors were saturated under the conditions of the experiment (see section 5.2 for discussion). Fortunately, this limitation did not apply to PET imaging in rhesus macaques (chapter 4). Thus, in order to study quantitative ObR binding in mice, we relied on biodistribution analysis (Figure 23, 23b, section 4.3). The unique properties of each tracer was required for a full elucidation of the uptake of the hormone in the kidney: while ^{18}F-FBA-leptin revealed uptake of the hormone in the cortex of the kidney (Figure 20, 19b), ^{68}Ga-DOTA-leptin allowed for quantitative analysis of uptake since it is a residualizing tracer. Furthermore, the fact that the biodistribution patterns of both tracers are similar gives confidence in the imaging results.

Using PET imaging in mice we were able to elucidate the role of the multiligand receptor megalin in the clearance of leptin by the kidney. Previous studies had revealed that leptin is cleared by the kidney in mice, nonhuman primates, and humans[84,85,87-91,96,158,163]. We also found high levels of uptake of leptin in the kidneys in mice, rats, and rhesus macaques (Figure 20). Quantification of uptake in the cortex of the kidney by PET revealed that 68.2 ± 1.5% of the tracer was cleared by the kidney over 30 minutes. Furthermore, by coinjection of a 30 fold excess of leptin, a substantial portion of the

hormone could be displaced from the kidney, as only 47.3 ± 2.0% was then taken up. Thus, there is a saturable reuptake system for leptin reuptake in the kidney. Recently, Hama et al. found that leptin binds to megalin, a protein abundantly expressed on the proximal tubules in the kidney[50]. Additionally, leptin had been previously shown to bind to the renal medulla in tissue sections, where ObR is known to be expressed[81,83]. In order to define which receptor was responsible for the clearance of the hormone *in vivo*, we obtained mice with a kidney-specific deficit of the multiligand clearance receptor megalin ($Megalin^{lox/lox}$, $ApoE^{cre}$), and mice deficient in ObR (ObRd/ob/ob). The finding that the megalin deficient mice lost leptin in the urine suggested that this receptor was required for the clearance of leptin. This finding was confirmed by PET imaging, where a significant reduction of leptin uptake in the kidney was observed in mice with a kidney specific deficit of megalin. By contrast, mice lacking ObR had no apparent change in kidney uptake of the hormone, as detected by PET imaging. At present, we cannot exclude the presence of a low level of ObR dependant uptake in the kidney, as biodistribution analysis revealed a small, non-statistically significant difference in the uptake of leptin in the kidney when comparing Ob/ob and ObRd/ob/ob mice (Figure 24c). Thus, taken together with the previous data regarding clearance of the hormone, our PET study reveals that leptin is freely filtered in the glomerulus of the kidney, where it is taken up in the cortex, in a manner that requires the transporter megalin. The implications of this finding are further discussed in section 5.3.

Chapter 4. Ex vivo biodistribution in mice and PET imaging in rhesus macaques reveals ObR dependant uptake of leptin in the brain and a role for leptin in hematopoiesis

Experiments performed in this chapter were the product of a close collaboration with G. Ceccarini (Friedman lab) and E. Butelman (Kreek lab)

Section 4.1. Why study ObR biodistribution and receptor occupancy?

The leptin receptor ObR is widely expressed in peripheral tissues and in the CNS, and its function in the hypothalamus is essential for normal body weight and energy homeostasis (see section 1.3)[19,24]. In addition, leptin modulates the function of several peripheral tissues, in part by direct action of ObR in those organs. To date, despite extensive study of ObR mRNA expression[15,37,176], and leptin binding in tissue sections[83], there is no comprehensive description of leptin biodistribution *in vivo*. The advantage of biodistribution analysis is that it takes into account the physiological (or pathological) pattern of functional cell surface receptor expression. Furthermore, by studying the appropriately genetically modified animals, uptake in organs and tissues can be ascribed to specific receptors. Additionally, current models of leptin resistance, which is present in most obese humans, predict altered biodistribution of the hormone[27,177,178]. Finally, biodistribution analysis could be used to discover novel roles of leptin in an unbiased approach.

Micro-PET imaging in mice using ^{68}Ga-DOTA-leptin and ^{18}F-FBA-leptin was used to elucidate the mechanism of leptin clearance by the multiligand receptor megalin

(see chapter 3). However, we were unable to study ObR mediated uptake using micro-PET in mice, owing to the fact that the specific activity of our tracers is moderate, and a relatively large dose of the hormone (15-30 μg) must be injected to enable visualization of the hormone. Unfortunately, this is a common problem in micro-PET imaging, and is particularly prevalent in mice, which are the most convenient animals for genetic modification[179,180]. One way to overcome this to this would be to improve the specific activity of our tracers, ^{18}F-FBA-leptin, and ^{68}Ga-DOTA-leptin. Potential methods to accomplish this are discussed in section 5.1. Another method would be to forgo PET imaging altogether, and rely on ex-vivo biodistribution analysis, in which a smaller quantity of a radiotracer is injected, the animal sacrificed, and the radioactivity in tissues counted. This technique suffers from the limitations that kinetic data is more difficult to obtain, and that the animal is destroyed in the experiment - this is particularly troublesome for animal models that are difficult or slow to breed (for example ObRΔ/ob/ob mice and Megalin$^{lox/lox}$, ApoE^{cre}). The final way to overcome issues of receptor saturation is to use larger animal models such as primates. This is because a much smaller dose relative to the mass of the animal need be injected (approximately 100 fold less in mg/kg). In this section, we describe the application of ex-vivo leptin biodistribution analysis to mice, and of PET-CT imaging of leptin biodistribution in rhesus macaques. Using these techniques, we found that a subset of tissues were able to take up leptin in an ObR-dependant manner. Most prominently, hematopoietic tissues have a very high level of uptake of the hormone, suggesting that leptin may play an important role in modulating the function of hematopoietic and immune systems by direct action of ObR on these cells.

4.2 Biodistribution analysis of leptin reveals sites of leptin receptor dependant uptake in mice

Biodistribution analysis has been previously applied to leptin (see section 1.6), principally for the purpose of studying the transport of leptin into the brain[17,39,92,181,182]. We chose to use ^{125}I-leptin for biodistribution analysis for several reasons. Firstly, the labeled hormone is commercially available at high specific activity (81 GBq/μmol). Secondly, the long half-life of the isotope (60 days) means that one batch can be used for a series of experiments. Finally, we chose to use ^{125}I in order to avoid the regulatory problems associated in moving animals or radioisotopes in between Rockefeller University (where the animals were housed) to Weill-Cornell Medical College (where ^{18}F and ^{68}Ga is generated).

Our goal was to define which tissues have ObR dependant uptake in mice. In order to assess this, we investigated four groups of mice on the C57Bl6 background - wild type, ob/ob (lacking intact leptin), ObRΔ (lacking all isoforms of the leptin receptor), and ObRΔ/ob/ob (mice lacking both leptin and leptin receptor). The generation and use of ObRΔ/ob/ob mice is necessitated because ObRΔ mice have very high circulating levels of leptin, which would saturate any high affinity binding. By comparing the biodistribution of leptin in an animal strain with or without competing leptin, saturable binding sites can be identified. Secondly, by comparing the biodistribution of leptin Ob/ob vs ObRΔ/ob/ob mice, ObR dependant binding sites can be identified. In a typical biodistribution experiment, approximately 10-15 KBq of ^{125}I leptin (specific activity 81.4 GBq/μmol), corresponding to approximately 150 fmol or 2.4 ng of leptin is injected, in the presence or absence of 650 μg competing leptin. It is important to note

that this injected dose is approximately a 10000 fold reduction in the amount of leptin injected in a typical micro-PET imaging experiment (20-30 μg), which could not saturate binding sites. After 15 minutes, the animals are sacrificed by decapitation, the organs harvested, weighed, and the radioactivity contained therein counted in a gamma counter.

Table 3A reveals the results of the biodistribution analysis of ^{125}I-leptin in various mouse strains. A comparison of wild type or Ob mice in the absence or presence of cold leptin reveals the presence of saturable uptake in the spleen, lung, liver, brain and bone in these animals (Figure 28a, c). In ObRΔ mice, no saturable uptake was seen in any organ. An increase was seen in the uptake of the hormone in the kidney in Ob and wild type mice when co-treated with cold leptin. As discussed in section 3.3, this is probably due to the increased delivery of leptin to the kidney, following saturation of peripheral ObR. No saturable uptake was seen in the heart in Ob/ob or wild type mice. Broadly speaking, our biodistribution results are consistent with prior reports, which found uptake of ^{125}I-leptin in the liver, kidney, brain, and bone marrow in mice[92], and in the kidney, lungs, spleen, and liver in chickens[183].

Next, we tested if ObR was required for the uptake of leptin in these tissues, by comparing the uptake in Ob/ob vs. ObRΔ/ob/ob mice. A comparison of Ob/ob vs. ObRΔ/ob/ob mice reveals that Ob/ob mice take up a greater amount of ^{125}I-leptin in the spleen, lung, liver, brain, bone and fat than their ObRΔ/ob/ob counterparts (Figure 28b, c). Thus, there is ObR dependant uptake in these tissues. The fact that there was a difference between Ob/ob vs. ObRΔ/ob/ob mice in the uptake of ^{125}I-leptin in the fat, and saturable uptake of leptin in the fat of Ob/ob but not wild type mice, suggests that there is functional leptin receptor in fat tissue, but that it is saturated under the conditions of the

experiment in wild type mice. Alternatively, Ob mice may upregulate ObR in fat tissue to compensate for their leptin starved state.

One major caveat in interpreting the data in this manner is that there is a significant variation in blood levels of leptin between the different strains of mice (Table 3a). The cause of this phenomenon is obscure, but may be due to saturation of circulating receptors (ObRe), or other intravascular binding sites. In order to correct for this phenomenon, we present the same data again on Table 3b, where the uptake in tissues is divided by the uptake in the blood, and then multiplied by 1000 by convention to enable comparison with published results[17,39]. This correction allows for a direct comparison of the binding potential for leptin in an organ of an animal to that of other organs within the same animal or others. A more rigorous method would be to serially take blood samples to define an "exposure time" parameter[17,184,185]. However, given the difficulty in generating the correct mouse strains in significant numbers (particularly ObRΔ/ob/ob mice, which must be generated from a cross of double ObRΔ/ob heterozygotes) this is an intractable problem from a technical standpoint. Nevertheless, given that we are simply seeking to define regions of saturable uptake, and to explain which receptor is responsible, this analysis is sufficient.

Broadly speaking, the results from the corrected biodistribution mimic those of the unmodified numbers, revealing saturable, leptin receptor dependant uptake in the spleen, lung, liver, brain, bone, and fat. An additional interesting observation is that there is higher binding in all tissues in Ob mice vs. wild type mice, suggesting either that Ob mice upregulate ObR to compensate for their leptin starved condition, or that wild type mice have their binding sites partially saturated under physiological conditions. Our data

reveal slightly higher uptake of ^{125}I-leptin in the brain than previous reports, possibly owing to either different specific activity of our ^{125}I-leptin preparation, different mouse strains (CD-1 vs. C57Bl6 in our study) or different dissection technique (Figure 29, value of 55 in wild type mice, compare to approximately 25 in intact animals[17], but ranging from 10-125 using perfusion techniques [39,182]). A comparison of the brain uptake of leptin in Ob/ob and ObRΔ/ob/ob mice reveals a significantly different level of uptake in the brain, implying that ObR is required for uptake of leptin in the brain. These data represent the first unambiguous demonstration that leptin receptor is required for full transport and binding of leptin to the brain under intact physiological conditions. Using a capillary perfusion technique, in which mouse brains were perfused with ^{125}I-leptin, Hileman et al. found a significant difference between the uptake of ^{125}I-leptin when comparing wild type and ObRΔ mice[39]. Our data confirm this finding, and extend it to find that the reduced uptake also occurs in mice under physiological, non-brain perfused conditions. Furthermore, this finding controls for the multiple endocrine and immune abnormalities found in Ob and ObRΔ mice.

Our data reveal that the highest level of uptake of leptin in the brain is in Ob mice. Wild type mice have lower uptake, suggesting that their uptake system into the brain is either lower capacity or partially saturated, consistent with previous observations[182]. All animals with competing cold leptin, or lacking leptin receptor altogether, have lower levels of leptin uptake in the brain. Taken together, our data reveal that in mice, that there is saturable, ObR dependant uptake of leptin in the spleen, lung, liver, brain, bone, fat, and possibly in the kidney.

A)

Organ	WT	WT + cold leptin	Ob/ob	Ob/ob + cold leptin	ObRΔ	ObRΔ + cold leptin	ObRΔ/ob/ob
Blood	7.24 ± 0.13	4.33 ± 0.09	3.90 ± 0.16	3.16 ± 0.21	4.33 ± 0.16	2.56 ± 0.38	6.05 ± 0.45
Spleen	20.40 ± 4.02	2.42 ± 0.31	15.70 ± 1.80	2.96 ± 0.73	1.50 ± 0.42	1.33 ± 0.39	5.84 ± 0.39
Lung	11.47 ± 2.93	3.23 ± 1.45	11.05 ± 0.56	3.37 ± 0.32	2.90 ± 0.84	1.86 ± 0.43	3.89 ± 0.43
Liver	4.28 ± 0.14	1.44 ± 0.13	4.08 ± 0.53	1.36 ± 0.22	1.09 ± 0.01	0.84 ± 0.22	1.80 ± 0.22
Heart	3.70 ± 0.36	2.66 ± 0.10	1.85 ± 0.15	2.03 ± 0.04	2.15 ± 0.16	1.98 ± 0.33	1.98 ± 0.33
Brain	0.40 ± 0.01	0.19 ± 0.02	0.26 ± 0.02	0.14 ± 0.01	0.15 ± 0.03	0.09 ± 0.02	0.18 ± 0.02
Bone	3.52 ± 0.055	1.23 ± 0.44	1.55 ± 0.06	0.71 ± 0.05	0.90 ± 0.06	0.65 ± 0.07	0.88 ± 0.07
Fat	1.04 ± 0.18	1.14 ± 0.07	0.50 ± 0.06	0.30 ± 0.05	0.37 ± 0.03	0.23 ± 0.03	0.35 ± 0.04
Kidney	49.1 ± 12.1	125 ± 13	27.6 ± 2.4	96.5 ± 13.9	60.7 ± 5.5	85.6 ± 3.1	29.9 ± 3.9

B)

Organ	WT	WT + cold leptin	Ob/ob	Ob/ob + cold leptin	ObRΔ	ObRΔ + cold leptin	ObRΔ/ob/ob
Spleen	2817 ± 557	558 ± 73	4028 ± 493	936 ± 240	348 ± 53	519 ± 171	966 ± 130
Lung	1584 ± 405	745 ± 335	2835 ± 187	1065 ± 123	672 ± 196	727 ± 200	644 ± 57
Liver	590 ± 22	333 ± 30	1047 ± 142	428 ± 76	253 ± 10	332 ± 100	298 ± 49
Heart	510 ± 51	615 ± 26	475 ± 44	644 ± 43	498 ± 42	773 ± 174	445 ± 31
Brain	55 ± 2	44 ± 6	66 ± 5	43 ± 5	36 ± 7	34 ± 9	30 ± 4
Bone	486 ± 12	295 ± 12	398 ± 22	225 ± 21	209 ± 17	254 ± 48	146 ± 14
Fat	145 ± 25	263 ± 18	127 ± 17	95 ± 16	86 ± 7	90 ± 18	58 ± 7
Kidney	6783 ± 414	28887 ± 336	7083 ± 66	30533 ± 2620	14017 ± 641	33497 ± 5041	4945 ± 450

Table 3. Summary of biodistribution analysis of ^{125}I-leptin in various mouse models. A) Uptake in % injected dose/g tissue (i.e., the percent of the total injected dose in a tissue, divided by the weight of that tissue). Results are an average of 3-4 experiments ± s.e.m. B) Uptake in the indicated tissues when corrected for blood values. Uptake values from A were divided by the blood uptake value, and multiplied by 1000 to obtain a normalized standard uptake value. Results are an average of 3-4 experiments ± s.e.m.

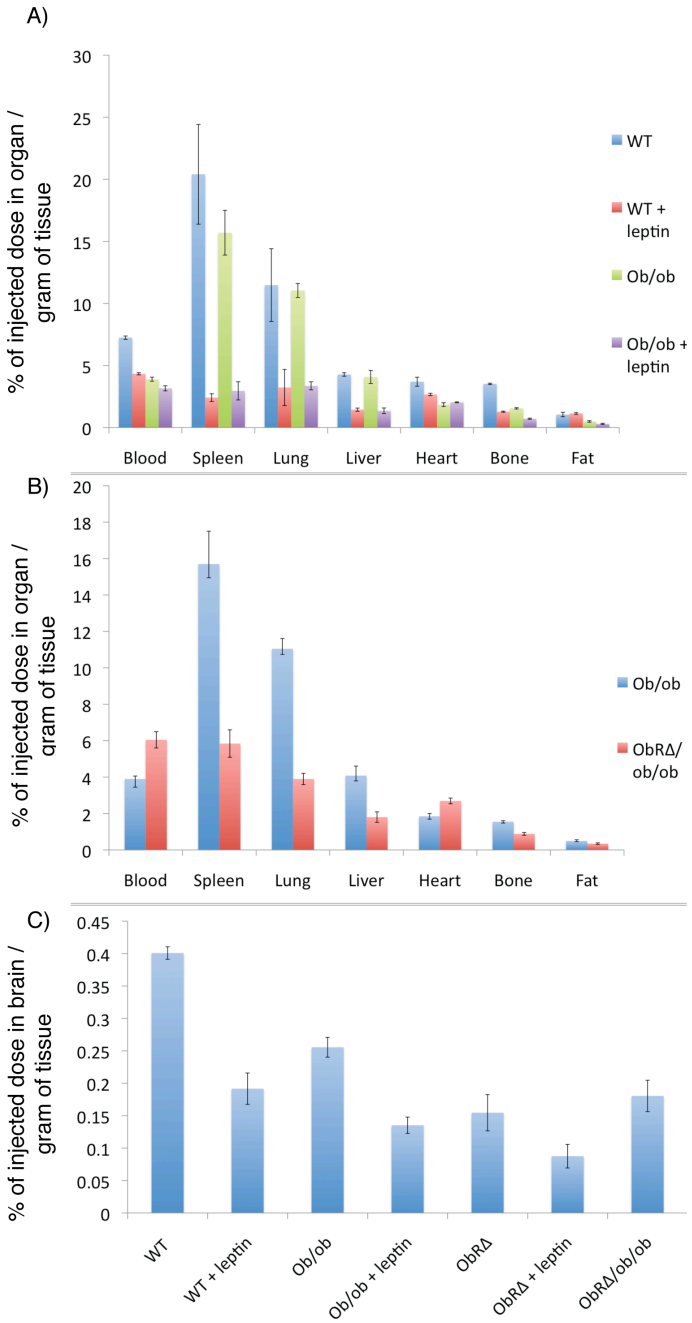

Figure 28. Biodistribution results using ^{125}I reveal saturable and leptin receptor dependant uptake in tissues. Animals were sacrificed 15 minutes after injection with 15 KBq ^{125}I-leptin, and the indicated tissues weighed and counted in a gamma counter. The % of the total injected dose in the indicated tissue, divided by the weight of the tissue is plotted on the Y-axis. A) A comparison of wild type and Ob/ob mice with and without coinjection with 650 μg leptin. B) A comparison of Ob/ob vs ObRΔ/ob/ob. C) A comparison of the uptake of leptin in the brain in various animal models.

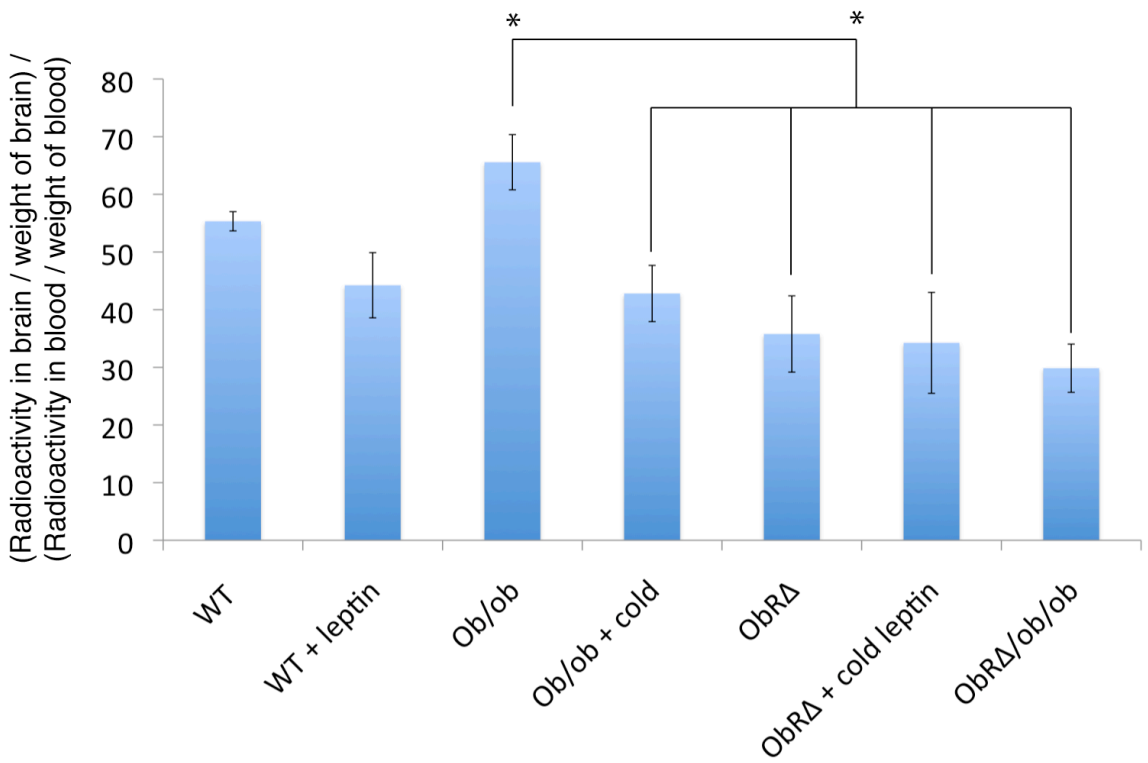

Figure 29. Uptake of ^{125}I-leptin in the brain is mediated in part by ObR. Animals were sacrificed 15 minutes after injection with 15 KBq ^{125}I-leptin, and the brain and blood were collected, weighed, and counted in a gamma counter. On the Y axis the uptake is represented as 1000 times (% Injected dose / mass of brain in mg) / (% injected dose in blood / mass of blood in mg), i.e. the standard uptake value of leptin in the brain when using the blood as a reference tissue (n = 3-4 ± s.e.m). Statistical significance was assessed between the Ob/ob group and the other groups connected by lines by Student's one-tailed t-test, $0.05 < p$.

Section 4.3. A rationale for imaging of leptin biodistribution in non-human primates

The encouraging results generated from micro-PET imaging and biodistribution studies in rodents led us to consider other animal model systems with greater relevance to leptin biology in man. Rhesus macaques are a commonly used species of laboratory monkey in which the basic physiology of leptin has been characterized, using essentially the same approaches followed in mice. The cloning of rhesus macaque leptin followed shortly after the cloning of mouse and human leptin[186]. The sequence homology of rhesus to mouse and human leptin is 84% and 91%, respectively (Figure 30). Rhesus ObR is

found in adipose tissue, liver, choroid plexus, and hypothalamus, where it is expressed principally in the arcuate and ventromedial hypothalamic nuclei in POMC and AgRP neurons[172,187]. Leptin levels in macaques are correlated with the total weight of the animal, and centrally administered human leptin is able to induce weight loss while peripherally administered leptin is not[188,189]. Leptin has a biphasic half-life in macaques with a second-phase half life of 96 minutes[86]. Leptin also appears to play a role in the immune system in macaques, as they produce leptin in response to endotoxin injection[190]. Furthermore, leptin treatment reduces the production of other inflammatory factors such as IL-6, TNF-α, and cortisol in endotoxin injected monkeys[191]. Thus, the role of leptin in energy homeostasis and regulation of immunity superficially resembles the homologous system in mice. It is likely that further study of leptin physiology in macaques will yield useful information of relevance to humans.

PET imaging of leptin biodistribution in rhesus macaques provides additional information which could not be obtained in mice. Firstly, leptin function and physiology is more likely to mimic that in humans due to the closer evolutionary relationship between the species. Secondly, due to their larger size, Macaques can be imaged in a clinical PET-CT scanner. Thus, the functional metabolic information provided by the PET scan can be fused to the anatomical information provided by the CT scan. Additionally, a lower dose of isotope relative to the size of the animal can be injected, which reduces saturation of receptor binding sites. Therefore, we decided to undertake a PET study of leptin biodistribution in rhesus macaques.

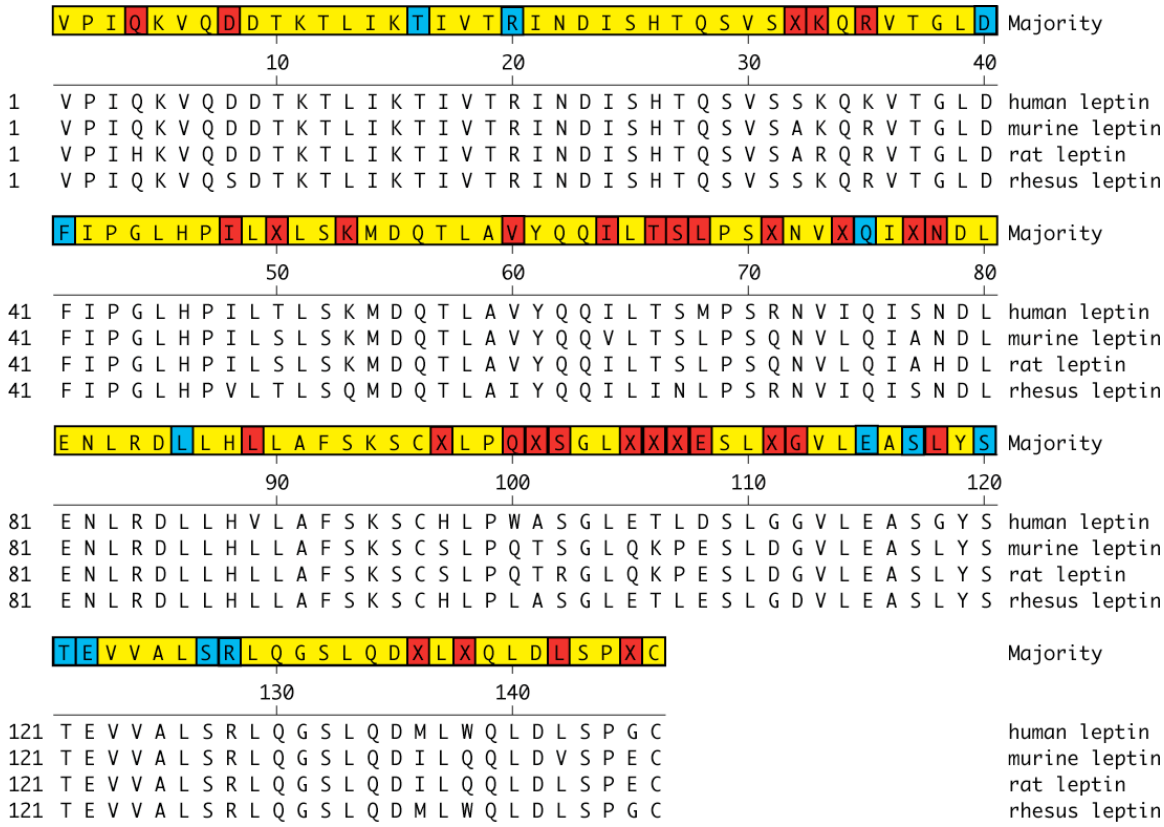

Figure 30. Sequence alignment of leptin in mammalian species referred to in this section. Sites of divergence are highlighted in red. Residues which are believed to be essential for ObR binding or activation[133,134] are highlighted in blue.

4.4. PET imaging of leptin biodistribution in rhesus macaques.

In a typical PET-CT imaging experiment, ^{68}Ga-DOTA-leptin is introduced via a venous catheter, with or without 1 mg of competing cold leptin administration prior to tracer administration. PET imaging of rhesus macaques injected with ^{68}Ga-DOTA-leptin revealed a high level of uptake in the sphenoid bone, mandibles, head of the humeri, vertebral bodies, pelvic bones, sternum, and kidney (Figure 31a-d). PET-CT fusion images reveal that the tracer is confined to the inner portion of these bones (Figure 32). One possibility is that this binding represents an artifact of imaging the biodistribution of murine leptin in a rhesus monkey. In order to exclude this possibility, we performed a

competition experiment in which rhesus leptin was used to displace ^{68}Ga-DOTA-(murine)-leptin in a PET imaging experiment. Thus, we expressed rhesus leptin in *E. coli* and purified and refolded it as described in the methods (Figure 33A, B). In the aforementioned (murine) ObRb-STAT3-luciferase activation assay (Figure 6), rhesus leptin had identical activity to human leptin (Figure 33C, EC_{50} of 0.44 nM). In a ^{68}Ga-DOTA-leptin scan with the coinjection of a 20-fold excess of rhesus leptin, a striking difference was observed, and the tracer localized almost exclusively to the kidney (Figure 31e, f). Nearly identical results were obtained with a similar competition scan with murine leptin (data not shown). Thus, the binding of ^{68}Ga-DOTA-leptin to these tissues almost certainly mimics the binding activity of rhesus leptin.

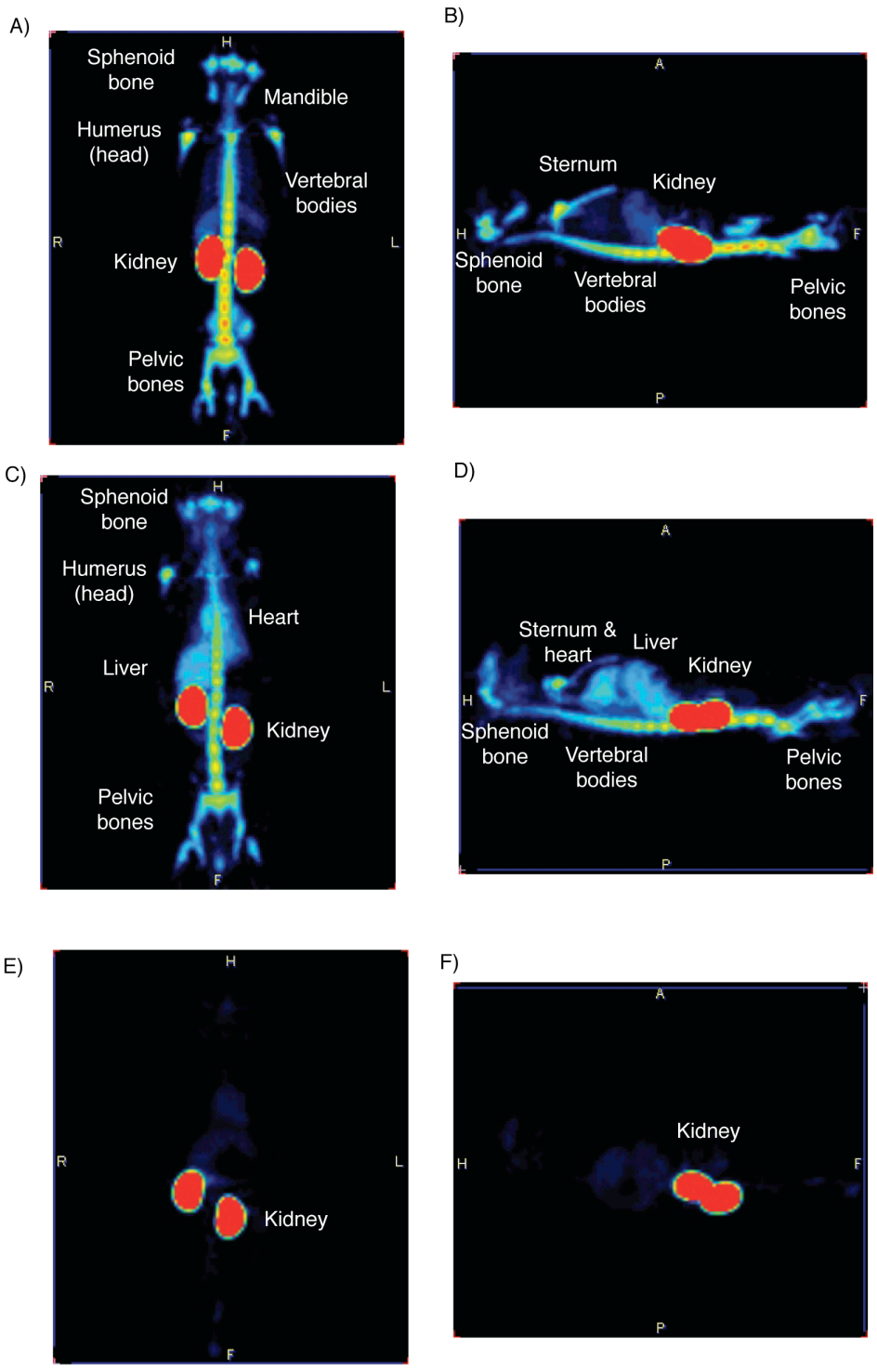

Figure 31. Maximum intensity projections (MIPs) of PET scans using 9 – 25 MBq of ^{68}Ga-DOTA-leptin (corresponding to approximately 50 μg) as a tracer in rhesus macaques. A,B) Subject #1, in coronal and sagittal planes. C,D) Subject #2 in coronal and sagittal planes. E,F) Subject #1, with 1 mg of competing cold rhesus leptin co-injection, in coronal and sagittal planes.

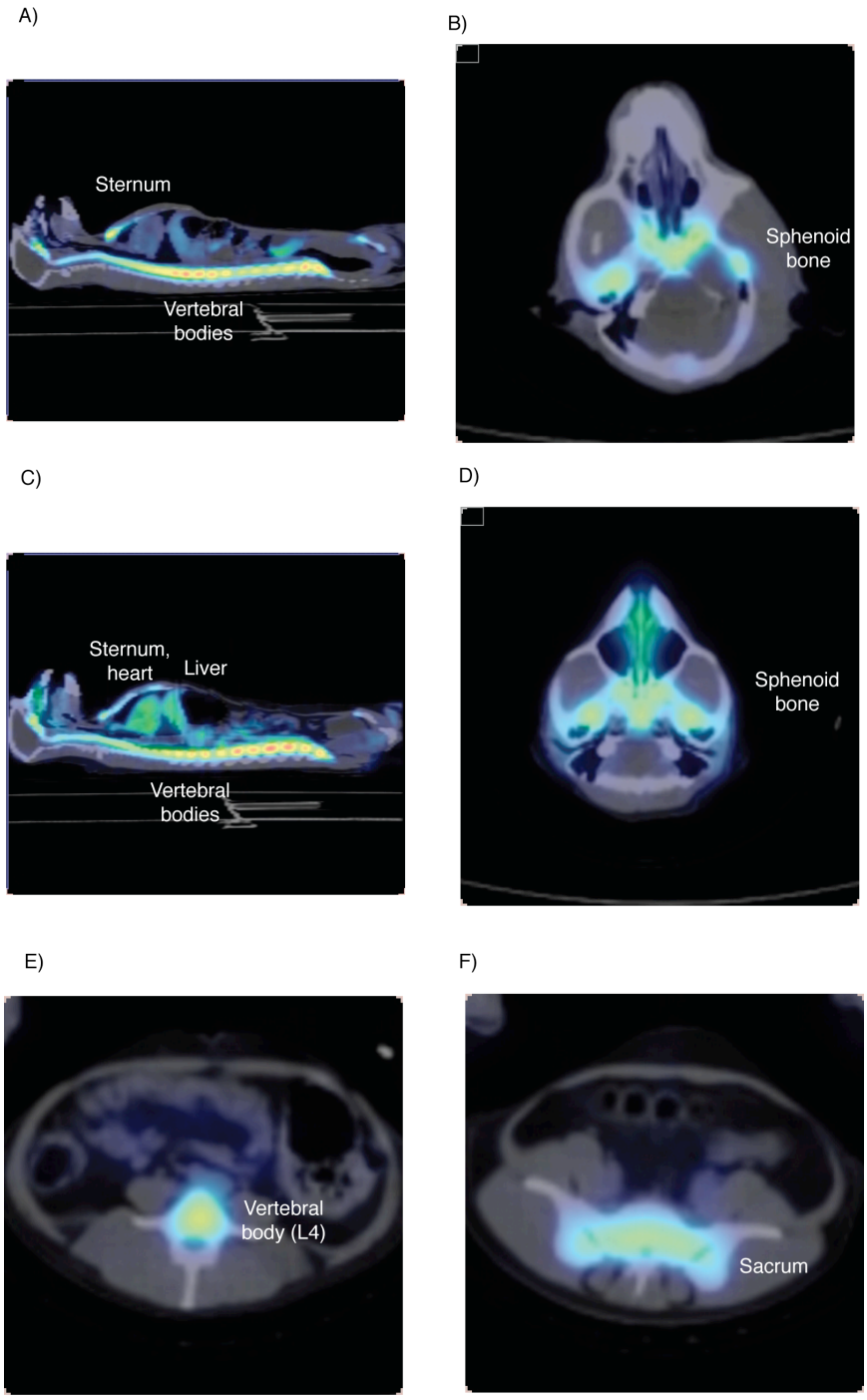

Figure 32. PET-CT fusions of two rhesus macaques injected with ^{68}Ga-DOTA-leptin (10-30 MBq per experiment). A) Subject #1, sagittal view at midline. B) Subject #1, axial view at the base of the skull. C) Subject #2, sagittal view at midline. D) Subject #2, axial view at the base of the skull. E) Subject #2, axial view through the L4 vertebral body. F) Subject #2, axial view through the sacrum.

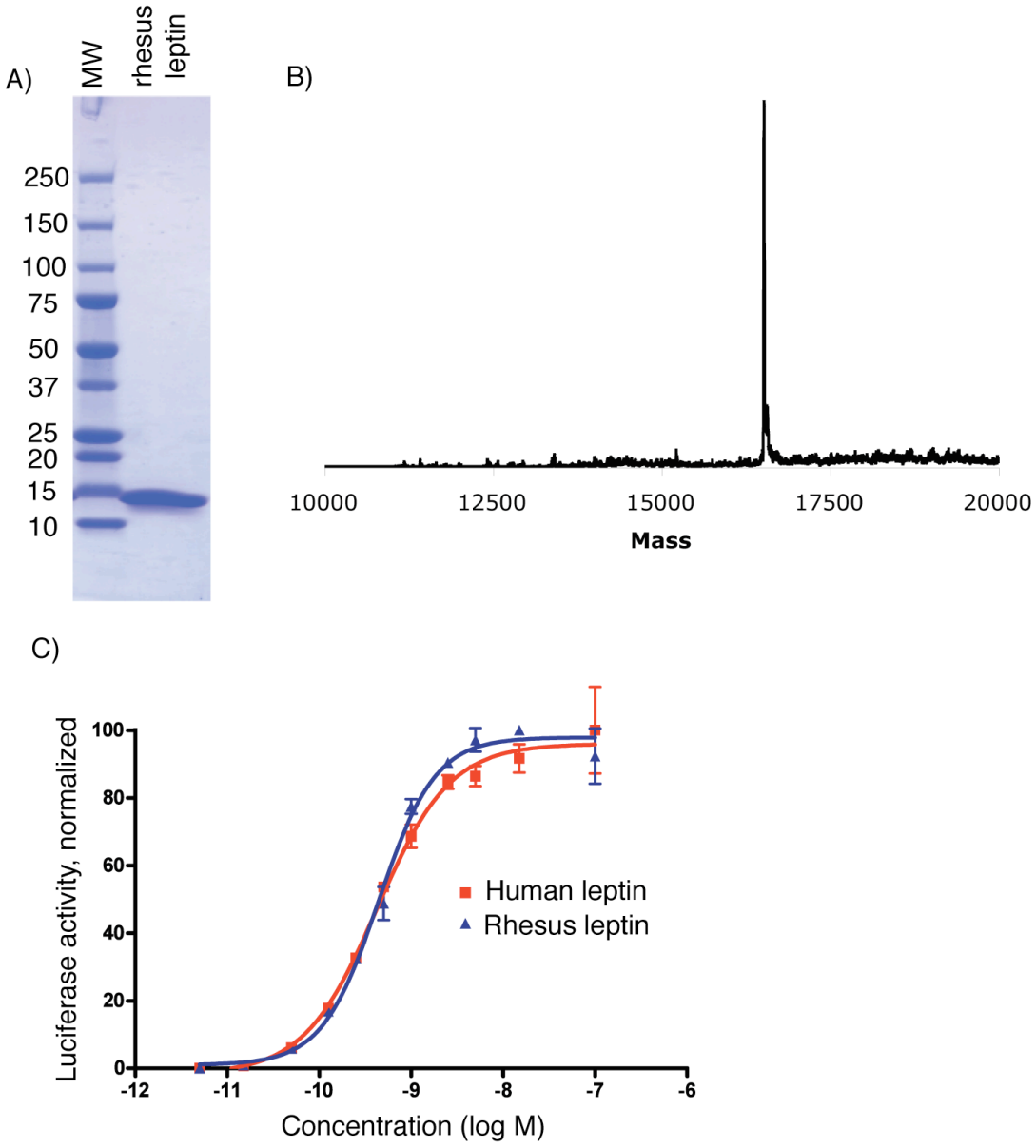

Figure 33. Expression and purification of rhesus leptin. a) SDS-PAGE on a 4-20% gradient gel of purified rhesus leptin, stained with Coomassie blue. b) ESI-MS reconstruct of purified rhesus leptin (Calculated mass 16529.1, obtained 16529.7 ± 4.1). c) Leptin receptor-STAT3 dependant luciferase assay comparing the activity of rhesus leptin and human leptin obtained from a commercial source. EC_{50} for rhesus leptin = 0.44 nM (95% confidence intervals 0.37 – 0.53 nM). EC_{50} for human leptin = 0.42 nM (95% confidence intervals 0.32 to 0.54 nM, n = 2 per group ± s.d).

The high level of uptake of the tracer in the kidney likely represents uptake in the proximal convoluted tubule by the endocytic receptor megalin (see chapter 3). The pattern of uptake in the sphenoid bone, sternum, head of the humerus, and vertebral bodies mimics that obtained with the bone marrow targeting tracer ^{18}F-fluorothymidine (FLT)[192]. Based on the similarity between the images generated with these two tracers, we propose that the high levels of uptake in the axial skeleton represent binding to red bone marrow. Red bone marrow is the site of hematopoiesis in adult rhesus macaques, and is composed of hematopoietic precursors, blood vessels, and stromal cells such as adipocytes and reticular cells.

Time activity curves of uptake of ^{68}Ga-DOTA-leptin are presented on Figure 34. Four distinct patterns of uptake were observed. Firstly, radioactivity in the bone marrow stays constant over time course of the scan, at a high level. This pattern suggests the presence of a very high level of saturable receptors. The tracer accumulates continually in the kidney over the course of the scan, mimicking the effect observed in mice (see Figure 22e). This pattern is consistent with the clearance of the hormone by the receptor megalin in the kidney (see chapter 3). Interestingly, displacement increased the activity observed in the kidneys. These results are consistent with a high affinity-binding site in the bone marrow (presumably leptin receptor), and a lower affinity site in the kidneys (presumably megalin). Thus, in the absence of competing leptin, the tracer is free to bind to peripheral leptin receptors. However, in the presence of saturating leptin, binding to the high affinity sites is blocked, and leptin is instead filtered by the kidney, where it binds to megalin, in a lower affinity interaction. In comparison with mice, the rate of clearance of ^{68}Ga-DOTA-leptin in rhesus macaques is slower, as judged by the uptake of the hormone in

the kidney (compare Figure 22e and 35); this is consistent with a previous comparison of leptin pharmacokinetics in mice and monkeys[86]. In the heart, an identical pattern of disappearance of the tracer is observed in the displacement and tracer-only scans. This pattern suggests that there is no saturable uptake in the organ, and that the observed radioactivity simply represents intravascular leptin. Finally, the liver initially has the same level of the tracer, but as the scan progresses, the tracer clears more rapidly from organs in the competing scan than in the tracer-only scan. This pattern suggests the presence of a low level of saturable receptors in the organ, which is initially overshadowed by the blood pool leptin. As the leptin in the blood clears to the kidney, the saturable uptake becomes detectable. Thus, collectively these data indicate that there is the presence of a very high level of saturable uptake leptin in the bone marrow, and lower levels of uptake in the liver.

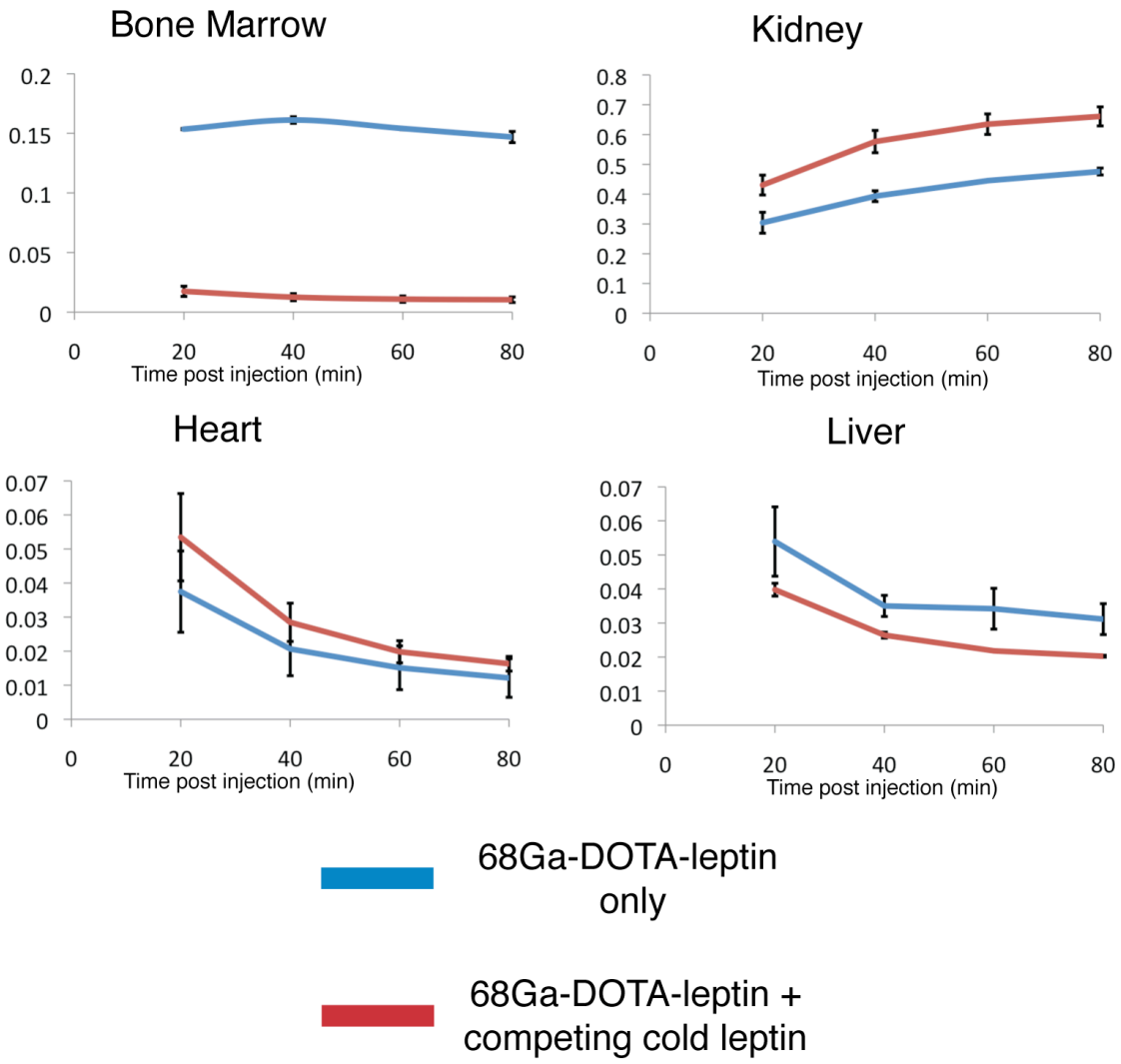

Figure 34. Time activity curves of uptake of ^{68}Ga-DOTA-leptin in rhesus macaques in selected organs. Uptake on the Y axis is the fraction of the injected dose in the corresponding tissue, i.e. the total radioactivity in the indicated tissue, divided by the total body radioactivity, as determined from ROI analysis of the PET-CT fusion scan (average of two animals per group +/- s.e.m.)

4.5. A comparison of mouse biodistribution and rhesus monkey PET results suggests a role for leptin in hematopoiesis

In order to define the molecular mechanism of leptin uptake in various tissues, we performed biodistribution analysis using ^{125}I leptin in mouse models. Using this method, saturable, ObR dependant uptake of the hormone was found in the brain, fat, spleen, lung, liver, and bone (Figure 28a). Of these tissues, the spleen and bone are sites of hematopoiesis in adult mice[193]. Additionally, biodistribution analysis in mice lacking leptin receptor reveals that the uptake in these sites is dependant on ObR (Figure 29). Uptake in the fat was relatively low, and saturated in wild type mice, suggesting that these receptors are generally saturated under normal physiological conditions. The low level of saturable uptake in the brain is consistent with previously published results[17,39]. Importantly, our results provide direct proof that leptin receptor mediates binding in the mouse brain, and that this system is not fully saturated under normal physiological conditions (Figure 29). At present, our results also suggest a low level of ObR mediated leptin uptake in the kidney, in addition to the much higher level of megalin mediated uptake, although a larger data set is needed to conclusively prove this hypothesis. Much higher levels of ObR dependant leptin uptake were also seen in the lungs, liver, bone, and especially in the spleen.

In rhesus macaques, saturable uptake of the hormone was found in the bone marrow and liver (Figure 34). Uptake in the bone marrow was particularly prominent (Figure 31, 32). In adult primates, the bone marrow is the site of hematopoiesis[193]. Unfortunately, the same quantitative technique could not be applied to understanding the

biodistribution of leptin using PET imaging in mice. This is because a relatively large amount of tracer must be injected in mice (15-30 μg per scan), potentially saturating peripheral binding sites. Nevertheless, we were able to see a low level of tracer uptake in the bone marrow in rats injected with ^{68}Ga-DOTA-leptin (see Figure 20c). Another important result is that the highest level of uptake was observed in the hematopoietic system in mice (in the spleen and bone marrow), and in rhesus macaques (the bone marrow). Taken together, these results strongly suggest that leptin plays a role in modulating the immune and hematopoietic systems by direct action on hematopoietic precursors.

Chapter 5. Discussion

5.1. A comparison of the properties of ^{18}F-FBA-leptin and ^{68}Ga-DOTA-leptin, and potential improvements to the tracers

The properties of the three radiolabeled tracers referred to in this thesis are presented on Table 4. ^{68}Ga-DOTA-leptin and ^{18}F-FBA-leptin emit positrons, allowing for PET imaging, while ^{125}I decays by electron capture to produce β^- particles which cannot be used for PET imaging. The specific activity of the PET-imaging tracers is comparable, with that of ^{18}F-FBA-leptin being slightly higher than ^{68}Ga-DOTA-leptin. The major advantage of the ^{18}F-FBA-leptin tracer is the resolution of the images generated. Thus, while imaging of ^{68}Ga-DOTA-leptin reveals uptake of the tracer in the kidney, the higher resolution of ^{18}F-FBA-leptin shows that the protein is absorbed principally in the renal cortex (Figure 20, 19). The labeling chemistry and protein labeling sites are different, but both PET tracers retain native-like bioactivity (Figures 7, 14). Finally, the fate of the labeled tracers following receptor binding and endocytosis are different: ^{68}Ga-DOTA-lysine a residualizing tracer, while the unidentified metabolite of ^{18}F-FBA-leptin diffuses freely from cells, as does ^{125}I-iodotyrosine from ^{125}I-leptin treated cells (Figure 21). It is important to note that there were no detectable physiological effects of any labeled tracers in any PET imaging experiments we performed, demonstrating that we were performing our imaging experiments at tracer levels. Furthermore, the similar biodistribution pattern generated by all tracers used provides confidence that the modified proteins mimic the behavior of intact leptin.

Tracer	^{68}Ga-DOTA-leptin	^{18}F-FBA-leptin	^{125}I-leptin
Specific activity	5.5 - 11 GBq / μmol	9 - 17 GBq / μmol	81 GBq / μmol
Half-life	68 minutes	110 minutes	60 days
Imaging resolution	2.3 - 11.5 mm	0.65 - 2.7 mm	No imaging
Labeling sites	Amines (lysine and N-terminus)	C-terminus	Tyrosines
Labeling method	Metal chelation	Oximation	Peroxidase mediated iodination
Intracellular metabolism	Residualizing	Diffusible	Diffusible

Table 4. A comparison of the properties of the three radioactive tracers used in this thesis. Resolution information is taken from the model study of Sanchez-Crespo et al[101].

A comparison of ^{68}Ga-DOTA-leptin to the other ^{68}Ga-chelate labeled proteins from the literature is presented on Table 5. The radiochemical properties of our tracer compares favorably with the previously reported ^{68}Ga labeled leptin derivative. The improved yield of the radiochemical synthesis for ^{68}Ga-DOTA-leptin is likely due to the high stoichiometry of chelator to protein (4:1), when compared to the prior report (1:1)[97]. The synthesis of ^{68}Ga-DOTA-leptin is highly optimized with respect to temperature, concentration of the protein, and time of reaction, and is not likely to improve. Thus, the only way to improve this tracer would be to start with more ^{68}Ga. During the course of our experiments the ^{68}Ge/^{68}Ga generator produced 0.15-0.3 GBq of ^{68}Ga, while generators

producing up to 3.7 GBq are commercially available. A 10-20 fold improvement in specific activity could easily be obtained by using such a generator. An alternate method would be to use ^{64}Cu to label DOTA-leptin. This isotope has recently become popular owing to the high resolution of the images it generates (Bmax of 0.65 MeV, comparable to 0.63 MeV for ^{18}F, see table 2)[105]. For example, a ^{64}Cu labeled vascular endothelial growth factor (VEGF) derivative has recently been applied to PET imaging in various animal models[194-197]. The major drawback in the use of this isotope is the half-life of 12.8 hours and the low percentage of positrons it emits (18%), which results in a high radiation burden to any animal in which it is injected.

Ref	Protein	Chelator	Yield (%)	Specific activity	Note
[198]	Antibody	DTPA	N.R.	N.R.	
[97]	Leptin	DTPA	N.R.	1.7 - 6 GBq/μmol	3.7 GBq generator
[137]	LDL	DTPA	N.R.	0.185-0.370 GBq/mg	
[199]	Albumin	DOTA	45	11 GBq/μmol	
[138]	EGF	DOTA	N.R.	12-20 GBq-μmol	90 degree microwave labeling
Chapter 2	**Leptin**	**DOTA**	**25.7 ± 4.7**	**5.5 - 11 GBq/μmol**	**0.15 - 0.37 Gbq generator**

Table 5. A comparison of ^{68}Ga-DOTA-leptin to previously reported ^{68}Ga protein tracers. N.R. = not reported.

^{18}F-FBA-leptin is compared to other ^{18}F labeled proteins reported in the literature on Table 6, and Figure 35. Our labeling method, based on expressed protein ligation[144,200], is unique among the ^{18}F labeling techniques in that it is intrinsically site-specific and directed to the C-terminus[163]. Furthermore, the yields of the two reactions in our synthesis, the preparation of ^{18}F-FBA and the aniline-accelerated oximation, are comparable to the best methods published. However, the specific activity of ^{18}F-FBA-leptin order of magnitude lower than the best prior reports of ^{18}F-labeled proteins[159,201,202]. This is for three reasons: firstly, the reformulation of ^{18}F-FBA into water is time consuming, and requires multiple handling steps. Furthermore, as our synthesis is manual, a relatively small amount of starting radioactivity can be used due to safety concerns. Finally, the recovered yield of our labeling reaction is relatively low owing to a

tendency of our labeled protein to precipitate. Finally, due to the tendency of leptin to precipitate, we must perform our labeling reaction on ice. Most prior ^{18}F labeling reactions have been conducted at elevated temperatures, which accelerates the conjugation. Optimization of the synthesis along the lines of several previous reports could considerably improve the specific activity of our protein, allowing for a superior imaging probe.

Ref	Protein	Target	Labeling reagent yield (%)	Protein labeling yield (%)	Overall yield (%)	Specific activity (GBq/μmol)	Reagent	Method
[125]	Albumin	Amine	67 ± 15.7	25-90	N.R.	N.R.	**7**	Manual
[203]	Albumin	Amine	50 - 60	90	N.R.	N.R.	**8**	Manual
[124]	Albumin	Amine	50	N.R.	15	N.R.	**9**	Manual
[204]	Annexin V	Amine	N.R.	N.R.	N.R.	0.02 - 0.033	**8**	Manual
[202]	Annexin V	Amine	N.R.	N.R.	15-20	35	**8**	Automated
[205]	Annexin V	Amine	N.R.	70	17.6 ± 5.6	1.3	**8**	Manual
[206]	Antibody	Amine	N.R.	N.R.	39	11	**8**	Manual
[207]	Antibody	Amine	25	50	N.R.	N.R.	**8**	Manual
[208]	Antibody	Amine	30 - 35	15 - 20	3	3.7 - 40	**8**	Manual
[209]	Antibody	Amine	25	N.R.	0.5	12-17	**8**	Manual
[210]	Antibody	Amine	N.R.	25 - 40	N.R.	18	**10**	Manual
[159]	Epo	Amine	16.5	19.8 ± 5.2	N.R.	147	**8**	Manual
[201]	Transferrin	Amine	N.R.	N.R.	N.R.	37 - 74	**8**	Manual
[163] **Chapter 2**	**Leptin**	**C-terminus**	**40 - 70**	**65**	**3**	**9.25 - 16.65**	**7**	**Manual**
[211]	Affibody	Cys	50-70	N.R.	13 - 18	10.4 - 20.8	**7**	Automated
[131]	Annexin V	Cys	45-69	43 - 58	N.R.	2 - 4	**11**	Manual
[132]	Annexin V	Cys	23 ± 4	37 ± 9	N.R.	N.R.	**12b**	Manual
[117]	Ab fragment	Cys	28-37	60-70	N.R.	N.R.	**12a**	Manual
[128]	LDL	Cys	29	17 ± 10	N.R.	50 - 300	**12c**	Manual
[212]	MS2 phage	Tyr	65 - 75	15 - 25	N.R.	N.R.	**7**	Manual

Table 6. A comparison of well characterized methods for labeling proteins with ^{18}F from the literature.

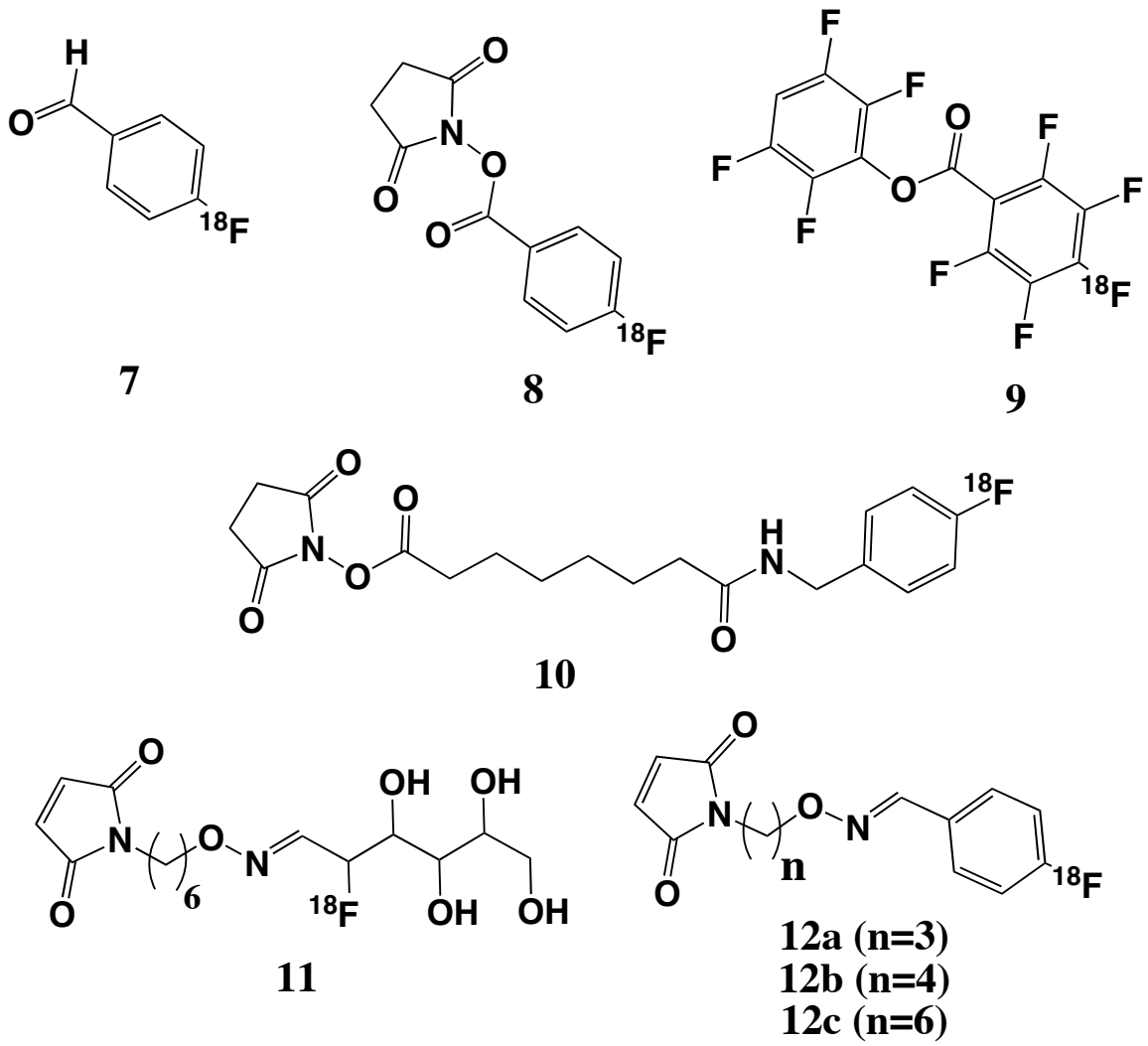

Figure 35. Previously described ^{18}F-based synthons for protein labeling, referred to on table 7.

The synthesis of ^{18}F-FBA-leptin could be improved in several ways. Firstly, automation of the synthesis of ^{18}F-FBA, as previously reported[211], would allow for an increase in starting radioactivity of up to five fold, since a limiting factor in the amount of radioactivity is the dose of radiation to the hands of the operator. In the labeling of ^{18}F-FBA-leptin, a paradoxical decrease of labeling efficiency was observed when increasing portions of the ^{18}F-FBA product was added to aminooxy-leptin **4**, suggesting that the ^{18}F-FBA prep contains impurities which interfere with or compete with the reaction.

Consistent with this was the finding that intact aminooxy-leptin **4** was not observed in the radiochemical product of the labeling reaction, but instead only a mixture of products with a higher mass were found (data not shown). Therefore it is likely that the specific activity of the ^{18}F-FBA is moderate and may represent the limiting factor in generating high specific activity leptin. Optimization of the purification conditions and reformulation of ^{18}F-FBA, along the lines of a recent report[132], would improve its specific activity. Another option would be to forgo the use of ^{18}F-FBA altogether, and to instead use ^{18}F-fluorodeoxyglucose (FDG). ^{18}F-FDG is the most commonly used PET tracer, and a recent study revealed that it could be used to label small molecule substrates (e.g. compound **11**, Figure 35) by oximation[131]. It is likely that using aniline to accelerate this reaction would render it useful for protein labeling. These improvements in the generation of the ^{18}F synthon for leptin labeling would likely lead to an improved radiotracer.

Finally, it is likely that altering the structure of the aminooxy-leptin used as a precursor would improve the stability of the labeled leptin. One simple method to accomplish this would be to dramatically shorten the linker length between the protein and the aminooxy group. For example, the length of the linker could be reduced from 29 atoms (Scheme 1) to 2 atoms by expressed protein ligation with the reagent in Scheme 5A. This compound could readily be synthesized from previously described N-[2-(tert-butyl-N-hydroxycarbamoyl)ethyl]amine[213] in two steps (Scheme 5B). This compound could be conjugated to leptin using expressed protein ligation, similar to the technique shown on Scheme 2. Based on experiments in which other small moieties were installed at the C-terminus of leptin (data not shown), the smaller linker would likely have greater

stability and bioactivity than the previously described ^{18}F-FBA-leptin. Alternatively, the lysine-directed aminooxyacetic acid / ^{18}F-FBA strategy (Section 2.5) could be further explored and applied to imaging *in vivo*. It is likely that implementing these improvements to both the protein chemistry and the radiochemistry would substantially increase the specific activity of the final tracer. In turn, the improved specific activity of these tracers could potentially allow for better visualization of high affinity, low capacity interactions of leptin, such as transport into the brain, by micro-PET imaging in mice. Furthermore, the optimization of the specific activity of the tracer is crucial for translation of the imaging methodologies to human subjects.

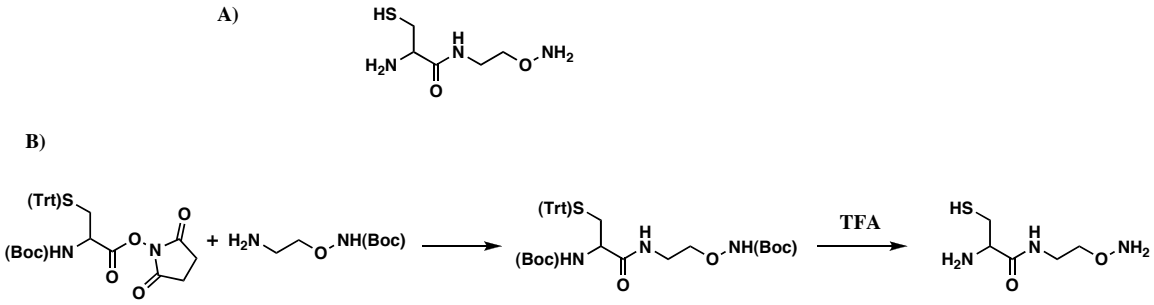

Scheme 5. A) Structure of proposed short-aminooxy Cys-linker. B) Proposed synthesis for short aminooxy Cys-linker.

5.2. Biodistribution results and discussion

Our study of leptin biodistribution represents the most extensive report to date. Van Heek et al. studied leptin biodistribution using ^{125}I leptin; however doses of the hormone were used which saturate peripheral receptors (injected dose of 0.3 mg/kg)[92]. Nevertheless, they were able to observe leptin binding in the bone marrow. Karonen et al. studied leptin biodistribution using SPECT, finding uptake in the liver, kidneys, lung, and

brain[96]. One study used ^{125}I-leptin to study leptin transport across the placenta in pregnancy in rats[214]. In chickens, leptin has a very high level of uptake in the kidney, but also in the testes, lung, and spleen[183]. Several studies have used ^{125}I-leptin to study the transport of leptin into the brain[17,39,182,215,216]. Collectively, these previous biodistribution studies have suffered from a lack of displacement studies using cold ligand, and no molecular characterization of binding sites has been performed. Thus, to date there is no comprehensive description of leptin biodistribution.

Our results incorporate data from three different labeled molecules, ^{68}Ga-DOTA-leptin, ^{18}F-FBA-leptin, and ^{125}I-leptin, in model systems including mice, rats, and rhesus macaques. A comparison of our experiments reveals largely consistent results, when the effect of injected dose is considered (see Table 7). The different results obtained in micro-PET and ex vivo biodistribution experiments are likely the result of receptor saturation at both high affinity receptors (ObR) and low affinity receptors (megalin) and can be summed up as follows. In the case where a very small amount of tracer is injected, relative to the size of the animal, such as in *ex vivo* biodistribution studies using ^{125}I-leptin and ^{68}Ga-DOTA-leptin, and in PET imaging in rhesus macaques using ^{68}Ga-DOTA-leptin, there is no saturation of high affinity receptors. In intermediate cases, including micro-PET imaging in mice using ^{68}Ga-DOTA-leptin and ^{18}F-FBA-leptin, or PET imaging in rhesus macaques with a small amount of competing leptin, high affinity peripheral receptors are saturated (ObR). Thus, micro-PET imaging in mice has been useful principally for studying the low affinity interaction of leptin with megalin. The final case is biodistribution and PET imaging experiments in mice, where a high dose of competing leptin is co-injected, saturating both high affinity (ObR) and low affinity

receptors (megalin). Collectively, our biodistribution and PET results suggest that megalin is a low affinity receptor for leptin in the kidney, and ObR is a high affinity receptor for leptin in the bone marrow, lung, liver, fat, spleen, and brain.

	Mouse biodistribution	**Micro Pet in mice**	**Mouse displacement experiments**	**Micro PET in rats**	**PET imaging in rhesus macaques**	**PET imaging in rhesus macaques with displacement**
Injected dose	<100 ng	20-30 μg	650 μg	60 μg	60 μg	1000 μg
Weight of animal	30g	30g	30g	500g	10 kg	10 kg
Injected dose (mg/kg)	<0.003	0.66-1	22	0.12	0.006	0.1

Table 7. Summary of effective doses delivered in different animal experiments performed in this thesis.

The uptake of leptin in the kidney by megalin is discussed in section 5.3, the uptake in the spleen and bone marrow by ObR is discussed in section 5.4, and in the brain in section 5.5. Our biodistribution results in mice and PET imaging in rhesus macaques also reveal uptake of leptin in the lung, liver, and fat. Although ObR mRNA is found in both lung and liver, its physiologic effects in these tissues remains unclear. ObRb is abundantly expressed in the lung[37], while the short isoforms (ObRa, c, and f) are more abundantly expressed in the liver[217]. The role of leptin in the physiology of the lung is less clear than in other organs. It is possible that our data represent binding to resident immune cells of the lung, as leptin receptor positive T-cells are present in large numbers in this organ[218]. Dal farra et al also found that leptin binding sites are present in the

pulmonary parenchyma as well as bronchiolar epithelium[83]. It is likely that these cells are the ones that leptin is bound to in our study.

The relatively low uptake of leptin in the liver compared to other organs (4.1 ± 0.1% ID/g for liver vs. 24.8 ± 4.0% ID/g for spleen in mice) suggests that leptin may only bind to a subset of cells in the liver, or that liver cells expressed relatively little ObR. Leptin induces IRS-1 phosphorylation in cultured HEP-G2 hepatocytes, in a manner that mimics insulin signaling[219-221]. However, a tissue specific knockout of leptin receptor in hepatocytes resulted in no apparent metabolic phenotype, revealing that this effect is not required for normal glucose homeostasis[18]. Leptin also has a direct effect on hepatic stellate cells, inducing collagen production and promoting fibrosis[222]. One study suggested that leptin receptor in the liver was induced by both leptin treatment and short-term starvation. In particular, ObRe production was enhanced, suggesting that the liver may act as a reservoir of the circulating leptin receptor[223]. Thus, while our results showing leptin:ObR binding in the lung and liver are consistent with mRNA expression data in mice, the physiological effect of leptin in these tissues remains unknown. The identification of which cell types leptin is binding to in the lung and liver could provide a starting point for identifying the physiological role of leptin in these tissues.

We also found saturable uptake of leptin in the fat of Ob, but not wild type mice (Table 3b). This suggests either that these receptors are saturated under physiological conditions, or that hypoleptinemic animals such as Ob mice upregulate ObR. The role of ObR in the fat tissue is currently obscure. Some experiments have suggested that the action of ObR is required for full lipolysis to take place in the tissue[71,72]. Our finding, that there is no saturable uptake of leptin in fat tissue in normal wild type mice, suggests that

the ObR receptor on fat may play a role in fasting or starving conditions. For example, under conditions of starvation, a lack of ObR signaling on adipocytes could act to alter the metabolism of the adipocytes. As a first step in evaluating this hypothesis, the uptake of ^{125}I-leptin adipose tissue in fasted wild type mice and rats could be evaluated and compared to well fed animals.

5.3 Leptin and megalin in the kidney, and potential implications of the megalin:leptin interaction

Our study is the first, to our knowledge, to utilize PET to systematically investigate leptin biodistribution in the kidney. We found a similar biodistribution pattern, in which leptin is taken up in the cortex of the kidney, in mice, rats, and rhesus macaques (Figure 20). In both humans and rodents, leptin has a short half-life, and kidneys are the major site of leptin metabolism from the circulation, accounting for over 80% of all clearance from plasma[12,84,87,88]. The half-life of leptin appears to be unaffected in ob/ob, db/db, or mice on a high fat diet[92,224]. Our finding of rapid and identical kidney uptake in ob/ob, ObRΔ/ob/ob, and wild type mice, with approximately 50% of the total hormone appearing in the kidney 3 min post injection, is consistent with these studies (Figure 24a). End stage renal disease (ESRD) causes increased leptin levels[164] and this increase could underlie the induction of anorexia, a symptom associated with ESRD[225]. Thus, the clearance of potent low molecular weight hormones such as leptin by the kidney is a problem of clinical significance.

Several studies have shown that leptin metabolism in the kidney is the result of an active process[165]. Conflicting reports suggested that leptin uptake in the kidney is

saturable[84] or non saturable[158]. The evidence that both the long (ObRb) and one of the short (ObRa) isoforms of leptin receptor are expressed mainly at the loop of Henle[50] in the kidney, and are capable of mediating internalization of leptin in vitro[93], makes them candidate leptin transporters in that organ. ObRb may also mediate a possible natriuretic effect of leptin[226]. *In vitro* binding experiments performed with ^{125}I-leptin on kidney preparations have shown binding exclusively at the level of the medulla, which could be compatible with ObR distribution[81].

However, we have presented several lines of evidence that unequivocally demonstrate that megalin (gp330/LRP2), and not ObR, is required for leptin metabolism in the kidney *in vivo*. Our results in 3 different mammalian species (mouse, rat, and rhesus macaques) show that leptin is actively taken up in the renal cortex, which is not compatible with the aforementioned pattern of leptin receptor expression. Furthermore, leptin uptake in the kidney was not significantly reduced in ObRΔ animals, which lack leptin receptor. Recently, Hama et al. found that megalin (gp330/LRP 2) binds leptin with an apparent affinity of 300 nM in QCM analysis and can mediate leptin uptake in an L2 yolk sac tumor cell line[50]. Megalin is highly expressed at the proximal convoluted tubule in the kidney cortex. It is involved in endocytosis of several ligands, including hormones and their precursors (PTH, insulin, prolactin, EGF, thyroglobulin) vitamin binding proteins (Vitamin-D binding protein, retinol binding protein, transcobalamin-VitB12) and carrier proteins (Haemoglobin, myoglobin, albumin, lactoferrin, transthyretin)[50,167]. Megalin knockout mice are severely compromised due to a deficit in the development of the forebrain (holoprosencephaly) and die perinatally[227]. Megalin kidney specific knockout mice (megalin$^{lox/lox}$, ApoE^{cre}) show a normal phenotype but reduced kidney

uptake of several megalin ligands[175,228,229]. We have demonstrated that megalin$^{lox/lox}$, ApoE^{cre} eliminate leptin in the urine (Figure 25). This finding was confirmed using micro-PET imaging (Figure 26). Thus, megalin, and not ObR, is required for the uptake and degradation of leptin in the kidney following filtration of the protein at the glomerulus.

To our knowledge, this is the first report of a non-ObR cell surface receptor playing a role in leptin physiology. Our results have broader implications since megalin is expressed in several organs such as lung, intestine, thyroid, parathyroid, placenta, endometrium, yolk sac, testicle, ovary and in brain microvessels and choroid plexus[230], anatomical structures that are part of the blood brain barrier that leptin actively crosses to enter in the brain[167]. For example, our findings support the need for intensive investigation on the interaction between leptin and megalin at the blood brain barrier[174]. We speculate that megalin mediated uptake and transport of leptin in different tissues and organs could become a target for pharmacological intervention useful for the treatment of obese patients.

5.4 Leptin in hematopoiesis

Our biodistribution results support the idea that leptin plays a significant role in hematopoiesis and immunity in mammals. In mice, leptin binds to bone marrow and spleen, in an ObR dependant manner (Table 3a, Figure 28). One previous biodistribution study also found uptake of ^{125}I-leptin in the bone marrow[92]. By PET imaging using ^{68}Ga-DOTA-leptin in rats, leptin localized to the proximal femur, a site of bone marrow production in rodents (fig 19). In rhesus macaques, binding to the spleen is very low,

while uptake in bone marrow is high (16% of total injected dose, Figures 33-34). These results are consistent with binding of leptin to tissues undergoing active hematopoiesis: in mice, spleen and bone marrow are sites of hematopoiesis, while in adult rhesus macaques and humans only the bone marrow is[193]. An ex vivo tissue section binding study found high affinity binding sites using ^{125}I-leptin in the fetal liver in mice, which decrease during development, as binding in the spleen increases[83]. This pattern of receptor distribution follows the development of hematopoietic tissues in mice, where the liver serves as the sites of hematopoiesis *in utero*, while the spleen and bone marrow serve this function in adult mice. Thus, taken together with the previous data, leptin binds to sites of active hematopoiesis, in an ObR dependant manner, in mice, rats, and rhesus macaques.

Several lines of evidence support an important role for leptin in regulating hematopoiesis and immune function[231,232]. Firstly, humans lacking a functional leptin gene are predisposed to frequent upper respiratory tract infections, and have reduced $CD4^+$ T-cells. Furthermore, lymphocytes isolated from these patients have reduced proliferative responses, and dysregulated cytokine production consistent with an excess of Th2/regulatory cytokines. This abnormal phenotype is corrected by treatment with recombinant leptin[21]. A similar syndrome is seen in ob and db mice, which have severely impaired humoral and cell-mediated immunity[233,234]. Ob mice have substantially reduced lymphopoiesis, particularly in the B-cell compartment, which is corrected by leptin treatment[235]. Furthermore, Ob mice are protected against experimental autoimmune encephalitis[69]. Thus, leptin is clearly required for normal immune function in humans and rodents.

Leptin also has effects on hematopoietic stem cells and mature immune cells *in vitro*. Leptin stimulates proliferation and granulocyte-macrophage colony formation in hematopoietic stem cells *in vitro*[236]. Leptin receptors are abundantly expressed by hematopoietic stem cells, and marrow isolated from db mice has a blunted response to leptin treatment[63,237]. Furthermore, leptin has clear effects on immune cells *in vitro*: it promotes the secretion of pro-inflammatory Th1 cytokines (such as IFN-γ) at the expense of Th2 cytokines (such as IL-4), and it substantially increases the proliferation of naïve T-cells[62]. Additionally, leptin activates monocytes, augmenting the release of Th1 cytokines[238]. Taken together, these data indicate that leptin plays a role in augmenting hematopoiesis (particularly lymphopoiesis) and plays a permissive role in immunity.

An interesting question raised by our biodistribution results is to what extent leptin is moderating the physiology of hematopoiesis and immunity directly, via receptors on bone marrow and mature immune cells. Our finding of extensive uptake of leptin in hematopoietic tissues in mice, rats and rhesus macaques, combined with ample evidence of leptin's effects on immune and hematopoietic cells *in vitro*[62,236-239], suggests that a key role of leptin in augmenting hematopoiesis and immunity is a direct effect on the hematopoietic cells. However, lethally irradiated db mice, with a wild type bone marrow transplant were unable to reconstitute a normal immune system, while db to wild type bone marrow chimeras had an essentially normal immune system[240]. These results suggest that the immune deficiency seen in db mice is not intrinsic to immune cells, but rather that it is due to a deficiency in either the bone marrow microenvironment or elsewhere in the organism. However, these results must be interpreted with caution, as the lethal irradiation technique does not completely destroy the host immune system, and

the degree of chimerism in these experiments is only 80%. Thus, it is possible that the remaining 20% of wild type immune cells mask the immune deficit. Furthermore, leptin can still induce granulocyte-macrophage colony formation, albeit to a lesser extent, in marrow isolated from db mice[236]. Thus, it is possible that leptin may still function via the truncated ObR[16] in db mouse marrow, or that it may act via an alternative mechanism in these cells. One potential approach to overcome these limitations would be to use lymphocyte specific promoters[241] to knock out ObR in specific hematopoietic tissues, or alternatively to drive ObRb expression in these tissues in mice lacking all isoforms of the leptin receptor. Thus, to date the relative contribution of leptin signaling to immune function via direct action on blood cells and precursors, versus indirect actions via other tissues, has not been fully addressed.

A second question raised by our study is which cell types leptin is binding to in the bone marrow. This question was partially addressed by Gainsford et al., who incubated a human bone marrow preparation with ^{125}I leptin in vitro, and then characterized which cell types took up the tracer by autoradiography[239]. In this assay, a variety of precursors, including blasts, myelocyte precursors, promonocytes, and monocytes took up the tracer. Only a small subset of lymphocytes took up the tracer, and some of these had "intense labeling." These results imply that leptin has different effects on different lymphocyte populations. A molecular characterization of leptin-binding to immune and hematopoietic cells using cell-specific antigens has not been performed to date. It is likely that the question of the specific substrates of leptin action in hematopoietic and immune tissues could be answered by flow cytometry using fluorescently labeled leptin in combination with cell-type specific antibodies.

A final intriguing possibility raised by our finding of intense uptake of leptin in the bone marrow is the possibility of using this tracer as a diagnostic imaging agent. In humans, leptin receptor is overexpressed in a subset of patients with acute myelogenous leukemia (AML), chronic myelogenous leukemia (CML) and in acute promyelocytic leukemia (APL)[242-244]. Leptin receptor is also expressed in solid tumors, including endometrial[245], hepatocellular,[246] breast,[247-249] colorectal,[250] and renal[251] cancers. Leptin receptor is being actively investigated as a marker for these cancers[249,251,252], and it is likely that using the tracers ^{68}Ga-DOTA-leptin and ^{18}F-FBA-leptin as an imaging agent in patients with these tumors could aid in visualizing, staging, and diagnosing these malignancies.

Section 5.5 Leptin transport into the brain

We found that uptake of leptin in the brain occurs at extremely low levels, with uptake values of between 0.1 to 0.4% of injected dose per gram of tissue in mice (Table 3A). These results are consistent with previous reports of leptin transport into the brain[17,92]. These experiments reveal that leptin is taken up in the brain in a saturable manner in an ObR dependant manner. To our knowledge, these results represent the first conclusive report that leptin uptake in the brain is dependant on ObR *in vivo*, as all previous experiments used ObR-deficient mice with high circulating levels of leptin, which would saturate any binding sites.

One possibility is that ObR itself mediates the transport of leptin across the BBB, as ObRa is abundantly expressed on choroid plexus and cerebral microvessels[39]. However, Banks et al. found no difference in the transport of leptin across the BBB in a

perfusion model in the Koletsky rat, which lacks functional leptin receptors altogether[40,253]. In this model, the brain is perfused with a saline solution containing leptin, and thusly corrects for serum components interfering with leptin brain transport. In contrast, Hileman et al found that mice lacking ObR had reduced transport of the protein in a similar brain perfusion system[39]. Thus, although the suggestion that ObR mediates the transport across the BBB is over a decade old, it has not been conclusively proven or disproven.

An intriguing question raised by our experiments and that of others is the relative role of megalin in the transport of leptin into the brain. A recent report showed that a transfection of a virus expressing siRNA directed against megalin reduced transport of leptin into the brain in mice[174]. Based on these results, the authors concluded that megalin mediates the transport of leptin into the CSF. These results are supported by our own finding that megalin mediates the uptake of leptin in the kidney. It is possible that either or both ObR and megalin mediate the transport of leptin into the brain, or that there is cross-talk between these systems. Furthermore, Banks et al. have suggested that there are two mechanisms of transport into the brain, a saturable and a non saturable one, and that transport varied in different regions of the brain[182]. Similarly, Thomas et al. found a saturable and non-saturable component of leptin transport into the CSF in a sheep choroid plexus model[216]. The molecular identity of these transporters remains obscure. Nevertheless, it is likely that either megalin or ObR, or both acting together, play a role in this mechanism. Animals with deletions of these receptors in the choroid plexus and capillary endothelium could be used to evaluate this hypothesis.

Chapter 6. Materials and methods

General Methods

Amino acid derivatives, resin and coupling reagents were purchased from Novabiochem (San Diego, CA) unless otherwise indicated. Boc-aminooxyacetic acid was purchased from Sigma-Aldrich (Milwaukee, WI). All other chemicals were purchased from Sigma-Aldrich (Milwaukee, WI) or Fisher Scientific (Pittsburgh, PA). Recombinant murine leptin was a gift of Amgen (Thousand Oaks, CA), or Amylin (San Diego, CA). Analytical gradient reversed phase HPLC was performed on a Hewlett Packard 1100 series instrument and a Vydac C18 or C4 column (5 micron, 4 X 150 mm). Flow rate was 1 mL/min and detection was at 214 and 280 nm. Preparative scale HPLC was performed on a Waters Delta Prep 4000 fitted with a Waters 486 tunable absorbance detector and using either a Vydac C4 process scale column (5 x 25 cm) at 30 mL/min, a Vydac C18 process scale column (5 x 25 cm) at 30 mL/min, or a Vydac C4 semiprep scale column (1 x 25 cm) at 5 mL/min. Radiochemical HPLC was performed on a Varian ProStar series instrument fitted with a model 320 UV detector and a Bioscan flowcount radiodetector (Bioscan Inc., Washington D.C.), and either a Vydac analytical C4 column (5 micron, 4 X 150 mm) at 1 mL/minute or a Waters μBondapak C18 (7.8 x 300 mm) column at 3 mL/min as indicated. HPLC mobile phase buffers A and B were 0.1% trifluoroacetic acid in water, and 90% acetonitrile, 0.1% trifluoroacetic acid in water, respectively. Electrospray mass spectrometry was routinely used on all peptides and proteins, using a Sciex API-100 single quadrapole spectrometer. Thin layer chromatographic (TLC) analysis was conducted using normal phase silica 60, F254, 250 μm, 2.5 x 7.5 cm plates

(Spectrum Chemical, Gardena, CA). Quantification of radiochemical thin layer chromatography plates was performed on a Bioscan Mini-Scan TLC scanner (Bioscan, Washington, D.C.). All enzymes involved in the construction of the plasmids were obtained from New England Biolabs (Ipswich, MA). All molecular biology kits were obtained from Qiagen unless otherwise specified. Metal free buffers were prepared by pre-treatment of the buffers with Chelex 100 resin (Biorad, Hercules, CA).

Animal Maintenance

Wild type C57BL/6J and Ob/ob mice were obtained from Jackson laboratory (Bar Harbor, ME). Megalin$^{lox/lox}$, ApoE^{cre} and megalin$^{lox/lox}$ mice were obtained from Dr. T. Willnow (Max-Delbrueck Molecular Cardiovascular Research and Medical Faculty, Free University of Berlin[175].) Rats used for PET scans were male Sprague-Dawley purchased from Charles River Laboratories. ObRΔ/ob/ob mice were generated in our laboratory crossing heterozygote mice for both the leptin receptor mutation (ObRΔ^{18}) and leptin gene mutation (ob). All mice were maintained in cages in temperature controlled rooms. All animals were subjected to a 12 h light/dark cycle. Procedures and measurements were performed between 10:00 and 17:00 hours. Animal care and experiments were conducted in accordance with approved guidelines of The Rockefeller University.

Rhesus macaque subjects were two gonadally intact adult male rhesus monkeys (Macaca mulatta). Subjects were approximately 14 years of age and weighed in the range 10-12 kg. Subjects were housed in a stable colony and were previously exposed to the experimental situation (e.g., pole and collar training, transfer into transport cage etc.).

Titration of leptin labeling with DOTA-NHS

Murine leptin (Amgen/Amylin) at 13.1 mg/mL was diluted to 5 mg/mL using 100 mM metal free sodium phosphate pH 7.0. To 10 μL of the resulting solution was added 2 μL of 10 mg/mL DOTA-NHS (Macrocyclics Inc., 40 nmol, 5 equivalents), or 4 μL 10 mg/mL DOTA-NHS (80 nmol, 10 equivalents). Additionally, to 262 μL of the same solution was added 100 equivalents of DOTA-NHS (8.2 μmol, 4.12 mg), and the pH was adjusted to 7.5 with metal free 1N NaOH. The reactions were allowed to proceed 1-3 hours at 4 degrees, and then analyzed by C4 RP-HPLC on a 0-100% B gradient, and by ESI-MS.

Preparation of DOTA-leptin

A lysine-directed labeling approach using DOTA-NHS ester (Macrocyclics) was employed. Briefly, to 100 μL mouse leptin solution at 13.1 mg/mL (Amylin) was added 162 μL metal free (by chelex resin treatment, Biorad) 100 mM sodium phosphate pH 7.5 (final concentration of 5 mg/mL). To this solution was as added 100 equivalents of DOTA-NHS (8.2 μmol, 4.1 mg), and the pH adjusted to 7.5 using 1N NaOH. The reaction proceeded for 3 h at 4 °C at which point it was purified by HPLC using a Hewlett Packard 1100 series instrument and a Vydac C4 column (5 micron, 4 X 150 mm) on a 45-60%B gradient (where buffer A is 0.1% trifluoroacetic acid in water, and buffer B is 90% acetonitrile, 0.1% trifluoroacetic acid in water.) The product was characterized by ESI-MS on a Sciex API-100 single quadrapole spectrometer, which indicated the incorporation of 2-6 DOTA moieties per leptin molecule. The solution was separated to 8

aliquots of DOTA-leptin and lyophilized.

Generation of a Stable Cell Line Overexpressing Leptin Receptor Long Isoform (Ob-Rb) and a Stat3-Responsive Element-Luciferase Reporter

A stable Flp-In 293 cell line[254] expressing the long isoform of the leptin receptor (Ob-Rb) that is capable of full signaling (kind donation of Dr. Cai Li, University of Texas Southwestern) was stably transfected with a p4xm67 luciferase plasmid, containing a STAT3 responsive element and luciferase DNA (kindly provided by Dr Jim Darnell, The Rockefeller University). Cells were transfected with p4xm67 luciferase and a puromicin resistance plasmid following the Lipofectamine 2000 method (Invitrogen). Stable integrants were selected in Dulbecco's modified Eagle's medium containing 10% fetal bovine serum and puromicin (1.5 μg/ml) for about 4 weeks. Single cell clones were then selected for leptin induced luciferase production and the clone with the best response to leptin used for further experiments.

Luciferase Reporter Assay of Leptin Receptor Activation

Ob-Rb-STAT3-luciferase cells were seeded into 24-well plates. At a confluence of 80% the cells were washed and replaced with serum-free medium. After 4 hours the medium was changed and replaced by serum-free medium containing dilutions of leptin or the appropriate semisynthetic derivative. Samples were assayed in duplicate for every dilution. After 24 hours cells were collected and luciferase activity measured in cell lysate using a luciferase assay system (Promega).

Leptin Administration to ob/ob Mice

Leptin or its semisynthetic derivatives were administered continuously with mini osmotic pumps (Alzet, Cupertino, CA, model 2002) to Ob/ob mice with an exchange rate of 450 ng/h for ob/ob mice. Pumps were filled aseptically according to the manufacturer instructions with either sterile PBS solution, leptin, or leptin derivatives. Recombinant leptin or leptin derivatives were diluted in sterile PBS buffer. Before surgery, pumps were incubated overnight in a sterile 0.9 % NaCl solution at 37 °C to achieve immediate and constant pumping rate at the time of implantation. During surgery mice were anesthetized with isofluorane. Pumps were implanted subcutaneously in the interscapular region of the mice. Body weight was measured on a daily basis following surgery.

^{68}Ga labeling of DOTA-leptin.

One DOTA-leptin aliquot consisting of approximately 70-100 μg of protein (see above) was resuspended in 40 μL of metal free 15 mM HCl. After incubation for 10 minutes on ice to allow full resuspension of the protein, 10 μL of 1.2M sodium acetate (pH 4.5) was added. Immediately prior to addition of the ^{68}Ga solution, the protein solution was centrifuged for 2 minutes at 10,000 x g to remove insoluble components.

DOTA-leptin was labeled using ^{68}Ga eluted from a ^{68}Ge generator (Isotope Products Laboratories) using a previously described procedure[199] with modifications. We found that reproducible labeling results were obtained by eluting the generator the evening prior to labeling, presumably to remove impurities. The gallium generator was eluted with 7 mL of 1M metal free HCl. The solution was diluted with 7 mL of concentrated HCl (trace metal grade, Fisher), and applied to 150 μL settled volume of

AG1-X8 resin (Biorad). The ^{68}Ga was then eluted from the resin using 300 μL 15 mM HCl and followed by 100 μL of 15 mM HCl. The dilute acid solution was evaporated at 160 degrees, and the ^{68}Ga was subsequently resuspended in 40 μL of metal free 15 mM HCl. The ^{68}Ga solution was then added to the leptin-DOTA solution (above), and incubated in a 35 °C water bath for 20 minutes. The solution was then centrifuged for 1 min at 10,000 x g, and the supernatant added to 2 μL of 0.1M diethylenetriaminepentaacetic acid (DTPA). After 2 min the solution was transferred to a micro bio-spin P6 column (Biorad), which had been pre-equilibrated with PBS according to the manufacturer's instructions. The ^{68}Ga -DOTA-leptin was eluted from the column by centrifuging at 1000 x g for 4 minutes. Following elution the solution was diluted to an appropriate volume for injection in PBS (typically to 0.5-1 mL), and filtered through a 0.22 μm filter. The specific activity of the conjugate at the end of synthesis was 9.1 ± 4.2 GBq/μmol (s.d., n = 30 syntheses) at greater than 90% pure as determined by radiochemical HPLC and iTLC. The amount of total protein in the reaction was determined by BCA assay (Pierce).

Radiochemical HPLC and iTLC analysis

Radiochemical HPLC was performed on a Varian ProStar series instrument fitted with a model 320 UV detector and a Bioscan flowcount radiodetector (Bioscan Inc., Washington D.C.), and a Vydac analytical C4 column (5 micron, 4 X 150 mm) at 1 mL/minute. HPLC mobile phase buffers A and B were 0.1% trifluoroacetic acid in water, and 90% acetonitrile, 0.1% trifluoroacetic acid in water, respectively. Linear gradients from 0-100%B over 30 minutes with a 2 minute isocratic were used.

iTLC was performed using ITLC SG silica impregnated glass fiber sheets (Pall, East Hill, NY), with 5 mM diethylenetriaminepentaacetic acid (DTPA) as an eluant. Quantification of radiochemical thin layer chromatography plates was performed on a Bioscan Mini-Scan TLC scanner (Bioscan, Washington, D.C.).

Stability of ^{18}F-FBA-leptin 5 and ^{68}Ga-DOTA-leptin *in vivo*

Approximately 20 MBq of ^{18}F-FBA-leptin **5** or ^{68}Ga-DOTA-leptin was injected into either ob/ob or wild type mice via the tail vein. After 20 - 30 minutes (as indicated in the text), the animals were sacrificed and 500 μL of whole blood was collected. The blood was centrifuged for 15 minutes at 7000 rpm, and the supernatant injected on a C4 analytical HPLC.

Radioactive Cell Binding Experiment

ObRb expressing cells were grown overnight in suspension in Dulbecco's modified Eagle's medium containing 10% fetal bovine serum at 37 °C and 5% CO_2. Cell viability and concentration was then determined using trypan blue staining. Cells were washed with serum free medium and re-suspended in HBSS supplemented with 0.1% BSA at a final concentration of 20 million/mL. For each cell binding assay, 750 μL of cell suspension was incubated with a constant amount of radiolabeled leptin corresponding to 80,000 cpm of radioactivity (either ^{68}Ga-DOTA-leptin or ^{18}F-FBA-leptin) $\pm$ 60 μg of cold leptin. The concentration of the labeled leptin was determined using the BCA method (BCA protein Assay Kit, microplate procedure, Pierce). Following incubation of the cells at room temperature for 2 hours at constant agitation, the cell suspension was washed twice with 0.5 mL of HBSS with 0.1% BSA and

centrifuged at 2000 rpm for 5 minutes. The radioactivity associated with cell pellet (cell bound activity) was determined by counting the tubes in a gamma counter with corresponding standards and blanks.

Cloning of Leptin(1-146)-GyrA-His_6

The sequence encoding the chitin binding domain in the pTXB vector (New England Biolabs, Ipswich, MA) was replaced with a His_6 tag sequence to facilitate protein purification under denaturing conditions. Synthetic oligonucleotides encoding a His_6 tag flanked by AgeI and PstI restriction sites (sense strand; 5'-CCGGTGGAGCGCATCATCATCATCATCATGGAGCGTAACTGCA and antisense strand; 3'-GTTACGCTCCATGATGATGATGATGATGCGCTCCA) were phosphorylated using T4 DNA kinase and annealed. The pTXB vector was digested with AgeI and PstI, and the annealed His-oligos inserted using T4 ligase to give plasmid pGyrAHis, the identity of which was verified by sequencing. cDNA encoding leptin(1-146) was amplified by PCR from a leptin-EGFP plasmid (obtained from A. Zeigerer, Friedman lab) using forward and reverse primers (GGAATTCCATATGGTGCCTATCCAGAAAGTCCAGG and GGACTAGTGCATCTCCCGTGATGCATTCAGGGCTAACATCCAACTG, respectively) encoding the NdeI and SpeI restriction sites. The PCR product was purified by gel extraction and ligated into the pre-digested pGyrAHis plasmid using T4 ligase to give the plasmid pLeptin-GyrA, the identity of which was verified by sequencing.

Overexpression and purification of Leptin(1-146)-GyrA-His_6

E. coli BL21(DE3) cells (Novagen, Darmstadt, Germany) were transformed using the plasmid pLeptin-GyrA. Cells were grown to an OD_{600} of 15-25 in a Bioflo 3000 Batch/Continuous bioreactor (New Brunswick Scientific, Edison, NJ) in superbroth media (Qbiogene, Irvine, CA) with 50 μg/mL ampicillin. The culture medium was supplemented with oxygen to keep oxygen gas levels constant at 30% and agitated at 350 RPM. The pH was maintained at 7.0 automatically using 5N sodium hydroxide. The culture medium was supplemented with 2 mL/min 50% glucose and 2 mL/min 3X superbroth solution during growth. Overexpression was induced with 1 mM IPTG, and the flow of glucose and superbroth was increased up to 10 mL/min. After four hours of induction at 37 °C, the cells were harvested by centrifugation. Using this protocol 200-250g of biomass was typically obtained per culture prep.

The cells were resuspended in lysis buffer consisting of 1% triton, 50 mM sodium phosphate buffer, pH 7.0, 200 mM sodium chloride supplemented with one complete protease inhibitor tablet, EDTA free (Roche, Basel, Switzerland) per 50 mL of buffer. The cells were lysed by passage through a French Press (Emulsiflex C5 homogenizer, Avestin, Ottawa, Canada.). The inclusion bodies were separated by centrifugation at 16,000 rpm for 30 minutes, and subsequently resuspended overnight in one volume (relative to the cell pellet) of resuspension buffer consisting of 8 M urea, 20 mM imidazole, 150 mM sodium chloride, 100 mM sodium phosphate, pH 7.5. This suspension was centrifuged again at 16,000 RPM for 30 minutes to remove insoluble debris, and applied to 100 mL of Ni-NTA beads which were pre-equilibrated with resuspension buffer supplemented with 20 mM imidazole. The beads were then washed

with resuspension buffer supplemented with 20 mM imidazole, and the fusion protein was eluted from the column with 10 x 50 mL fractions of resuspension buffer supplemented with 500 mM imidazole. The fractions were analyzed by SDS-PAGE and those containing the 39 kDa fusion protein were pooled.

Optimization of intein cleavage

100 μL of pure leptin-GyrA-His6 was refolded by dialysis overnight using four buffer changes of 250 mL, in buffer containing 200 mM sodium phosphate, 200 mM NaCl, 5 mM EDTA, pH 7.0, in the presence of varying additives, including 1 & 2M guanidine, and 2, 3, 4 and 5M Urea. Following dialysis, ethanethiol was added to 3%, and the samples were cleaved overnight at room temperature or at 4° C. Samples were analyzed by SDS-PAGE and Coomassie staining.

Generation of Leptin(1-146) α-thioester, 1

The combined Leptin(1-146)-GyrA-His_6 fractions were refolded by extensive dialysis against 4 M urea, 100 mM sodium phosphate, 150 mM sodium chloride pH 7.0 at 4 °C. The first dialysis buffer was further supplemented with 10 mM EDTA to remove trace amounts of contaminating nickel. Intein cleavage to form the leptin (1-146) α-thioester **1** was initiated by adding sodium 2-mercaptoethane sulfonate to a final concentration of 100 mM. Cleavage was allowed to proceed for 2 days at 4 °C. The crude cleavage reaction was reapplied to 100 mL of nickel-NTA beads, which were pre-equilibrated with dialysis buffer supplemented with 20 mM imidazole. The beads were washed with dialysis buffer supplemented with 20 mM imidazole and 100 mM sodium 2-

mercaptoethane sulfonate. The pooled flowthrough and washes from the Ni-NTA column containing principally the leptin(1-146) α-thioester **1** were then purified by process scale C4 RP-HPLC using a gradient of 50-65% buffer B. Fractions were analyzed by analytical RP-HPLC and ESI-MS, and those containing pure leptin α-thioester **1** were pooled and lyophilized. Residual uncleaved fusion protein on the Ni-NTA column could be recovered from the column by elution with 8 M urea, 500 mM imidazole, 500 mM sodium chloride, 100 mM sodium phosphate pH 7.0, and refolded and recleaved as above. Using this procedure, ~60 mg of pure leptin(1-146) a-α-thioester **1** could be obtained from an initial 5L culture.

Synthesis of native murine leptin by EPL

Leptin-GyrA-His_6 was expressed, purified, and refolded as indicated above. EPL with cysteine was initiated using 100 mM sodium 2-mercaptoethanesulfonate and 10 mM cysteine, and the reaction was allowed to proceed for 3 days at 4 °C. After the reaction was complete, it was diluted to 0.25 mg/mL in 6 M guanidine hydrochloride, 20 mM tris pH 7.4, 5 mM dithiothreitol. The product was then dialyzed at 4 °C sequentially against 6 M urea, 2.5 mM dithiothreitol, 2.5 mM 2-mercaptoethanol, 20 mM tris pH 7.4, then against 4 and 2 M urea containing 5 mM 2-mercaptoethanol, 20 mM tris pH 7.4, then against 20 mM tris pH 7.4, and finally overnight against 20 mM tris pH 7.4, 5 mM oxidized glutathione, 0.5 mM reduced glutathione, 150 mM sodium chloride. The crude refolded mixture was purified on a C4 semiprep RP-HPLC column using a gradient of

45-60% buffer B (buffer A = 0.1% TFA in water, buffer B = 90% acetonitrile, 0.1% TFA in water.) Fractions containing pure murine leptin were pooled and lyophilized.

Synthesis of Peptide 2

The peptide was prepared using manual Fmoc-based solid phase peptide synthesis, as indicated on Scheme 3. Agitation was achieved using a flow of nitrogen gas. Fmoc deprotection was achieved using 5 mL of 20% piperidine in DMF for 3 minutes followed by another treatment for 10 minutes. The resin was acetylated after every coupling using 5 mL of 10% acetic anhydride, 10% diisopropylethylamine (DIEA) in DMF for 10 minutes. Washes with DMF were performed in between all coupling, acetylation, and deprotection steps.

Fmoc-Lys(ivDde) (0.379 g, 0.66 mmoles) was coupled to Rink amide AM resin (420 mg, 0.71 mmol/g) using 2-(1H-benzotriazole-1-yl)-1,1,3,3-tetramethyluronium hexafluorophosphate (HBTU, 0.228 g, 0.6 mmoles), 0.5 mL DIEA, in 4 mL DMF for two hours. After capping and deprotection, Fmoc-NH-PEG_2(20 atoms)-COOH linker (0.2 g, 0.36 mmoles) was coupled to the resin using HBTU (0.125 g, 0.33 mmoles), 0.5 mL DIEA in 4 mL DMF for two hours. The coupling reaction was repeated. Following capping and deprotection, Boc-Cys(Trt)-OH (1.02 g, 2.2 mmoles) was coupled using diisopropylcarbodiimide (310 μL, 2 mmoles), N-hydroxybenzotriazole (0.270 g, 2 mmoles) for 20 minutes. The coupling was then repeated. The ivDde group was deprotected using 2% hydrazine in DMF three times for one hour. Boc-aminooxyacetic acid (0.460 g, 2.4 mmoles) was then coupled using DIC (370 μL, 2.4 mmoles) for 10 minutes as described[255]. The resin was washed with DCM and dried. Cleavage from the

resin and deprotection was achieved using 5 mL of 1% triisopropyl silane, 2.5% ethanedithiol, 2.5% water in trifluoroacetic acid (TFA) for 2.5 hours. The peptide was precipitated using 50 mL of 5% 2-mercaptoethanol in diethyl ether, centrifuged at 4800 rpm for 10 minutes, resuspended in 5 mL of HPLC buffer A, and lyophilized. The crude residue was then purified by process scale RP-HPLC on a C18 column using a gradient of 5-20% B. Fractions containing the purified peptide **2** were identified by HPLC/MS, pooled, and lyophilized. Yield from 0.3 mmol scale: 120 mg, (0.19 mmol), 63%.

Semisynthesis of Aminooxy-leptin 4

Leptin(1-146) a-α-thioester **1** was dissolved to a concentration of 20 mg/mL in 6 M guanidine hydrochloride, 100 mM sodium 2-mercaptoethane sulfonate, 200 mM sodium phosphate, 150 mM sodium chloride, pH 7.2. Peptide **2** (10-20 mg, 25 equivalents) was added to 10 mg/mL, and the pH was adjusted to 7.2 using 1 N NaOH. After overnight reaction at room temperature, the crude mixture containing unfolded aminooxy-leptin derivative **3** was diluted to 0.25 mg/mL in 6 M guanidine hydrochloride, 20 mM tris pH 7.4, 5 mM dithiothreitol. The product was then dialyzed at 4 °C sequentially against 6 M urea, 2.5 mM dithiothreitol, 2.5 mM 2-mercaptoethanol, 500 μM aminooxyacetic acid, 20 mM tris pH 7.4, then against 4 and 2 M urea containing 5 mM 2-mercaptoethanol, 500 μM aminooxyacetic acid, 20 mM tris pH 7.4, then against 500 μM aminooxyacetic acid, 20 mM tris pH 7.4, and finally overnight against 20 mM tris pH 7.4, 5 mM oxidized glutathione, 0.5 mM reduced glutathione, 500 μM aminooxyacetic acid, 150 mM sodium chloride. The crude refolded mixture was purified on a C4 semiprep RP-HPLC column using a gradient of 45-60% buffer B (buffer A =

0.1% TFA in water, buffer B = 90% acetonitrile, 0.1% TFA in water.) Fractions containing pure refolded AOA-leptin **4** were identified by HPLC and ESI-MS and pooled and lyophilized into 250 μg aliquots. Yield from a 1 μmol scale: 5 mg, (0.3 μmol), 30%.

Tryptic Digestion of Aminooxy-leptin 4 and Recombinant Leptin

20 μg of sequencing grade trypsin (Promega, Madison, WI) was dissolved in 100 μL of trypsin resuspension buffer (provided by the manufacturer), and incubated at 30 °C for 15 minutes. The trypsin solution was added to 150 μg of either aminooxy-leptin **4** (dissolved in 15 mM HCl) or recombinant leptin (Amgen, Thousand Oaks, CA), and the pH was adjusted to 8.3 using 1 M sodium bicarbonate. The reaction was incubated at 37 °C for 3 hours, and analyzed by analytical RP-HPLC on a C4 analytical column using a gradient of 0-100% B. Peaks were collected and identified by ESI-MS.

Synthesis of ^{19}FBA-leptin 5

Aminooxy-leptin **4** (5 mg, 0.3 mmole) was dissolved in 2 mL of 15 mM HCl. 250 μL 1 M sodium acetate pH 4.5 was added, followed by 250 μL of 10 mM 4-fluorobenzaldehyde in DMF. The reaction was vortexed, and incubated at 4 °C overnight. The reaction was then purified by C4 semipreperative RP-HPLC on a gradient of 46-61% B. Fractions containing pure FBA-leptin **5** were pooled and lyophilized, yielding 1.7 mg pure protein (Yield of 34%).

Synthesis and Reformulation of ^{18}F-FBA

The radiosynthesis of ^{18}F-FBA was accomplished essentially as previously described, however in order to facilitate labeling of leptin, which precipitates in solutions containing a high proportion of organic solvents, it was reformulated into 5 μL of DMF. The precursor (4-formylphenyl)trimethylammonium trifluoromethanesulfonate was synthesized as previously described[155]. This precursor was dried under vacuum and stored under argon atmosphere. Cyclotron produced ^{18}F in ^{18}O water was loaded onto a QMA light cartridge (Waters), which had been preconditioned with 5 mL 0.5M potassium carbonate and 10 mL water. The cartridge was eluted with a solution of 20 mg kryptofix 222 (4,7,13,16,21,24-hexaoxa-1,10-diazabicyclo[8.8.8]hexacosane), 2 mg potassium carbonate in 1:1 acetonitrile:water into a 3 mL reactivial (Pierce, Rockford, IL) equipped with a stir bar. The resulting solution was evaporated at 95 °C with a gentle nitrogen stream, and dried azeotropically using 3 x 1 mL dry acetonitrile. The resulting solid was resuspended in 400 μL of dry DMSO and transferred to a second 3 mL reactivial equipped with a stir bar and containing 1-2 mg of (4-formylphenyl)trimethylammonium trifluoromethanesulfonate. The vial was incubated for 8 minutes at 120 °C, and then cooled to room temperature. The reaction was then diluted with 1.5 mL of water, and filtered through a GHP filter (Pall, East Hill, NY) and loaded on a Waters μBondapak C18 (7.8 x 300 mm) semiprep column, and eluted isocratically using 13:87 acetonitrile:water with 0.1% TFA at a flow rate of 3 mL/min. The peak eluting at 14 minutes was diluted with 15 mL water, and loaded onto a C18 sep-pak plus cartridge (Waters). The cartridge was then eluted with 1 mL of diethyl ether. A small amount of DMF (5 μL) was added during this step to minimize loss of the FBA during evaporation.

The diethyl ether was then evaporated at 45° C, leaving a small organic residue (about 5-10 μL in a typical reaction). The product had the same R_f in 3:1 hexanes:ethyl acetate as authentic 4-fluorobenzaldehyde (0.65) and the same retention time on C18 HPLC as the authentic sample. Starting from 9.25-13 GBq, typically 1.3-1.85 GBq of reformulated ^{18}FBA could be recovered with a synthesis time of 90 minutes.

Rate of Oximation of Aminooxyleptin 4 with ^{18}F-FBA

Lyophilized aminooxy-leptin **4** (150 μg, 9.1 nmol) was dissolved in 55 μL 15 mM HCl, and 15 μL of either 0.5 M sodium acetate pH 4.5 or anilinium acetate pH 4.5 was added, giving a final volume of 70 μL (final concentration of **4** = 125 μM). 2 μL of ^{18}F-FBA in DMF (prepared as described in the supporting information) was added to each reaction, which was vortexed and placed on ice. Aliquots of the reaction were spotted on TLC plates at the indicated times and run with 4:1 DCM methanol with 2% acetic acid. ^{18}F-FBA leptin **5** was retained at the origin while ^{18}F-FBA migrated at the solvent front. At t = 30 minutes, a small portion of the anilinium acetate reaction was injected on a C4 analytical HPLC column and eluted on a 0-100% B gradient over 30 minutes. The ^{18}F-FBA eluted at 3.5 minutes while the ^{18}F-FBA-leptin **5** eluted at 21 minutes on this gradient.

Synthesis of ^{18}F-FBA-leptin 5

Lyophilized aminooxy-leptin **4** (500 μg, 30 nmol) was dissolved in 100 μL of 15 mM HCl. To this solution was added 25 μL of 0.5 M anilinium acetate, pH 4.5. The aforementioned DMF solution of ^{18}F-FBA was then added, and the mixture was vortexed

and incubated on ice for 15 minutes. The reaction was then purified through two micro bio-spin P-6 columns (Biorad, Hercules, CA), which had been pre-equilibrated with PBS according to the manufacturer's instructions. The eluate from the columns was filtered though a 0.22 μM filter. The purity of the oxime product was analyzed by both RP-HPLC using a 0-100% B gradient on a C4 analytical column, and by iTLC (ITLC SG silica impregnated glass fiber sheets, Pall, East Hill, NY) using 1% acetic acid in water as an eluant. While the labeling yield as detected by HPLC or iTLC was typically over 50%, the recovered yield was generally 25%, probably due to precipitation of the protein. Starting from 9.25-13 GBq of aqueous $K^{18}F$, typically 93-200 MBq of ^{18}F-FBA-leptin **5** was recovered with a total synthesis time of 120 minutes. The total amount of protein in the final sample was determined using the BCA assay (BCA assay micro plate kit, Pierce, Rockford, MD). The specific activity at the end of synthesis was 9.25-13 GBq/μmol (n=4).

Stability of ^{18}F-FBA-leptin 5 *in vitro*

Approximately 200 kBq of ^{18}F-FBA-leptin **5** in 2 μL was diluted in either 100 mM sodium acetate pH 4.5 (10 mM sodium phosphate, 140 mM sodium chloride, pH 7.4), PBS, or mouse serum. After 60 minutes a sample of each was injected on a C4 analytical HPLC. Integration of the radiochemical HPLC peaks was used to estimate the purity of the sample, and if no other peaks could be detected above background the sample was assumed to be greater than 95% pure.

Synthesis of Isopropylidene-aminooxyacetic acid, succinimide ester (6)

Isopopylidene-aminooxyacetic acid was synthesized as previously described[162]. To 500 mg (3.8 mmol) of isopopylidene-aminooxyacetic acid in 30 mL dichlooromethane, cooled on ice, was added 3.8 mmol (439 mg) N-hydroxysuccinimide, and 3.8 mmol dicyclohexylcarbodiimide (782.8 mg). The mixture was stirred and allowed to warm to room temperature overnight. The reaction was filtered to remove insoluble dicyclohexylurea. The mixture was washed with 1N HCl, water, 1% sodium bicarbonate, then dried over sodium sulfate. The reaction was then filtered and evaporated to dryness, and triturated with dichloromethane to remove residual dicyclohexylurea. Yield 450 mg. 1.97 mmol, 52%. ^{1}H NMR (400 MHz, $CDCl_3$) δ 4.90 (s, 2H), 2.84 (s, 4H), 1.92 (s, 2H), 1.88 (s, 2H).

Conjugation of Isopropylidene-aminooxyacetic, succinimide ester (6) to leptin

To 20 uL of leptin solution (13.1 mg/mL, 16.4 nmol total) was added 32 uL of 100 mM sodium phosphate, pH 7.5, to generate a 5 mg/mL solution. Two 25 uL aliquots were prepared, and to each aliquot was added either 32.8 or 164 nmol isopropylidene-aminooxyacetic acid-NHS (corresponding to 7.5 or 37 μg) in 2.5 μL DMF. The reactions was allowed to stand for 5-6 hours and then analyzed by RP-HPLC and ESI-MS.

Preparation of aminooxyleptin by lysine side chain modification strategy

To 30 μL of leptin solution at 13.1 mg/mL was added 48 μL of 100 mM sodium phosphate pH 7.5, and 22.5 μg of isopropylidene-aminooxyacetic acid, succinimide ester (**6**) in 5 μL DMF. The reaction was allowed to proceed at room temperature overnight,

then chilled on ice. The reaction was diluted 1:1 with 1M methoxylamine hemihydrochloride, and allowed to stand on ice for five hours. The reaction was then analyzed by HPLC and ESI-MS.

Micro-PET imaging experiments

Imaging was conducted using a MicroPET (Focus TM 220, CTI Concord Microsystems, LLC) camera, with a bore size of 22 cm and an axial field of view of 7.6 cm. This enables imaging of the entire mouse. The resolution at the center of field of view (FOV) is <1.3 mm. Mice ranged in age from four to seven months of age.

Following induction of anesthesia with ketamine, each mouse was injected with 3.7-5.4 MBq of ^{18}F-FBA-leptin **5** or ^{68}Ga-DOTA-leptin in the tail vein. Rats were injected with 6-10 MBq of ^{68}Ga-DOTA-leptin. The distribution of radioactivity was studied by acquiring dynamic imaging for 30 - 60 minutes. 3D histograms of emission data were generated (span3, rig difference 47) using dead time correction. Images were reconstructed using OSEM2D algorithm without any attenuation or scatter correction. All data were analyzed on PMOD software (Zurich, Switzerland). Regions of interest were drawn by two independent operators, with similar results.

Metabolite analysis of blood, kidney, and urine by radiochemical HPLC

Approximately 20 MBq of ^{68}Ga -DOTA-leptin or ^{18}F-FBA-leptin was injected into the appropriate mice via the tail vein after induction of anesthesia with ketamine-xylazine. At the indicated time point, the animals were sacrificed, and the blood, urine, and kidneys harvested. Alternately, urine samples could be recovered by massaging the

bladder of the mice. Blood samples were centrifuged for 10 min at 8000 RPM (x g) prior to injection on HPLC. Kidney samples were solubilized by homogenization in 25 mM Tris pH 7.8, 1% triton X-100, 0.25% BSA, with one Compete mini EDTA-free protease inhibitor tablet (Roche) added per 10 mL, and centrifuged for 10 minutes at 8000 RPM prior to injection on HPLC.

Leptin ELISA in urine samples

Urine samples for ELISA were collected at 16 weeks of age. Urine samples from megalin$^{lox/lox}$,ApoE^{cre} and megalin$^{lox/lox}$ were diluted 10 fold in calibrator diluent of the mouse Elisa assay kit (R & D biosystems). A standard curve was build with known amounts of mouse recombinant leptin diluted in calibrator diluent and 10% urine from leptin deficient ob/ob mice. Instructions from the manufacturer were followed. Samples were measured in duplicate, and the assay sensitivity was 0.4 ng/ml.

Western blotting from urine samples

After concentration (10 fold from the starting volume) of the urine of megalin$^{lox/lox}$,ApoE^{cre} and megalin$^{lox/lox}$ using vivaspin concentrators (Sartorius), samples were boiled at 95 C in loading buffer with 10% 2-mercaptoethanol. 30 microliters of each sample were loaded on a 5-12% acrylamide gel (Biorad) and then transferred to nitrocellulose membranes for western blot analysis. Blots were blocked in TBST and 5% milk and then incubated overnight in TBST and 5% milk with rabbit polyclonal anti-leptin antibody A-20 (Santa Cruz) diluted 1:500. After wash with TBST blot was incubated with a secondary antibody anti-rabbit IgG conjugated with HRP (GE

Healthcare) and ECL reaction performed using ECL plus western blotting detection system kit (GE Healthcare).

Mouse biodistribution experiments

Approximately 10-15 KBq of ^{125}I-leptin (New England Nuclear, 81.4 GBq/umol, 20 uL of the solution provided by the manufacturer) was diluted in 300 uL of sterile PBS and injected in the tail vein of the appropriate mouse strains in the presence or absence of 50 uL of murine leptin solution (13.1 mg/mL, Amgen/Amylin). After 15 minutes, the animals were sacrificed, and tissues were collected and weighed. Radioactivity associated with each sample was counted in a gamma counter with corresponding standards and blanks, and residual activity from each injection. The total injected dose was computed by preparing a standard of 20 uL of the manufacturers solution, and subtracting the residual dose remaining in the syringe post injection, and the radioactivity in the tail of the animal.

Subcloning of Rhesus-leptin in a pET 15b vector

Rhesus leptin was subcloned into a PET15b vector, to facilitate purification using the His_6 tag encoded for in the vector. A plasmid containing a synthetic gene, codon optimized for expression in bacteria, encoding the 146 amino acids of intact rhesus leptin following a methionine, was ordered from Integrated DNA technologies. The 2 μg of DNA obtained from the manufacturer was resuspended in 200 μL TE buffer. The cDNA encoding rhesus leptin was amplified by PCR from using forward and reverse primers (GGAATTCCATATGGTGCCAATCCAGAAAGTTCA and

CGGGATCCTTAACAACCCGGAGACAGGTC, respectively) encoding the NdeI and BamHI restriction sites. The PCR reaction was then purified by gel extraction. The PCR product and the PET15b vector was digested with NdeI and BamHI, and the vector was treated with calf intestinal phosphatase. The vector was then purified by gel extraction, and the PCR product using a PCR purification kit (Qiagen). The rhesus leptin PCR product was then ligated into the PET15b vector, and transformed into DH5α *E. coli*. The identity of the correct plasmids were screened by digestion with NdeI and BamHI, and confirmed by sequencing.

Expression and purification of rhesus leptin

Expression of rhesus leptin was similar to a previously described protocol[256]. PET15b-Rhesus leptin plasmid was transformed into BL21(DE3) *E. coli*. An overnight culture was prepared in LB broth, which was diluted the following day by a factor of 100 into 6 X 1L shaking flasks. The bacteria grew at 37°C with shaking at 250 RPM, and protein expression was induced with 1 mM Isopropyl β-D-1-thiogalactopyranoside (IPTG) at an OD590 of 0.8. After six hours of induction, the cells were harvested by centrifugation. From a typical prep, 30g of biomass could be obtained. Initial experiments revealed the presence of an approximately 16 kDa protein in the insoluble fraction, in induced but not uninduced cells, and thus preparation of the protein from inclusion bodies was used in future experiments.

The cells were resuspended in two volumes lysis buffer consisting of 1% triton, 50 mM sodium phosphate buffer, pH 7.0, 200 mM sodium chloride supplemented with one complete protease inhibitor tablet, EDTA free (Roche, Basel, Switzerland) per 50 mL

of buffer. The cells were lysed by passage through a French Press (Emulsiflex C5 homogenizer, Avestin, Ottawa, Canada.) The inclusion bodies were separated by centrifugation at 16,000 rpm for 30 minutes, and washed with an equal volume of lysis buffer. The pellet was subsequently resuspended overnight in one volume (relative to the cell pellet) of resuspension buffer consisting of 8 M urea, 10 mM imidazole, 500 mM sodium chloride, 100 mM sodium phosphate, pH 7.5. This suspension was centrifuged again at 16,000 RPM for 30 minutes to remove insoluble debris, and applied to 25 mL of Ni-NTA beads which were pre-equilibrated with resuspension buffer supplemented with 10 mM imidazole. The beads were then washed with resuspension buffer supplemented with 20 mM imidazole, and the fusion protein was eluted from the column with 5 x 20 mL fractions of resuspension buffer supplemented with 500 mM imidazole. The fractions were analyzed by SDS-PAGE and those containing the fusion protein were pooled. The protein was then refolded by dropwise infusion of 0.1M Tris pH 7.4 at 1 mL/min over approximately 90 minutes. Reduced and oxidized glutathione were added to 10 and 1 mM, respectively, and the solution was allowed to stir overnight at 4 °C. The solution was then centrifuged at 16,000 RPM for 30 minutes to remove insoluble debris, and then dialyzed against thrombin cleavage buffer consisting of 50 mM tris pH 8.3, 150 mM NaCl, 2.5 mM $CaCl_2$ in order to remove imidazole. The resulting solution was again centrifuged to remove insoluble debris, and 100 units of thrombin (Sigma) was added to the supernatant. Following overnight cleavage at 4 °C, the resulting solution was purified by process scale C4 RP-HPLC on a 47-62%B gradient. The fractions containing the intact rhesus leptin were then resuspended in 6M guandine, 100 mM Tris pH 8.0, and purified by gel filtration on an S75 10/300 GL column, using 10 mM sodium phosphate,

140 mM NaCl, pH 7.4 as an eluant. From a typical 6L prep, 2 – 3 mg of rhesus leptin could be obtained using this protocol. The sequence of the final protein is GSHM-rhesus leptin(1-146).

Rhesus macaque PET-CT imaging experiments

On experiment days, the subjects were individually transported to the PET center in a purpose - built transfer cage. They were then injected with ketamine (10 mg/kg, i.m.) and atropine (0.05 mg/kg, i.m). Subjects were then intubated and anesthesia was induced with isoflurane (3%). Subjects' vital signs (respiratory rate, heart rate, temperature and pulse oximetry) were monitored throughout, anesthesia was typically then maintained at 1.5-2% isoflurane for the remainder of the experiment.

The subject was placed supine on a heating pad (37ºC) in the bed of the PET scanner for the remainder of the experiment. Primate PET/CT scans were performed using a GE Discovery LS PET/CT scanner (GE Healthcare, Waukesha, Wis.). A low-dose CT scan was obtained and the scanner bed was moved into PET position. Competing cold leptin was administered by a femoral catheter 10 min prior to injection of the radiotracer. Immediately following an intravenous injection of 0.25-1 mCi of ^{68}Ga-DOTA-leptin, 4 sequential 18 min whole-body images were obtained (3 beds, 6 minutes each) in 3D acquisition mode. Images were reconstructed using the FORE-Iterative reconstruction method.

Following completion of the transmission scan, isoflurane was discontinued and the subject was extubated when gagging reflex is observed, and carefully observed until recovery (which was rapid and uneventful).

References

(1) Weigle, D. S. Appetite and the regulation of body composition. *FASEB J* **1994**, *8*, 302-10.

(2) Walley, A. J.; Blakemore, A. I.; Froguel, P. Genetics of obesity and the prediction of risk for health. *Hum Mol Genet* **2006**, *15 Spec No 2*, R124-30.

(3) http://www.cdc.gov/nccdphp/dnpa/obesity/index.htm.

(4) Maes, H. H.; Neale, M. C.; Eaves, L. J. Genetic and environmental factors in relative body weight and human adiposity. *Behav Genet* **1997**, *27*, 325-51.

(5) Barsh, G. S.; Farooqi, I. S.; O'Rahilly, S. Genetics of body-weight regulation. *Nature* **2000**, *404*, 644-51.

(6) King, B. M. The rise, fall, and resurrection of the ventromedial hypothalamus in the regulation of feeding behavior and body weight. *Physiol Behav* **2006**, *87*, 221-44.

(7) Kennedy, G. C. The role of depot fat in the hypothalamic control of food intake in the rat. *Proc R Soc Lond B Biol Sci* **1953**, *140*, 578-96.

(8) Coleman, D. L. Obese and diabetes: two mutant genes causing diabetes-obesity syndromes in mice. *Diabetologia* **1978**, *14*, 141-8.

(9) Coleman, D. L.; Hummel, K. P. Effects of parabiosis of normal with genetically diabetic mice. *Am J Physiol* **1969**, *217*, 1298-304.

(10) Zhang, Y.; Proenca, R.; Maffei, M.; Barone, M.; Leopold, L.; Friedman, J. M. Positional cloning of the mouse obese gene and its human homologue. *Nature* **1994**, *372*, 425-32.

(11) Maffei, M.; Fei, H.; Lee, G. H.; Dani, C.; Leroy, P.; Zhang, Y.; Proenca, R.; Negrel, R.; Ailhaud, G.; Friedman, J. M. Increased expression in adipocytes of ob RNA in mice with lesions of the hypothalamus and with mutations at the db locus. *Proc Natl Acad Sci U S A* **1995**, *92*, 6957-60.

(12) Klein, S.; Coppack, S. W.; Mohamed-Ali, V.; Landt, M. Adipose tissue leptin production and plasma leptin kinetics in humans. *Diabetes* **1996**, *45*, 984-7.

(13) Maffei, M.; Halaas, J.; Ravussin, E.; Pratley, R. E.; Lee, G. H.; Zhang, Y.; Fei, H.; Kim, S.; Lallone, R.; Ranganathan, S.; Kern, P. A.; Friedman, J. M. Leptin levels in human and rodent: measurement of plasma leptin and ob RNA in obese and weight-reduced subjects. *Nat Med* **1995**, *1*, 1155-61.

(14) Halaas, J. L.; Gajiwala, K. S.; Maffei, M.; Cohen, S. L.; Chait, B. T.; Rabinowitz, D.; Lallone, R. L.; Burley, S. K.; Friedman, J. M. Weight-reducing effects of the plasma protein encoded by the obese gene. *Science* **1995**, *269*, 543-6.

(15) Tartaglia, L. A.; Dembski, M.; Weng, X.; Deng, N.; Culpepper, J.; Devos, R.; Richards, G. J.; Campfield, L. A.; Clark, F. T.; Deeds, J.; Muir, C.; Sanker, S.; Moriarty, A.; Moore, K. J.; Smutko, J. S.; Mays, G. G.; Wool, E. A.; Monroe, C. A.; Tepper, R. I. Identification and expression cloning of a leptin receptor, OB-R. *Cell* **1995**, *83*, 1263-71.

(16) Lee, G. H.; Proenca, R.; Montez, J. M.; Carroll, K. M.; Darvishzadeh, J. G.; Lee, J. I.; Friedman, J. M. Abnormal splicing of the leptin receptor in diabetic mice. *Nature* **1996**, *379*, 632-5.

(17) Banks, W. A.; Kastin, A. J.; Huang, W.; Jaspan, J. B.; Maness, L. M. Leptin enters the brain by a saturable system independent of insulin. *Peptides* **1996**, *17*, 305-11.

(18) Cohen, P.; Zhao, C.; Cai, X.; Montez, J. M.; Rohani, S. C.; Feinstein, P.; Mombaerts, P.; Friedman, J. M. Selective deletion of leptin receptor in neurons leads to obesity. *J Clin Invest* **2001**, *108*, 1113-21.

(19) Friedman, J. M.; Halaas, J. L. Leptin and the regulation of body weight in mammals. *Nature* **1998**, *395*, 763-70.

(20) Montague, C. T.; Farooqi, I. S.; Whitehead, J. P.; Soos, M. A.; Rau, H.; Wareham, N. J.; Sewter, C. P.; Digby, J. E.; Mohammed, S. N.; Hurst, J. A.; Cheetham, C. H.; Earley, A. R.; Barnett, A. H.; Prins, J. B.; O'Rahilly, S. Congenital leptin deficiency is associated with severe early-onset obesity in humans. *Nature* **1997**, *387*, 903-8.

(21) Farooqi, I. S.; Matarese, G.; Lord, G. M.; Keogh, J. M.; Lawrence, E.; Agwu, C.; Sanna, V.; Jebb, S. A.; Perna, F.; Fontana, S.; Lechler, R. I.; DePaoli, A. M.; O'Rahilly,

S. Beneficial effects of leptin on obesity, T cell hyporesponsiveness, and neuroendocrine/metabolic dysfunction of human congenital leptin deficiency. *J Clin Invest* **2002**, *110*, 1093-103.

(22) Farooqi, I. S.; Wangensteen, T.; Collins, S.; Kimber, W.; Matarese, G.; Keogh, J. M.; Lank, E.; Bottomley, B.; Lopez-Fernandez, J.; Ferraz-Amaro, I.; Dattani, M. T.; Ercan, O.; Myhre, A. G.; Retterstol, L.; Stanhope, R.; Edge, J. A.; McKenzie, S.; Lessan, N.; Ghodsi, M.; De Rosa, V.; Perna, F.; Fontana, S.; Barroso, I.; Undlien, D. E.; O'Rahilly, S. Clinical and molecular genetic spectrum of congenital deficiency of the leptin receptor. *N Engl J Med* **2007**, *356*, 237-47.

(23) Farooqi, I. S.; O'Rahilly, S. Monogenic obesity in humans. *Annu Rev Med* **2005**, *56*, 443-58.

(24) Coll, A. P.; Farooqi, I. S.; O'Rahilly, S. The hormonal control of food intake. *Cell* **2007**, *129*, 251-62.

(25) Heymsfield, S. B.; Greenberg, A. S.; Fujioka, K.; Dixon, R. M.; Kushner, R.; Hunt, T.; Lubina, J. A.; Patane, J.; Self, B.; Hunt, P.; McCamish, M. Recombinant leptin for weight loss in obese and lean adults: a randomized, controlled, dose-escalation trial. *JAMA* **1999**, *282*, 1568-75.

(26) Caro, J. F.; Kolaczynski, J. W.; Nyce, M. R.; Ohannesian, J. P.; Opentanova, I.; Goldman, W. H.; Lynn, R. B.; Zhang, P. L.; Sinha, M. K.; Considine, R. V. Decreased cerebrospinal-fluid/serum leptin ratio in obesity: a possible mechanism for leptin resistance. *Lancet* **1996**, *348*, 159-61.

(27) Myers, M. G.; Cowley, M. A.; Munzberg, H. Mechanisms of leptin action and leptin resistance. *Annu Rev Physiol* **2008**, *70*, 537-56.

(28) Roth, J. D.; Roland, B. L.; Cole, R. L.; Trevaskis, J. L.; Weyer, C.; Koda, J. E.; Anderson, C. M.; Parkes, D. G.; Baron, A. D. Leptin responsiveness restored by amylin agonism in diet-induced obesity: evidence from nonclinical and clinical studies. *Proc Natl Acad Sci U S A* **2008**, *105*, 7257-62.

(29) Trevaskis, J. L.; Coffey, T.; Cole, R.; Lei, C.; Wittmer, C.; Walsh, B.; Weyer, C.; Koda, J.; Baron, A. D.; Parkes, D. G.; Roth, J. D. Amylin-Mediated Restoration of Leptin Responsiveness in Diet-Induced Obesity: Magnitude and Mechanisms. *Endocrinology* **2008**.

(30) Gorden, P.; Gavrilova, O. The clinical uses of leptin. *Curr Opin Pharmacol* **2003**, *3*, 655-9.

(31) Bluher, S.; Mantzoros, C. S. Leptin in reproduction. *Curr Opin Endocrinol Diabetes Obes* **2007**, *14*, 458-64.

(32) Cohen, S. L.; Halaas, J. L.; Friedman, J. M.; Chait, B. T.; Bennett, L.; Chang, D.; Hecht, R.; Collins, F. Human leptin characterization. *Nature* **1996**, *382*, 589.

(33) Zhang, F.; Basinski, M. B.; Beals, J. M.; Briggs, S. L.; Churgay, L. M.; Clawson, D. K.; DiMarchi, R. D.; Furman, T. C.; Hale, J. E.; Hsiung, H. M.; Schoner, B. E.; Smith, D. P.; Zhang, X. Y.; Wery, J. P.; Schevitz, R. W. Crystal structure of the obese protein leptin-E100. *Nature* **1997**, *387*, 206-9.

(34) Peelman, F.; Iserentant, H.; De Smet, A. S.; Vandekerckhove, J.; Zabeau, L.; Tavernier, J. Mapping of binding site III in the leptin receptor and modeling of a hexameric leptin.leptin receptor complex. *J Biol Chem* **2006**, *281*, 15496-504.

(35) Mistrik, P.; Moreau, F.; Allen, J. M. BiaCore analysis of leptin-leptin receptor interaction: evidence for 1:1 stoichiometry. *Anal Biochem* **2004**, *327*, 271-7.

(36) Fruhbeck, G. Intracellular signalling pathways activated by leptin. *Biochem J* **2006**, *393*, 7-20.

(37) Fei, H.; Okano, H. J.; Li, C.; Lee, G. H.; Zhao, C.; Darnell, R.; Friedman, J. M. Anatomic localization of alternatively spliced leptin receptors (Ob-R) in mouse brain and other tissues. *Proc Natl Acad Sci U S A* **1997**, *94*, 7001-5.

(38) Murakami, T.; Yamashita, T.; Iida, M.; Kuwajima, M.; Shima, K. A short form of leptin receptor performs signal transduction. *Biochem Biophys Res Commun* **1997**, *231*, 26-9.

(39) Hileman, S. M.; Pierroz, D. D.; Masuzaki, H.; Bjorbaek, C.; El-Haschimi, K.; Banks, W. A.; Flier, J. S. Characterizaton of short isoforms of the leptin receptor in rat cerebral microvessels and of brain uptake of leptin in mouse models of obesity. *Endocrinology* **2002**, *143*, 775-83.

(40) Banks, W. A.; Niehoff, M. L.; Martin, D.; Farrell, C. L. Leptin transport across the blood-brain barrier of the Koletsky rat is not mediated by a product of the leptin receptor gene. *Brain Res* **2002**, *950*, 130-6.

(41) Sinha, M. K.; Opentanova, I.; Ohannesian, J. P.; Kolaczynski, J. W.; Heiman, M. L.; Hale, J.; Becker, G. W.; Bowsher, R. R.; Stephens, T. W.; Caro, J. F. Evidence of free and bound leptin in human circulation. Studies in lean and obese subjects and during short-term fasting. *J Clin Invest* **1996**, *98*, 1277-82.

(42) Lammert, A.; Kiess, W.; Bottner, A.; Glasow, A.; Kratzsch, J. Soluble leptin receptor represents the main leptin binding activity in human blood. *Biochem Biophys Res Commun* **2001**, *283*, 982-8.

(43) Liu, C.; Liu, X. J.; Barry, G.; Ling, N.; Maki, R. A.; De Souza, E. B. Expression and characterization of a putative high affinity human soluble leptin receptor. *Endocrinology* **1997**, *138*, 3548-54.

(44) Patel, N.; Brinkman-Van der Linden, E. C.; Altmann, S. W.; Gish, K.; Balasubramanian, S.; Timans, J. C.; Peterson, D.; Bell, M. P.; Bazan, J. F.; Varki, A.; Kastelein, R. A. OB-BP1/Siglec-6. a leptin- and sialic acid-binding protein of the immunoglobulin superfamily. *J Biol Chem* **1999**, *274*, 22729-38.

(45) Chen, K.; Li, F.; Li, J.; Cai, H.; Strom, S.; Bisello, A.; Kelley, D. E.; Friedman-Einat, M.; Skibinski, G. A.; McCrory, M. A.; Szalai, A. J.; Zhao, A. Z. Induction of leptin resistance through direct interaction of C-reactive protein with leptin. *Nat Med* **2006**, *12*, 425-32.

(46) Gertler, A.; Niv-Spector, L.; Reicher, S. Is leptin an important physiological regulator of CRP? *Nat Med* **2007**, *13*, 18-9; author reply 19-21.

(47) Hutchinson, W. L.; Coll, A. P.; Gallimore, J. R.; Tennent, G. A.; Pepys, M. B. Is leptin an important physiological regulator of CRP? *Nat Med* **2007**, *13*, 17-8; author reply 19-21.

(48) Farooqi, I. S.; O'Rahilly, S. Is leptin an important physiological regulator of CRP? *Nat Med* **2007**, *13*, 16-7; author reply 19-21.

(49) Birkenmeier, G.; Kampfer, I.; Kratzsch, J.; Schellenberger, W. Human leptin forms complexes with alpha 2-macroglobulin which are recognized by the alpha 2-

macroglobulin receptor/low density lipoprotein receptor-related protein. *Eur J Endocrinol* **1998**, *139*, 224-30.

(50) Hama, H.; Saito, A.; Takeda, T.; Tanuma, A.; Xie, Y.; Sato, K.; Kazama, J. J.; Gejyo, F. Evidence indicating that renal tubular metabolism of leptin is mediated by megalin but not by the leptin receptors. *Endocrinology* **2004**, *145*, 3935-40.

(51) Sahu, A. Minireview: A hypothalamic role in energy balance with special emphasis on leptin. *Endocrinology* **2004**, *145*, 2613-20.

(52) de Luca, C.; Kowalski, T. J.; Zhang, Y.; Elmquist, J. K.; Lee, C.; Kilimann, M. W.; Ludwig, T.; Liu, S. M.; Chua, S. C., Jr. Complete rescue of obesity, diabetes, and infertility in db/db mice by neuron-specific LEPR-B transgenes. *J Clin Invest* **2005**, *115*, 3484-93.

(53) Halaas, J. L.; Boozer, C.; Blair-West, J.; Fidahusein, N.; Denton, D. A.; Friedman, J. M. Physiological response to long-term peripheral and central leptin infusion in lean and obese mice. *Proc Natl Acad Sci U S A* **1997**, *94*, 8878-83.

(54) Anand, B. K.; Brobeck, J. R. Localization of a "feeding center" in the hypothalamus of the rat. *Proc Soc Exp Biol Med* **1951**, *77*, 323-4.

(55) Flier, J. S. AgRP in energy balance: Will the real AgRP please stand up? *Cell Metab* **2006**, *3*, 83-5.

(56) Coll, A. P.; Farooqi, I. S.; Challis, B. G.; Yeo, G. S.; O'Rahilly, S. Proopiomelanocortin and energy balance: insights from human and murine genetics. *J Clin Endocrinol Metab* **2004**, *89*, 2557-62.

(57) Ollmann, M. M.; Wilson, B. D.; Yang, Y. K.; Kerns, J. A.; Chen, Y.; Gantz, I.; Barsh, G. S. Antagonism of central melanocortin receptors in vitro and in vivo by agouti-related protein. *Science* **1997**, *278*, 135-8.

(58) Schwartz, M. W.; Woods, S. C.; Porte, D., Jr.; Seeley, R. J.; Baskin, D. G. Central nervous system control of food intake. *Nature* **2000**, *404*, 661-71.

(59) Kieffer, T. J.; Heller, R. S.; Habener, J. F. Leptin receptors expressed on pancreatic beta-cells. *Biochem Biophys Res Commun* **1996**, *224*, 522-7.

(60) Hoggard, N.; Mercer, J. G.; Rayner, D. V.; Moar, K.; Trayhurn, P.; Williams, L. M. Localization of leptin receptor mRNA splice variants in murine peripheral tissues by RT-PCR and in situ hybridization. *Biochem Biophys Res Commun* **1997**, *232*, 383-7.

(61) Hoggard, N.; Hunter, L.; Duncan, J. S.; Williams, L. M.; Trayhurn, P.; Mercer, J. G. Leptin and leptin receptor mRNA and protein expression in the murine fetus and placenta. *Proc Natl Acad Sci U S A* **1997**, *94*, 11073-8.

(62) Lord, G. M.; Matarese, G.; Howard, J. K.; Baker, R. J.; Bloom, S. R.; Lechler, R. I. Leptin modulates the T-cell immune response and reverses starvation-induced immunosuppression. *Nature* **1998**, *394*, 897-901.

(63) Cioffi, J. A.; Shafer, A. W.; Zupancic, T. J.; Smith-Gbur, J.; Mikhail, A.; Platika, D.; Snodgrass, H. R. Novel B219/OB receptor isoforms: possible role of leptin in hematopoiesis and reproduction. *Nat Med* **1996**, *2*, 585-9.

(64) Sierra-Honigmann, M. R.; Nath, A. K.; Murakami, C.; Garcia-Cardena, G.; Papapetropoulos, A.; Sessa, W. C.; Madge, L. A.; Schechner, J. S.; Schwabb, M. B.; Polverini, P. J.; Flores-Riveros, J. R. Biological action of leptin as an angiogenic factor. *Science* **1998**, *281*, 1683-6.

(65) Matsunuma, A.; Horiuchi, N. Leptin attenuates gene expression for renal 25-hydroxyvitamin D3-1alpha-hydroxylase in mice via the long form of the leptin receptor. *Arch Biochem Biophys* **2007**, *463*, 118-27.

(66) Kim, Y. B.; Uotani, S.; Pierroz, D. D.; Flier, J. S.; Kahn, B. B. In vivo administration of leptin activates signal transduction directly in insulin-sensitive tissues: overlapping but distinct pathways from insulin. *Endocrinology* **2000**, *141*, 2328-39.

(67) Morioka, T.; Asilmaz, E.; Hu, J.; Dishinger, J. F.; Kurpad, A. J.; Elias, C. F.; Li, H.; Elmquist, J. K.; Kennedy, R. T.; Kulkarni, R. N. Disruption of leptin receptor expression in the pancreas directly affects beta cell growth and function in mice. *J Clin Invest* **2007**, *117*, 2860-8.

(68) Martin-Romero, C.; Santos-Alvarez, J.; Goberna, R.; Sanchez-Margalet, V. Human leptin enhances activation and proliferation of human circulating T lymphocytes. *Cell Immunol* **2000**, *199*, 15-24.

(69) Matarese, G.; Di Giacomo, A.; Sanna, V.; Lord, G. M.; Howard, J. K.; Di Tuoro, A.; Bloom, S. R.; Lechler, R. I.; Zappacosta, S.; Fontana, S. Requirement for leptin in the induction and progression of autoimmune encephalomyelitis. *J Immunol* **2001**, *166*, 5909-16.

(70) Torday, J. S.; Sun, H.; Wang, L.; Torres, E.; Sunday, M. E.; Rubin, L. P. Leptin mediates the parathyroid hormone-related protein paracrine stimulation of fetal lung maturation. *Am J Physiol Lung Cell Mol Physiol* **2002**, *282*, L405-10.

(71) Wang, M. Y.; Orci, L.; Ravazzola, M.; Unger, R. H. Fat storage in adipocytes requires inactivation of leptin's paracrine activity: implications for treatment of human obesity. *Proc Natl Acad Sci U S A* **2005**, *102*, 18011-6.

(72) Park, B. H.; Wang, M. Y.; Lee, Y.; Yu, X.; Ravazzola, M.; Orci, L.; Unger, R. H. Combined leptin actions on adipose tissue and hypothalamus are required to deplete adipocyte fat in lean rats: implications for obesity treatment. *J Biol Chem* **2006**, *281*, 40283-91.

(73) Siegrist-Kaiser, C. A.; Pauli, V.; Juge-Aubry, C. E.; Boss, O.; Pernin, A.; Chin, W. W.; Cusin, I.; Rohner-Jeanrenaud, F.; Burger, A. G.; Zapf, J.; Meier, C. A. Direct effects of leptin on brown and white adipose tissue. *J Clin Invest* **1997**, *100*, 2858-64.

(74) Lappas, M.; Permezel, M.; Rice, G. E. Leptin and adiponectin stimulate the release of proinflammatory cytokines and prostaglandins from human placenta and maternal adipose tissue via nuclear factor-kappaB, peroxisomal proliferator-activated receptor-gamma and extracellularly regulated kinase 1/2. *Endocrinology* **2005**, *146*, 3334-42.

(75) Minokoshi, Y.; Kim, Y. B.; Peroni, O. D.; Fryer, L. G.; Muller, C.; Carling, D.; Kahn, B. B. Leptin stimulates fatty-acid oxidation by activating AMP-activated protein kinase. *Nature* **2002**, *415*, 339-43.

(76) Lynn, R. B.; Cao, G. Y.; Considine, R. V.; Hyde, T. M.; Caro, J. F. Autoradiographic localization of leptin binding in the choroid plexus of ob/ob and db/db mice. *Biochem Biophys Res Commun* **1996**, *219*, 884-9.

(77) Malik, K. F.; Young, W. S., 3rd Localization of binding sites in the central nervous system for leptin (OB protein) in normal, obese (ob/ob), and diabetic (db/db) C57BL/6J mice. *Endocrinology* **1996**, *137*, 1497-500.

(78) Devos, R.; Richards, J. G.; Campfield, L. A.; Tartaglia, L. A.; Guisez, Y.; van der Heyden, J.; Travernier, J.; Plaetinck, G.; Burn, P. OB protein binds specifically to the choroid plexus of mice and rats. *Proc Natl Acad Sci U S A* **1996**, *93*, 5668-73.

(79) Williams, L. M.; Adam, C. L.; Mercer, J. G.; Moar, K. M.; Slater, D.; Hunter, L.; Findlay, P. A.; Hoggard, N. Leptin receptor and neuropeptide Y gene expression in the sheep brain. *J Neuroendocrinol* **1999**, *11*, 165-9.

(80) Baskin, D. G.; Breininger, J. F.; Bonigut, S.; Miller, M. A. Leptin binding in the arcuate nucleus is increased during fasting. *Brain Res* **1999**, *828*, 154-8.

(81) Serradeil-Le Gal, C.; Raufaste, D.; Brossard, G.; Pouzet, B.; Marty, E.; Maffrand, J. P.; Le Fur, G. Characterization and localization of leptin receptors in the rat kidney. *FEBS Lett* **1997**, *404*, 185-91.

(82) Cao, G. Y.; Considine, R. V.; Lynn, R. B. Leptin receptors in the adrenal medulla of the rat. *Am J Physiol* **1997**, *273*, E448-52.

(83) Dal Farra, C.; Zsurger, N.; Vincent, J. P.; Cupo, A. Binding of a pure 125I-monoiodoleptin analog to mouse tissues: a developmental study. *Peptides* **2000**, *21*, 577-87.

(84) Zeng, J.; Patterson, B. W.; Klein, S.; Martin, D. R.; Dagogo-Jack, S.; Kohrt, W. M.; Miller, S. B.; Landt, M. Whole body leptin kinetics and renal metabolism in vivo. *Am J Physiol* **1997**, *273*, E1102-6.

(85) Hill, R. A.; Margetic, S.; Pegg, G. G.; Gazzola, C. Leptin: its pharmacokinetics and tissue distribution. *Int J Obes Relat Metab Disord* **1998**, *22*, 765-70.

(86) Ahren, B.; Baldwin, R. M.; Havel, P. J. Pharmacokinetics of human leptin in mice and rhesus monkeys. *Int J Obes Relat Metab Disord* **2000**, *24*, 1579-85.

(87) Cumin, F.; Baum, H. P.; Levens, N. Leptin is cleared from the circulation primarily by the kidney. *Int J Obes Relat Metab Disord* **1996**, *20*, 1120-6.

(88) Meyer, C.; Robson, D.; Rackovsky, N.; Nadkarni, V.; Gerich, J. Role of the kidney in human leptin metabolism. *Am J Physiol* **1997**, *273*, E903-7.

(89) Garibotto, G.; Russo, R.; Franceschini, R.; Robaudo, C.; Saffioti, S.; Sofia, A.; Rolandi, E.; Deferrari, G.; Barreca, T. Inter-organ leptin exchange in humans. *Biochem Biophys Res Commun* **1998**, *247*, 504-9.

(90) Jensen, M. D.; Moller, N.; Nair, K. S.; Eisenberg, P.; Landt, M.; Klein, S. Regional leptin kinetics in humans. *Am J Clin Nutr* **1999**, *69*, 18-21.

(91) Sharma, K.; Considine, R. V.; Michael, B.; Dunn, S. R.; Weisberg, L. S.; Kurnik, B. R.; Kurnik, P. B.; O'Connor, J.; Sinha, M.; Caro, J. F. Plasma leptin is partly cleared by the kidney and is elevated in hemodialysis patients. *Kidney Int* **1997**, *51*, 1980-5.

(92) Van Heek, M.; Mullins, D. E.; Wirth, M. A.; Graziano, M. P.; Fawzi, A. B.; Compton, D. S.; France, C. F.; Hoos, L. M.; Casale, R. L.; Sybertz, E. J.; Strader, C. D.; Davis, H. R., Jr. The relationship of tissue localization, distribution and turnover to feeding after intraperitoneal 125I-leptin administration to ob/ob and db/db mice. *Horm Metab Res* **1996**, *28*, 653-8.

(93) Hileman, S. M.; Tornoe, J.; Flier, J. S.; Bjorbaek, C. Transcellular transport of leptin by the short leptin receptor isoform ObRa in Madin-Darby Canine Kidney cells. *Endocrinology* **2000**, *141*, 1955-61.

(94) Maness, L. M.; Banks, W. A.; Kastin, A. J. Persistence of blood-to-brain transport of leptin in obese leptin-deficient and leptin receptor-deficient mice. *Brain Res* **2000**, *873*, 165-7.

(95) Banks, W. A.; DiPalma, C. R.; Farrell, C. L. Impaired transport of leptin across the blood-brain barrier in obesity. *Peptides* **1999**, *20*, 1341-5.

(96) Karonen, S. L.; Koistinen, H. A.; Nikkinen, P.; Koivisto, V. A. Is brain uptake of leptin in vivo saturable and reduced by fasting? *Eur J Nucl Med* **1998**, *25*, 607-12.

(97) McCarthy, T. J.; Banks, W. A.; Farrell, C. L.; Adamu, S.; Derdeyn, C. P.; Snyder, A. Z.; Laforest, R.; Litzinger, D. C.; Martin, D.; LeBel, C. P.; Welch, M. J. Positron emission tomography shows that intrathecal leptin reaches the hypothalamus in baboons. *J Pharmacol Exp Ther* **2002**, *301*, 878-83.

(98) Levin, C. S. Primer on molecular imaging technology. *Eur J Nucl Med Mol Imaging* **2005**, *32 Suppl 2*, S325-45.

(99) Ametamey, S. M.; Honer, M.; Schubiger, P. A. Molecular imaging with PET. *Chem Rev* **2008**, *108*, 1501-16.

(100) McQuade, P.; Rowland, D. J.; Lewis, J. S.; Welch, M. J. Positron-emitting isotopes produced on biomedical cyclotrons. *Curr Med Chem* **2005**, *12*, 807-18.

(101) Alejandro Sanchez-Crespo, P. A., Stig A. Larsson Positron flight in human tissues and its influence on PET image spatial resolution. *European Journal of Nuclear Medicine and Molecular Imaging* **2004**, *31*, 44-51.

(102) Heppeler, A.; Froidevaux, S.; Eberle, A. N.; Maecke, H. R. Receptor targeting for tumor localisation and therapy with radiopeptides. *Curr Med Chem* **2000**, *7*, 971-94.

(103) H. J. Wester, M. S. Fluorine-18 Labeling of Peptides and Proteins. *Ernst Schering Research Foundation Workshop* **2007**, *62*, 79-111.

(104) Velikyan, I.; Beyer, G. J.; Bergstrom-Pettermann, E.; Johansen, P.; Bergstrom, M.; Langstrom, B. The importance of high specific radioactivity in the performance of 68Ga-labeled peptide. *Nucl Med Biol* **2008**, *35*, 529-36.

(105) Wadas, T. J.; Wong, E. H.; Weisman, G. R.; Anderson, C. J. Copper chelation chemistry and its role in copper radiopharmaceuticals. *Curr Pharm Des* **2007**, *13*, 3-16.

(106) De Leon-Rodriguez, L. M.; Kovacs, Z. The synthesis and chelation chemistry of DOTA-peptide conjugates. *Bioconjug Chem* **2008**, *19*, 391-402.

(107) Wilbur, D. S. Radiohalogenation of proteins: an overview of radionuclides, labeling methods, and reagents for conjugate labeling. *Bioconjug Chem* **1992**, *3*, 433-70.

(108) Ting, R.; Harwig, C.; Auf dem Keller, U.; McCormick, S.; Austin, P.; Overall, C. M.; Adam, M. J.; Ruth, T. J.; Perrin, D. M. Toward [(18)F]-Labeled Aryltrifluoroborate Radiotracers: In Vivo Positron Emission Tomography Imaging of Stable Aryltrifluoroborate Clearance in Mice. *J Am Chem Soc* **2008**.

(109) Schirrmacher, R.; Bradtmoller, G.; Schirrmacher, E.; Thews, O.; Tillmanns, J.; Siessmeier, T.; Buchholz, H. G.; Bartenstein, P.; Wangler, B.; Niemeyer, C. M.; Jurkschat, K. 18F-labeling of peptides by means of an organosilicon-based fluoride acceptor. *Angew Chem Int Ed Engl* **2006**, *45*, 6047-50.

(110) Okarvi, S. M. Recent progress in fluorine-18 labeled peptide radiopharmaceuticals. *Eur J Nucl Med* **2001**, *28*, 929-38.

(111) Wester, H. J.; Schottelius, M. Fluorine-18 labeling of peptides and proteins. *Ernst Schering Res Found Workshop* **2007**, 79-111.

(112) *Positron Emission Tomography*; Bailey, D. L.; Townsend, D. W.; Valk, P. E.; Maisey, M. N., Eds.; Springer-Verlag: London, 2005, pp 369.

(113) Vaidyanathan, G.; Zalutsky, M. R. Fluorine-18 labeled chemotactic peptides: a potential approach for the PET imaging of bacterial infection. *Nucl Med Biol* **1995**, *22*, 759-64.

(114) Poethko, T.; Schottelius, M.; Thumshirn, G.; Hersel, U.; Herz, M.; Henriksen, G.; Kessler, H.; Schwaiger, M.; Wester, H. J. Two-step methodology for high-yield routine radiohalogenation of peptides: (18)F-labeled RGD and octreotide analogs. *J Nucl Med* **2004**, *45*, 892-902.

(115) Schottelius, M.; Poethko, T.; Herz, M.; Reubi, J. C.; Kessler, H.; Schwaiger, M.; Wester, H. J. First (18)F-labeled tracer suitable for routine clinical imaging of sst receptor-expressing tumors using positron emission tomography. *Clin Cancer Res* **2004**, *10*, 3593-606.

(116) Glaser, M.; Karlsen, H.; Solbakken, M.; Arukwe, J.; Brady, F.; Luthra, S. K.; Cuthbertson, A. 18F-fluorothiols: a new approach to label peptides chemoselectively as potential tracers for positron emission tomography. *Bioconjug Chem* **2004**, *15*, 1447-53.

(117) de Bruin, B.; Kuhnast, B.; Hinnen, F.; Yaouancq, L.; Amessou, M.; Johannes, L.; Samson, A.; Boisgard, R.; Tavitian, B.; Dolle, F. 1-[3-(2-[18F]fluoropyridin-3-yloxy)propyl]pyrrole-2,5-dione: design, synthesis, and radiosynthesis of a new [18F]fluoropyridine-based maleimide reagent for the labeling of peptides and proteins. *Bioconjug Chem* **2005**, *16*, 406-20.

(118) Bruus-Jensen, K.; Poethko, T.; Schottelius, M.; Hauser, A.; Schwaiger, M.; Wester, H. J. Chemoselective hydrazone formation between HYNIC-functionalized peptides and (18)F-fluorinated aldehydes. *Nucl Med Biol* **2006**, *33*, 173-83.

(119) Marik, J.; Hausner, S. H.; Fix, L. A.; Gagnon, M. K.; Sutcliffe, J. L. Solid-phase synthesis of 2-[18F]fluoropropionyl peptides. *Bioconjug Chem* **2006**, *17*, 1017-21.

(120) Prante, O.; Einsiedel, J.; Haubner, R.; Gmeiner, P.; Wester, H. J.; Kuwert, T.; Maschauer, S. 3,4,6-Tri-O-acetyl-2-deoxy-2-[18F]fluoroglucopyranosyl phenylthiosulfonate: a thiol-reactive agent for the chemoselective 18F-glycosylation of peptides. *Bioconjug Chem* **2007**, *18*, 254-62.

(121) Schirrmacher, E.; Wangler, B.; Cypryk, M.; Bradtmoller, G.; Schafer, M.; Eisenhut, M.; Jurkschat, K.; Schirrmacher, R. Synthesis of p-(Di-tert-butyl[(18)F]fluorosilyl)benzaldehyde ([(18)F]SiFA-A) with high specific activity by isotopic exchange: a convenient labeling synthon for the (18)F-labeling of N-amino-oxy derivatized peptides. *Bioconjug Chem* **2007**, *18*, 2085-9.

(122) Vaidyanathan, G.; Bigner, D. D.; Zalutsky, M. R. Fluorine-18-labeled monoclonal antibody fragments: a potential approach for combining radioimmunoscintigraphy and positron emission tomography. *J Nucl Med* **1992**, *33*, 1535-41.

(123) Vaidyanathan, G.; Zalutsky, M. R. Labeling proteins with fluorine-18 using N-succinimidyl 4-[18F]fluorobenzoate. *Int J Rad Appl Instrum B* **1992**, *19*, 275-81.

(124) Herman, L. W.; Fischman, A. J.; Tompkins, R. G.; Hanson, R. N.; Byon, C.; Strauss, H. W.; Elmaleh, D. R. The use of pentafluorophenyl derivatives for the 18F labelling of proteins. *Nucl Med Biol* **1994**, *21*, 1005-10.

(125) Chang, Y. S.; Jeong, J. M.; Lee, Y. S.; Kim, H. W.; Rai, G. B.; Lee, S. J.; Lee, D. S.; Chung, J. K.; Lee, M. C. Preparation of 18F-human serum albumin: a simple and efficient protein labeling method with 18F using a hydrazone-formation method. *Bioconjug Chem* **2005**, *16*, 1329-33.

(126) Wang, H.; Chen, X. Site-specifically modified fusion proteins for molecular imaging. *Front Biosci* **2008**, *13*, 1716-32.

(127) Zhao, W.; Zhang, Y.; Cui, C.; Li, Q.; Wang, J. An efficient on-column expressed protein ligation strategy: application to segmental triple labeling of human apolipoprotein E3. *Protein Sci* **2008**, *17*, 736-47.

(128) Berndt, M.; Pietzsch, J.; Wuest, F. Labeling of low-density lipoproteins using the 18F-labeled thiol-reactive reagent N-[6-(4-[18F]fluorobenzylidene)aminooxyhexyl]maleimide. *Nucl Med Biol* **2007**, *34*, 5-15.

(129) Vogler, L., Berndt, M., Pietzsch, J., Wust, F. (18F)FBAM and (18F)FBOM: novel prosthetic groups for the mild labeling of thiol group-containing biomacromolecules. *Journal of Labeled Compounds and Radiopharmaceuticals* **2007**, *50*, S117.

(130) Namavari, M.; Padilla De Jesus, O.; Cheng, Z.; De, A.; Kovacs, E.; Levi, J.; Zhang, R.; Hoerner, J. K.; Grade, H.; Syud, F. A.; Gambhir, S. S. Direct site-specific radiolabeling of an Affibody protein with 4-[18F]fluorobenzaldehyde via oxime chemistry. *Mol Imaging Biol* **2008**, *10*, 177-81.

(131) Wuest, F.; Berndt, M.; Bergmann, R.; van den Hoff, J.; Pietzsch, J. Synthesis and application of [18F]FDG-maleimidehexyloxime ([18F]FDG-MHO): a [18F]FDG-based prosthetic group for the chemoselective 18F-labeling of peptides and proteins. *Bioconjug Chem* **2008**, *19*, 1202-10.

(132) Li, X.; Link, J. M.; Stekhova, S.; Yagle, K. J.; Smith, C.; Krohn, K. A.; Tait, J. F. Site-Specific Labeling of Annexin V with F-18 for Apoptosis Imaging. *Bioconjug Chem* **2008**.

(133) Verploegen, S. A.; Plaetinck, G.; Devos, R.; Van der Heyden, J.; Guisez, Y. A human leptin mutant induces weight gain in normal mice. *FEBS Lett* **1997**, *405*, 237-40.

(134) Peelman, F.; Van Beneden, K.; Zabeau, L.; Iserentant, H.; Ulrichts, P.; Defeau, D.; Verhee, A.; Catteeuw, D.; Elewaut, D.; Tavernier, J. Mapping of the leptin binding sites and design of a leptin antagonist. *J Biol Chem* **2004**, *279*, 41038-46.

(135) With the exception of residue K15, which when mutated to serine reduced the affinity for the receptor CRH2 domain, without reducing the ability of the protein to activate the receptor.

(136) Hnatowich, D. J. Labeling of tin-soaked albumin microspheres with 68Ga. *J Nucl Med* **1976**, *17*, 57-60.

(137) Moerlein, S. M.; Daugherty, A.; Sobel, B. E.; Welch, M. J. Metabolic imaging with gallium-68- and indium-111-labeled low-density lipoprotein. *J Nucl Med* **1991**, *32*, 300-7.

(138) Velikyan, I.; Sundberg, A. L.; Lindhe, O.; Hoglund, A. U.; Eriksson, O.; Werner, E.; Carlsson, J.; Bergstrom, M.; Langstrom, B.; Tolmachev, V. Preparation and

evaluation of (68)Ga-DOTA-hEGF for visualization of EGFR expression in malignant tumors. *J Nucl Med* **2005**, *46*, 1881-8.

(139) Heppeler, A.; Andre, J. P.; Buschmann, I.; Wang, X.; Reubi, J. C.; Hennig, M.; Kaden, T. A.; Maecke, H. R. Metal-ion-dependent biological properties of a chelator-derived somatostatin analogue for tumour targeting. *Chemistry* **2008**, *14*, 3026-34.

(140) Maecke, H. R.; Hofmann, M.; Haberkorn, U. (68)Ga-labeled peptides in tumor imaging. *J Nucl Med* **2005**, *46 Suppl 1*, 172S-8S.

(141) Neundorf, I.; Rennert, R.; Franke, J.; Kozle, I.; Bergmann, R. Detailed Analysis Concerning the Biodistribution and Metabolism of Human Calcitonin-Derived Cell-Penetrating Peptides. *Bioconjug Chem* **2008**.

(142) Schottelius, M.; Berger, S.; Poethko, T.; Schwaiger, M.; Wester, H. J. Development of novel 68Ga- and 18F-labeled GnRH-I analogues with high GnRHR-targeting efficiency. *Bioconjug Chem* **2008**, *19*, 1256-68.

(143) Decristoforo, C.; Hernandez Gonzalez, I.; Carlsen, J.; Rupprich, M.; Huisman, M.; Virgolini, I.; Wester, H. J.; Haubner, R. (68)Ga- and (111)In-labelled DOTA-RGD peptides for imaging of alphavbeta3 integrin expression. *Eur J Nucl Med Mol Imaging* **2008**, *35*, 1507-15.

(144) Muir, T. W. Semisynthesis of proteins by expressed protein ligation. *Annu Rev Biochem* **2003**, *72*, 249-89.

(145) Dawson, P. E.; Muir, T. W.; Clark-Lewis, I.; Kent, S. B. Synthesis of proteins by native chemical ligation. *Science* **1994**, *266*, 776-9.

(146) Dawson, P. E.; Kent, S. B. Synthesis of native proteins by chemical ligation. *Annu. Rev. Biochem.* **2000**, *69*, 923-960.

(147) Giriat, I.; Muir, T. W.; Perler, F. B. Protein splicing and its applications. *Genet. Eng. (N Y)* **2001**, *23*, 171-199.

(148) Muir, T. W.; Sondhi, D.; Cole, P. A. Expressed protein ligation: a general method for protein engineering. *Proc Natl Acad Sci U S A* **1998**, *95*, 6705-10.

(149) Severinov, K.; Muir, T. W. Expressed protein ligation, a novel method for studying protein-protein interactions in transcription. *J Biol Chem* **1998**, *273*, 16205-16209.

(150) Evans, T. C., Jr.; Benner, J.; Xu, M. Q. Semisynthesis of cytotoxic proteins using a modified protein splicing element. *Protein Sci* **1998**, *7*, 2256-2264.

(151) Varnerin, J. P.; Smith, T.; Rosenblum, C. I.; Vongs, A.; Murphy, B. A.; Nunes, C.; Mellin, T. N.; King, J. J.; Burgess, B. W.; Junker, B.; Chou, M.; Hey, P.; Frazier, E.; MacIntyre, D. E.; Van der Ploeg, L. H.; Tota, M. R. Production of leptin in Escherichia coli: a comparison of methods. *Protein Expr Purif* **1998**, *14*, 335-42.

(152) Valiyaveetil, F. I.; MacKinnon, R.; Muir, T. W. Semisynthesis and folding of the potassium channel KcsA. *J Am Chem Soc* **2002**, *124*, 9113-20.

(153) Hackeng, T. M.; Griffin, J. H.; Dawson, P. E. Protein synthesis by native chemical ligation: expanded scope by using straightforward methodology. *Proc Natl Acad Sci U S A* **1999**, *96*, 10068-73.

(154) Kalia, J.; Raines, R. T. Reactivity of intein thioesters: appending a functional group to a protein. *Chembiochem* **2006**, *7*, 1375-83.

(155) Haka, M. S., Kilbourn, M.R., Watkins, G.L. and Toorongian, S.A. Aryltrimethylammonium trifluoromethanesulfonates as precursors to aryl [18F]Fluorides: improved synthesis of [18F]GBR-13119. *Journal of Labeled Compounds and Radiopharmaceuticals* **1988**, *XXVII*, 823-833.

(156) Cordes, E. H., Jencks, William P. Nucleophilic catalysis of semicarbazone formation by anilines. *Journal of the American Chemical Society* **1962**, *84*, 826-831.

(157) Dirksen, A.; Hackeng, T. M.; Dawson, P. E. Nucleophilic catalysis of oxime ligation. *Angew Chem Int Ed Engl* **2006**, *45*, 7581-4.

(158) Cumin, F.; Baum, H. P.; Levens, N. Mechanism of leptin removal from the circulation by the kidney. *J Endocrinol* **1997**, *155*, 577-85.

(159) Lang, L.; Eckelman, W. C. Labeling proteins at high specific activity using N-succinimidyl 4-[18F](fluoromethyl) benzoate. *Appl Radiat Isot* **1997**, *48*, 169-73.

(160) Dirksen, A.; Dirksen, S.; Hackeng, T. M.; Dawson, P. E. Nucleophilic catalysis of hydrazone formation and transimination: implications for dynamic covalent chemistry. *J Am Chem Soc* **2006**, *128*, 15602-3.

(161) Kalia, J.; Raines, R. T. Hydrolytic stability of hydrazones and oximes. *Angew Chem Int Ed Engl* **2008**, *47*, 7523-6.

(162) Shao, H.; Crnogorac, M. M.; Kong, T.; Chen, S. Y.; Williams, J. M.; Tack, J. M.; Gueriguian, V.; Cagle, E. N.; Carnevali, M.; Tumelty, D.; Paliard, X.; Miranda, L. P.; Bradburne, J. A.; Kochendoerfer, G. G. Site-specific polymer attachment to a CCL-5 (RANTES) analogue by oxime exchange. *J Am Chem Soc* **2005**, *127*, 1350-1.

(163) Flavell, R. R.; Kothari, P.; Bar-Dagan, M.; Synan, M.; Vallabhajosula, S.; Friedman, J. M.; Muir, T. W.; Ceccarini, G. Site-specific (18)F-labeling of the protein hormone leptin using a general two-step ligation procedure. *J Am Chem Soc* **2008**, *130*, 9106-12.

(164) Merabet, E.; Dagogo-Jack, S.; Coyne, D. W.; Klein, S.; Santiago, J. V.; Hmiel, S. P.; Landt, M. Increased plasma leptin concentration in end-stage renal disease. *J Clin Endocrinol Metab* **1997**, *82*, 847-50.

(165) Sharma, K.; Considine, R. V. The Ob protein (leptin) and the kidney. *Kidney Int* **1998**, *53*, 1483-7.

(166) Moestrup, S. K.; Verroust, P. J. Megalin- and cubilin-mediated endocytosis of protein-bound vitamins, lipids, and hormones in polarized epithelia. *Annu Rev Nutr* **2001**, *21*, 407-28.

(167) Christensen, E. I.; Birn, H. Megalin and cubilin: multifunctional endocytic receptors. *Nat Rev Mol Cell Biol* **2002**, *3*, 256-66.

(168) Marx, K. A. Quartz crystal microbalance: a useful tool for studying thin polymer films and complex biomolecular systems at the solution-surface interface. *Biomacromolecules* **2003**, *4*, 1099-120.

(169) Konikowski, T.; Glenn, H. J.; Haynie, T. P. Kinetics of 67 Ga compounds in brain sarcomas and kidneys of mice. *J Nucl Med* **1973**, *14*, 164-71.

(170) Tsai, S. W.; Li, L.; Williams, L. E.; Anderson, A. L.; Raubitschek, A. A.; Shively, J. E. Metabolism and renal clearance of 111In-labeled DOTA-conjugated antibody fragments. *Bioconjug Chem* **2001**, *12*, 264-70.

(171) Strobel, J. L.; Baynes, J. W.; Thorpe, S. R. 125I-glycoconjugate labels for identifying sites of protein catabolism in vivo: effect of structure and chemistry of coupling to protein on label entrapment in cells after protein degradation. *Arch Biochem Biophys* **1985**, *240*, 635-45.

(172) Hotta, K.; Gustafson, T. A.; Ortmeyer, H. K.; Bodkin, N. L.; Hansen, B. C. Monkey leptin receptor mRNA: sequence, tissue distribution, and mRNA expression in the adipose tissue of normal, hyperinsulinemic, and type 2 diabetic rhesus monkeys. *Obes Res* **1998**, *6*, 353-60.

(173) Orlando, R. A.; Farquhar, M. G. Identification of a cell line that expresses a cell surface and a soluble form of the gp330/receptor-associated protein (RAP) Heymann nephritis antigenic complex. *Proc Natl Acad Sci U S A* **1993**, *90*, 4082-6.

(174) Dietrich, M. O.; Spuch, C.; Antequera, D.; Rodal, I.; de Yebenes, J. G.; Molina, J. A.; Bermejo, F.; Carro, E. Megalin mediates the transport of leptin across the blood-CSF barrier. *Neurobiol Aging* **2008**, *29*, 902-12.

(175) Leheste, J. R.; Melsen, F.; Wellner, M.; Jansen, P.; Schlichting, U.; Renner-Muller, I.; Andreassen, T. T.; Wolf, E.; Bachmann, S.; Nykjaer, A.; Willnow, T. E. Hypocalcemia and osteopathy in mice with kidney-specific megalin gene defect. *FASEB J* **2003**, *17*, 247-9.

(176) Lollmann, B.; Gruninger, S.; Stricker-Krongrad, A.; Chiesi, M. Detection and quantification of the leptin receptor splice variants Ob-Ra, b, and, e in different mouse tissues. *Biochem Biophys Res Commun* **1997**, *238*, 648-52.

(177) El-Haschimi, K.; Pierroz, D. D.; Hileman, S. M.; Bjorbaek, C.; Flier, J. S. Two defects contribute to hypothalamic leptin resistance in mice with diet-induced obesity. *J Clin Invest* **2000**, *105*, 1827-32.

(178) Banks, W. A.; Farr, S. A.; Morley, J. E. The effects of high fat diets on the blood-brain barrier transport of leptin: failure or adaptation? *Physiol Behav* **2006**, *88*, 244-8.

(179) Eckelman, W. C.; Frank, J. A.; Brechbiel, M. Theory and practice of imaging saturable binding sites. *Invest Radiol* **2002**, *37*, 101-6.

(180) Kung, M. P.; Kung, H. F. Mass effect of injected dose in small rodent imaging by SPECT and PET. *Nucl Med Biol* **2005**, *32*, 673-8.

(181) Zlokovic, B. V.; Jovanovic, S.; Miao, W.; Samara, S.; Verma, S.; Farrell, C. L. Differential regulation of leptin transport by the choroid plexus and blood-brain barrier and high affinity transport systems for entry into hypothalamus and across the blood-cerebrospinal fluid barrier. *Endocrinology* **2000**, *141*, 1434-41.

(182) Banks, W. A.; Clever, C. M.; Farrell, C. L. Partial saturation and regional variation in the blood-to-brain transport of leptin in normal weight mice. *Am J Physiol Endocrinol Metab* **2000**, *278*, E1158-65.

(183) McMurtry, J. P.; Ashwell, C. M.; Brocht, D. M.; Caperna, T. J. Plasma clearance and tissue distribution of radiolabeled leptin in the chicken. *Comp Biochem Physiol A Mol Integr Physiol* **2004**, *138*, 27-32.

(184) Patlak, C. S.; Blasberg, R. G.; Fenstermacher, J. D. Graphical evaluation of blood-to-brain transfer constants from multiple-time uptake data. *J Cereb Blood Flow Metab* **1983**, *3*, 1-7.

(185) Blasberg, R. G.; Fenstermacher, J. D.; Patlak, C. S. Transport of alpha-aminoisobutyric acid across brain capillary and cellular membranes. *J Cereb Blood Flow Metab* **1983**, *3*, 8-32.

(186) Hotta, K.; Gustafson, T. A.; Ortmeyer, H. K.; Bodkin, N. L.; Nicolson, M. A.; Hansen, B. C. Regulation of obese (ob) mRNA and plasma leptin levels in rhesus monkeys. Effects of insulin, body weight, and non-insulin-dependent diabetes mellitus. *J Biol Chem* **1996**, *271*, 25327-31.

(187) Finn, P. D.; Cunningham, M. J.; Pau, K. Y.; Spies, H. G.; Clifton, D. K.; Steiner, R. A. The stimulatory effect of leptin on the neuroendocrine reproductive axis of the monkey. *Endocrinology* **1998**, *139*, 4652-62.

(188) Bodkin, N. L.; Nicolson, M.; Ortmeyer, H. K.; Hansen, B. C. Hyperleptinemia: relationship to adiposity and insulin resistance in the spontaneously obese rhesus monkey. *Horm Metab Res* **1996**, *28*, 674-8.

(189) Ramsey, J. J.; Kemnitz, J. W.; Colman, R. J.; Cunningham, D.; Swick, A. G. Different central and peripheral responses to leptin in rhesus monkeys: brain transport may be limited. *J Clin Endocrinol Metab* **1998**, *83*, 3230-5.

(190) Landman, R. E.; Puder, J. J.; Xiao, E.; Freda, P. U.; Ferin, M.; Wardlaw, S. L. Endotoxin stimulates leptin in the human and nonhuman primate. *J Clin Endocrinol Metab* **2003**, *88*, 1285-91.

(191) Xiao, E.; Xia-Zhang, L.; Vulliemoz, N. R.; Ferin, M.; Wardlaw, S. L. Leptin modulates inflammatory cytokine and neuroendocrine responses to endotoxin in the primate. *Endocrinology* **2003**, *144*, 4350-3.

(192) Shields, A. F.; Grierson, J. R.; Dohmen, B. M.; Machulla, H. J.; Stayanoff, J. C.; Lawhorn-Crews, J. M.; Obradovich, J. E.; Muzik, O.; Mangner, T. J. Imaging proliferation in vivo with [F-18]FLT and positron emission tomography. *Nat Med* **1998**, *4*, 1334-6.

(193) Galloway, J. L.; Zon, L. I. Ontogeny of hematopoiesis: examining the emergence of hematopoietic cells in the vertebrate embryo. *Curr Top Dev Biol* **2003**, *53*, 139-58.

(194) Chen, K.; Cai, W.; Li, Z. B.; Wang, H.; Chen, X. Quantitative PET Imaging of VEGF Receptor Expression. *Mol Imaging Biol* **2008**.

(195) Rodriguez-Porcel, M.; Cai, W.; Gheysens, O.; Willmann, J. K.; Chen, K.; Wang, H.; Chen, I. Y.; He, L.; Wu, J. C.; Li, Z. B.; Mohamedali, K. A.; Kim, S.; Rosenblum, M. G.; Chen, X.; Gambhir, S. S. Imaging of VEGF receptor in a rat myocardial infarction model using PET. *J Nucl Med* **2008**, *49*, 667-73.

(196) Cai, W.; Chen, K.; Mohamedali, K. A.; Cao, Q.; Gambhir, S. S.; Rosenblum, M. G.; Chen, X. PET of vascular endothelial growth factor receptor expression. *J Nucl Med* **2006**, *47*, 2048-56.

(197) Backer, M. V.; Levashova, Z.; Patel, V.; Jehning, B. T.; Claffey, K.; Blankenberg, F. G.; Backer, J. M. Molecular imaging of VEGF receptors in angiogenic vasculature with single-chain VEGF-based probes. *Nat Med* **2007**, *13*, 504-9.

(198) Otsuka, F. L.; Welch, M. J.; Kilbourn, M. R.; Dence, C. S.; Dilley, W. G.; Wells, S. A., Jr. Antibody fragments labeled with fluorine-18 and gallium-68: in vivo

comparison with indium-111 and iodine-125-labeled fragments. *Int J Rad Appl Instrum B* **1991**, *18*, 813-6.

(199) Hoffend, J.; Mier, W.; Schuhmacher, J.; Schmidt, K.; Dimitrakopoulou-Strauss, A.; Strauss, L. G.; Eisenhut, M.; Kinscherf, R.; Haberkorn, U. Gallium-68-DOTA-albumin as a PET blood-pool marker: experimental evaluation in vivo. *Nucl Med Biol* **2005**, *32*, 287-92.

(200) Muralidharan, V.; Muir, T. W. Protein ligation: an enabling technology for the biophysical analysis of proteins. *Nat Methods* **2006**, *3*, 429-38.

(201) Aloj, L.; Lang, L.; Jagoda, E.; Neumann, R. D.; Eckelman, W. C. Evaluation of human transferrin radiolabeled with N-succinimidyl 4-[fluorine-18](fluoromethyl) benzoate. *J Nucl Med* **1996**, *37*, 1408-12.

(202) Zijlstra, S.; Gunawan, J.; Burchert, W. Synthesis and evaluation of a 18F-labelled recombinant annexin-V derivative, for identification and quantification of apoptotic cells with PET. *Appl Radiat Isot* **2003**, *58*, 201-7.

(203) Wester, H. J.; Hamacher, K.; Stocklin, G. A comparative study of N.C.A. fluorine-18 labeling of proteins via acylation and photochemical conjugation. *Nucl Med Biol* **1996**, *23*, 365-72.

(204) Yagle, K. J.; Eary, J. F.; Tait, J. F.; Grierson, J. R.; Link, J. M.; Lewellen, B.; Gibson, D. F.; Krohn, K. A. Evaluation of 18F-annexin V as a PET imaging agent in an animal model of apoptosis. *J Nucl Med* **2005**, *46*, 658-66.

(205) Toretsky, J.; Levenson, A.; Weinberg, I. N.; Tait, J. F.; Uren, A.; Mease, R. C. Preparation of F-18 labeled annexin V: a potential PET radiopharmaceutical for imaging cell death. *Nucl Med Biol* **2004**, *31*, 747-52.

(206) Choi, C. W.; Lang, L.; Lee, J. T.; Webber, K. O.; Yoo, T. M.; Chang, H. K.; Le, N.; Jagoda, E.; Paik, C. H.; Pastan, I.; et al. Biodistribution of 18F- and 125I-labeled anti-Tac disulfide-stabilized Fv fragments in nude mice with interleukin 2 alpha receptor-positive tumor xenografts. *Cancer Res* **1995**, *55*, 5323-9.

(207) Vaidyanathan, G.; Zalutsky, M. R. Improved synthesis of N-succinimidyl 4-[18F]fluorobenzoate and its application to the labeling of a monoclonal antibody fragment. *Bioconjug Chem* **1994**, *5*, 352-6.

(208) Page, R. L.; Garg, P. K.; Garg, S.; Archer, G. E.; Bruland, O. S.; Zalutsky, M. R. PET imaging of osteosarcoma in dogs using a fluorine-18-labeled monoclonal antibody Fab fragment. *J Nucl Med* **1994**, *35*, 1506-13.

(209) Zalutsky, M. R.; Garg, P. K.; Johnson, S. H.; Utsunomiya, H.; Coleman, R. E. Fluorine-18-antimyosin monoclonal antibody fragments: preliminary investigations in a canine myocardial infarct model. *J Nucl Med* **1992**, *33*, 575-80.

(210) Garg, P. K.; Garg, S.; Zalutsky, M. R. Fluorine-18 labeling of monoclonal antibodies and fragments with preservation of immunoreactivity. *Bioconjug Chem* **1991**, *2*, 44-9.

(211) Cheng, Z.; De Jesus, O. P.; Namavari, M.; De, A.; Levi, J.; Webster, J. M.; Zhang, R.; Lee, B.; Syud, F. A.; Gambhir, S. S. Small-Animal PET Imaging of Human Epidermal Growth Factor Receptor Type 2 Expression with Site-Specific 18F-Labeled Protein Scaffold Molecules. *J Nucl Med* **2008**, *49*, 804-13.

(212) Hooker, J. M.; O'Neil, J. P.; Romanini, D. W.; Taylor, S. E.; Francis, M. B. Genome-free viral capsids as carriers for positron emission tomography radiolabels. *Mol Imaging Biol* **2008**, *10*, 182-91.

(213) Gaertner, H.; Offord, R.; Botti, P.; Kuenzi, G.; Hartley, O. Semisynthetic analogues of PSC-RANTES, a potent anti-HIV protein. *Bioconjug Chem* **2008**, *19*, 480-9.

(214) Smith, J. T.; Waddell, B. J. Leptin distribution and metabolism in the pregnant rat: transplacental leptin passage increases in late gestation but is reduced by excess glucocorticoids. *Endocrinology* **2003**, *144*, 3024-30.

(215) Irani, B. G.; Dunn-Meynell, A. A.; Levin, B. E. Altered hypothalamic leptin, insulin, and melanocortin binding associated with moderate-fat diet and predisposition to obesity. *Endocrinology* **2007**, *148*, 310-6.

(216) Thomas, S. A.; Preston, J. E.; Wilson, M. R.; Farrell, C. L.; Segal, M. B. Leptin transport at the blood--cerebrospinal fluid barrier using the perfused sheep choroid plexus model. *Brain Res* **2001**, *895*, 283-90.

(217) Wang, M. Y.; Zhou, Y. T.; Newgard, C. B.; Unger, R. H. A novel leptin receptor isoform in rat. *FEBS Lett* **1996**, *392*, 87-90.

(218) Bruno, A.; Chanez, P.; Chiappara, G.; Siena, L.; Giammanco, S.; Gjomarkaj, M.; Bonsignore, G.; Bousquet, J.; Vignola, A. M. Does leptin play a cytokine-like role within the airways of COPD patients? *Eur Respir J* **2005**, *26*, 398-405.

(219) Cohen, B.; Novick, D.; Rubinstein, M. Modulation of insulin activities by leptin. *Science* **1996**, *274*, 1185-8.

(220) Szanto, I.; Kahn, C. R. Selective interaction between leptin and insulin signaling pathways in a hepatic cell line. *Proc Natl Acad Sci U S A* **2000**, *97*, 2355-60.

(221) Zhao, A. Z.; Shinohara, M. M.; Huang, D.; Shimizu, M.; Eldar-Finkelman, H.; Krebs, E. G.; Beavo, J. A.; Bornfeldt, K. E. Leptin induces insulin-like signaling that antagonizes cAMP elevation by glucagon in hepatocytes. *J Biol Chem* **2000**, *275*, 11348-54.

(222) Cao, Q.; Mak, K. M.; Ren, C.; Lieber, C. S. Leptin stimulates tissue inhibitor of metalloproteinase-1 in human hepatic stellate cells: respective roles of the JAK/STAT and JAK-mediated H2O2-dependant MAPK pathways. *J Biol Chem* **2004**, *279*, 4292-304.

(223) Cohen, P.; Yang, G.; Yu, X.; Soukas, A. A.; Wolfish, C. S.; Friedman, J. M.; Li, C. Induction of leptin receptor expression in the liver by leptin and food deprivation. *J Biol Chem* **2005**, *280*, 10034-9.

(224) Vila, R.; Adan, C.; Rafecas, I.; Fernandez-Lopez, J. A.; Remesar, X.; Alemany, M. Plasma leptin turnover rates in lean and obese Zucker rats. *Endocrinology* **1998**, *139*, 4466-9.

(225) Young, G. A.; Woodrow, G.; Kendall, S.; Oldroyd, B.; Turney, J. H.; Brownjohn, A. M.; Smith, M. A. Increased plasma leptin/fat ratio in patients with chronic renal failure: a cause of malnutrition? *Nephrol Dial Transplant* **1997**, *12*, 2318-23.

(226) Jackson, E. K.; Herzer, W. A. A comparison of the natriuretic/diuretic effects of rat vs. human leptin in the rat. *Am J Physiol* **1999**, *277*, F761-5.

(227) Nykjaer, A.; Dragun, D.; Walther, D.; Vorum, H.; Jacobsen, C.; Herz, J.; Melsen, F.; Christensen, E. I.; Willnow, T. E. An endocytic pathway essential for renal uptake and activation of the steroid 25-(OH) vitamin D3. *Cell* **1999**, *96*, 507-15.

(228) de Jong, M.; Barone, R.; Krenning, E.; Bernard, B.; Melis, M.; Visser, T.; Gekle, M.; Willnow, T. E.; Walrand, S.; Jamar, F.; Pauwels, S. Megalin is essential for renal proximal tubule reabsorption of (111)In-DTPA-octreotide. *J Nucl Med* **2005**, *46*, 1696-700.

(229) Raila, J.; Willnow, T. E.; Schweigert, F. J. Megalin-mediated reuptake of retinol in the kidneys of mice is essential for vitamin A homeostasis. *J Nutr* **2005**, *135*, 2512-6.

(230) Zlokovic, B. V.; Martel, C. L.; Matsubara, E.; McComb, J. G.; Zheng, G.; McCluskey, R. T.; Frangione, B.; Ghiso, J. Glycoprotein 330/megalin: probable role in receptor-mediated transport of apolipoprotein J alone and in a complex with Alzheimer disease amyloid beta at the blood-brain and blood-cerebrospinal fluid barriers. *Proc Natl Acad Sci U S A* **1996**, *93*, 4229-34.

(231) Fantuzzi, G.; Faggioni, R. Leptin in the regulation of immunity, inflammation, and hematopoiesis. *J Leukoc Biol* **2000**, *68*, 437-46.

(232) Lam, Q. L.; Lu, L. Role of leptin in immunity. *Cell Mol Immunol* **2007**, *4*, 1-13.

(233) Fernandes, G.; Handwerger, B. S.; Yunis, E. J.; Brown, D. M. Immune response in the mutant diabetic C57BL/Ks-dt+ mouse. Discrepancies between in vitro and in vivo immunological assays. *J Clin Invest* **1978**, *61*, 243-50.

(234) Chandra, R. K. Cell-mediated immunity in genetically obese C57BL/6J ob/ob) mice. *Am J Clin Nutr* **1980**, *33*, 13-6.

(235) Claycombe, K.; King, L. E.; Fraker, P. J. A role for leptin in sustaining lymphopoiesis and myelopoiesis. *Proc Natl Acad Sci U S A* **2008**, *105*, 2017-21.

(236) Umemoto, Y.; Tsuji, K.; Yang, F. C.; Ebihara, Y.; Kaneko, A.; Furukawa, S.; Nakahata, T. Leptin stimulates the proliferation of murine myelocytic and primitive hematopoietic progenitor cells. *Blood* **1997**, *90*, 3438-43.

(237) Bennett, B. D.; Solar, G. P.; Yuan, J. Q.; Mathias, J.; Thomas, G. R.; Matthews, W. A role for leptin and its cognate receptor in hematopoiesis. *Curr Biol* **1996**, *6*, 1170-80.

(238) Zarkesh-Esfahani, H.; Pockley, G.; Metcalfe, R. A.; Bidlingmaier, M.; Wu, Z.; Ajami, A.; Weetman, A. P.; Strasburger, C. J.; Ross, R. J. High-dose leptin activates human leukocytes via receptor expression on monocytes. *J Immunol* **2001**, *167*, 4593-9.

(239) Gainsford, T.; Willson, T. A.; Metcalf, D.; Handman, E.; McFarlane, C.; Ng, A.; Nicola, N. A.; Alexander, W. S.; Hilton, D. J. Leptin can induce proliferation, differentiation, and functional activation of hemopoietic cells. *Proc Natl Acad Sci U S A* **1996**, *93*, 14564-8.

(240) Palmer, G.; Aurrand-Lions, M.; Contassot, E.; Talabot-Ayer, D.; Ducrest-Gay, D.; Vesin, C.; Chobaz-Peclat, V.; Busso, N.; Gabay, C. Indirect effects of leptin receptor deficiency on lymphocyte populations and immune response in db/db mice. *J Immunol* **2006**, *177*, 2899-907.

(241) de Boer, J.; Williams, A.; Skavdis, G.; Harker, N.; Coles, M.; Tolaini, M.; Norton, T.; Williams, K.; Roderick, K.; Potocnik, A. J.; Kioussis, D. Transgenic mice with hematopoietic and lymphoid specific expression of Cre. *Eur J Immunol* **2003**, *33*, 314-25.

(242) Konopleva, M.; Mikhail, A.; Estrov, Z.; Zhao, S.; Harris, D.; Sanchez-Williams, G.; Kornblau, S. M.; Dong, J.; Kliche, K. O.; Jiang, S.; Snodgrass, H. R.; Estey, E. H.; Andreeff, M. Expression and function of leptin receptor isoforms in myeloid leukemia and myelodysplastic syndromes: proliferative and anti-apoptotic activities. *Blood* **1999**, *93*, 1668-76.

(243) Tabe, Y.; Konopleva, M.; Munsell, M. F.; Marini, F. C.; Zompetta, C.; McQueen, T.; Tsao, T.; Zhao, S.; Pierce, S.; Igari, J.; Estey, E. H.; Andreeff, M. PML-RARalpha is associated with leptin-receptor induction: the role of mesenchymal stem cell-derived adipocytes in APL cell survival. *Blood* **2004**, *103*, 1815-22.

(244) Diaz-Blanco, E.; Bruns, I.; Neumann, F.; Fischer, J. C.; Graef, T.; Rosskopf, M.; Brors, B.; Pechtel, S.; Bork, S.; Koch, A.; Baer, A.; Rohr, U. P.; Kobbe, G.; Haeseler, A.; Gattermann, N.; Haas, R.; Kronenwett, R. Molecular signature of CD34(+) hematopoietic stem and progenitor cells of patients with CML in chronic phase. *Leukemia* **2007**, *21*, 494-504.

(245) Wincewicz, A.; Koda, M.; Sulkowska, M.; Kanczuga-Koda, L.; Sulkowski, S. Comparison of STAT3 with HIF-1alpha, Ob and ObR expressions in human endometrioid adenocarcinomas. *Tissue Cell* **2008**.

(246) Zhou, J.; Lei, W.; Shen, L.; Luo, H. S.; Shen, Z. X. Primary study of leptin and human hepatocellular carcinoma in vitro. *World J Gastroenterol* **2008**, *14*, 2900-4.

(247) Jarde, T.; Caldefie-Chezet, F.; Damez, M.; Mishellany, F.; Penault-Llorca, F.; Guillot, J.; Vasson, M. P. Leptin and leptin receptor involvement in cancer development: a study on human primary breast carcinoma. *Oncol Rep* **2008**, *19*, 905-11.

(248) Saxena, N. K.; Vertino, P. M.; Anania, F. A.; Sharma, D. leptin-induced growth stimulation of breast cancer cells involves recruitment of histone acetyltransferases and mediator complex to CYCLIN D1 promoter via activation of Stat3. *J Biol Chem* **2007**, *282*, 13316-25.

(249) Revillion, F.; Charlier, M.; Lhotellier, V.; Hornez, L.; Giard, S.; Baranzelli, M. C.; Djiane, J.; Peyrat, J. P. Messenger RNA expression of leptin and leptin receptors and their prognostic value in 322 human primary breast cancers. *Clin Cancer Res* **2006**, *12*, 2088-94.

(250) Koda, M.; Sulkowska, M.; Kanczuga-Koda, L.; Cascio, S.; Colucci, G.; Russo, A.; Surmacz, E.; Sulkowski, S. Expression of the obesity hormone leptin and its receptor correlates with hypoxia-inducible factor-1 alpha in human colorectal cancer. *Ann Oncol* **2007**, *18 Suppl 6*, vi116-9.

(251) Horiguchi, A.; Sumitomo, M.; Asakuma, J.; Asano, T.; Zheng, R.; Nanus, D. M.; Hayakawa, M. Increased serum leptin levels and over expression of leptin receptors are associated with the invasion and progression of renal cell carcinoma. *J Urol* **2006**, *176*, 1631-5.

(252) Miyoshi, Y.; Funahashi, T.; Tanaka, S.; Taguchi, T.; Tamaki, Y.; Shimomura, I.; Noguchi, S. High expression of leptin receptor mRNA in breast cancer tissue predicts poor prognosis for patients with high, but not low, serum leptin levels. *Int J Cancer* **2006**, *118*, 1414-9.

(253) Takaya, K.; Ogawa, Y.; Hiraoka, J.; Hosoda, K.; Yamori, Y.; Nakao, K.; Koletsky, R. J. Nonsense mutation of leptin receptor in the obese spontaneously hypertensive Koletsky rat. *Nat Genet* **1996**, *14*, 130-1.

(254) Ge, H.; Huang, L.; Pourbahrami, T.; Li, C. Generation of soluble leptin receptor by ectodomain shedding of membrane-spanning receptors in vitro and in vivo. *J Biol Chem* **2002**, *277*, 45898-903.

(255) Jimenez-Castells, C.; de la Torre, B. G.; Gutierrez Gallego, R.; Andreu, D. Optimized synthesis of aminooxy-peptides as glycoprobe precursors for surface-based sugar-protein interaction studies. *Bioorg Med Chem Lett* **2007**, *17*, 5155-8.

(256) Lado-Abeal, J.; Hickox, J. R.; Cheung, T. L.; Veldhuis, J. D.; Hardy, D. M.; Norman, R. L. Neuroendocrine consequences of fasting in adult male macaques: effects of recombinant rhesus macaque leptin infusion. *Neuroendocrinology* **2000**, *71*, 196-208.